Energy Efficiency in Ad-hoc Wireless Networks

Wei Feng

School of Electronic and Electrical Engineering

University of Leeds

A thesis submitted for the degree of

Doctor of Philosophy

March 2010

Acknowledgements

It would not have been possible to write this doctoral thesis without the help and support of the kind people around me, to only some of whom it is possible to give particular mention here.

Above all, I would like to thank my supervisor, Prof. Jaafar Elmighani for his tremendous support all during my research study. His encouragements, motivation and endless enlightening ideas were very helpful to the success of this work.

I am also grateful to the friends and colleagues in the Communication Network and Systems Group.

At last I deeply appreciate all the support and great patience of my parents, my wife and my sister.

Abstract

In ad-hoc wireless networks, nodes are typically battery-powered, therefore energy limitations are among the critical constraints in ad-hoc wireless networks' development. The approaches investigated in this thesis to achieve energy efficient performance in wireless networks can be grouped into three main categories.

1. Each wireless network node has four energy consumption states: transmitting, receiving, listening and sleeping states. The power consumed in the listening state is less than the power consumed in the transmitting and receiving states, but significantly greater than that in the sleeping state. Energy efficiency is achieved if as many nodes as possible are put into the sleeping states.

2. Since energy is consumed for transmission nonlinearly in terms of the transmission range, transmission range adjustment is another energy saving approach. In this work, the optimal transmission range is derived and applied to achieve energy efficient performance in a number of scenarios.

3. Since energy can be saved by properly arranging the communication algorithms, network topology management or network routing is the third approach, which can be utilised in combination with the above two approaches. In this work, Geographical Adaptive Fidelity (GAF) algorithms, clustering algorithms and Geographic Routing (GR) algorithms are all utilised to reduce the energy consumption of wireless networks, such as Sensor Networks and Vehicular Networks.

These three approaches are used in this work to reduce the energy consumption of wireless networks. With the GAF algorithm, we derived the optimal transmission range and optimal grid size in both linear and rectangular networks, and as a result we show how the network energy consumptions can be reduced and how the network lifetime can be prolonged. With Geographic Routing algorithms, the author proposed the Optimal Range Forward (ORF) algorithm and Optimal Forward with Energy Balance (OFEB) algorithm to reduce the energy consumption and to prolong the network lifetime. The results show that, compared to the traditional GR algorithms (Most Forward within Radius, Nearest Forward Progress), the network lifetime is prolonged. Other approaches have also been considered to improve the networks's energy efficient operation utilising Genetic Algorithms to find the optimal size of the grid or cluster. Furthermore, realistic physical layer models, Rayleigh fading and LogNormal fading, are considered in evaluating energy efficiency in a realistic network environment.

Abbreviations

ACK	Acknowledge
AODV	Ad-hoc On-demand Distance Vector
AP	Access point
ATIM	Ad-hoc Traffic Indication Message
BI	Beacon Interval
BS	Base Station
DSR	Dynamic Source Routing
EPP	Energy-Proportional Principle
GA	Genetic Algorithm
GAF	Geographic Adaptive Fidelity
GPER	Geographic Power Efficient Routing
GPS	Global Positioning System
GR	Geographic Routing
GRS	Greedy Routing Scheme
HHRs	Hop by Hop Retransmissions
ICT	Information and Communication Technology
LAN	Local Area Networks
LEACH	Low Energy Adaptive Clustering Hierarchy

$MANET$	Mobile Ad-hoc NETworks
$MECH$	Maximum Energy Cluster-Head
MFR	Most Forward within Radius
MHC	Multi-Hop Communication
$MSPS$	Multiple States Power Saving
NFP	Nearest Forward Progress
$OFEB$	Optimal Forward with Energy Balance
ORF	Optimal Range Forward
OTR	Optimal Transmission Range
PDA	Personal Digital Assistances
PSM	Power Saving Mechanism
QoS	Quality of Service
$RREP$	Route REPly
$RREQ$	Route REQuest
SHC	Single Hop Communication
$SINR$	Signal-to-Interference-plus-Noise power Ratio
$VANET$	Vehicular Ad-hoc NETworks
$WASNET$	Wireless Ad-hoc Sensor NETworks

Symbols

D	traffic data bits
E	energy consumption
e_t	energy consumed for transceiver electronic
e_a	energy consumed for transmitter amplifier
e_p	energy consumed for processing data
f	carrier frequency
L	length of network
m	number of hops
N	number of nodes
n	propagation loss factor
$Power$	power consumption
P_b	probability
P_r	reception power
P_t	transmission power
P_{thr}	power threshold
R	transmission range
r	grid length
R_{opt}	optimal transmission range
W	width of network
λ	node density

Contents

List of Figures

Chapter 1

Introduction

Energy efficiency is one of the most important aspects in ad-hoc wireless networks and has been widely investigated in recent years. In this chapter, the communication networks are introduced. Following that, the energy constraints in ad-hoc wireless networks are described, and the network lifetime is defined. Furthermore, the energy consumption states of wireless node are summarised. The transmission techniques employed in ad-hoc wireless networks are introduced and discussed. Finally, popular topology management algorithms and routing algorithms in ad-hoc wireless networks are introduced and analysed.

1.1 Classification of communication networks

A communication network is a group of communication devices, such as computer and mobile phones, which are connected to each other for the purpose of communication [1–4]. Depending on the communication manners, communication networks may be classified as wired networks and wireless networks, which communicate with and without a wire, respectively. For example, Ethernet and optical fiber networks are wired networks, whereas wireless LAN, mobile cellular networks, ad-hoc wireless networks, Paging systems, Cordless telephone networks, and satellite networks are wireless networks, in which the devices use radio waves or infrared signals as transmission medium.
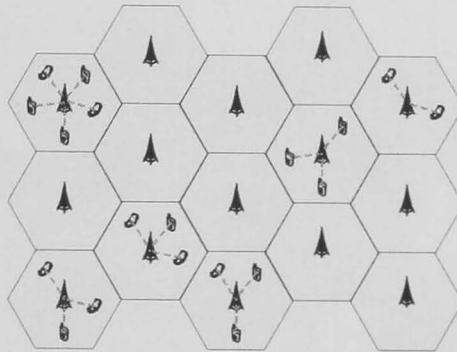
Figure 1.1: Cellular network structure

Since the mid of the 1990s, wireless networks have become much more pervasive than anything people could have imagined [1]. Wireless networks are traditionally classified as fixed infrastructure networks and ad-hoc networks [5–7]. The former usually contains one or more centralised nodes such as access points or base stations, which are connected to the Internet backbone. In these networks, mobile nodes can communicate directly with an access point which performs the key networking and control functions for them. There is no peer-to-peer communication between mobile nodes and all communication is done via the access point through single-hop routing.

Ad-hoc is a Latin phrase which means 'for this purpose' and ad-hoc networks are networks constructed to solve specific problems or tasks. The earliest wireless ad hoc networks were the 'packet radio' networks (PRNETs) dating to the 1970s, sponsored by DARPA after the ALOHAnet project [8]. Nodes in ad-hoc wireless networks, however, can communicate in peer-to-peer mode or perform some distributed networking and control functions. They can communicate directly with other nodes whenever they are within their transmission ranges and communicate through intermediate nodes (relays) using multi-hop routing to extend their communication ranges and consequently forward their information packets to other nodes which are out of their transmission ranges [4]. A centralised cel-
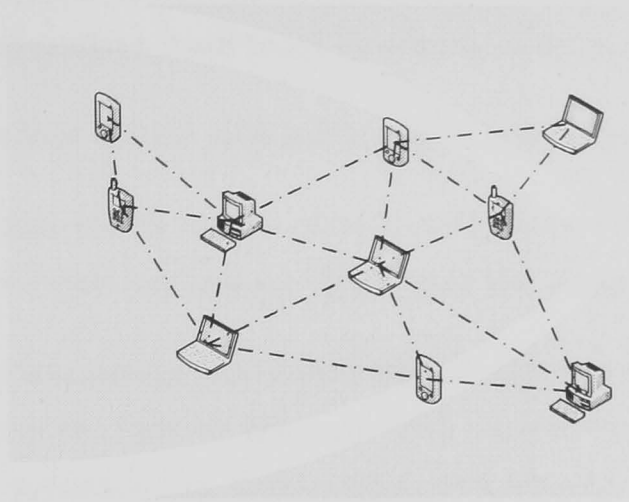
Figure 1.2: Ad-hoc network structure

lular network structure is shown in Fig. 1.1 and an ad-hoc network structure is shown in Fig. 1.2.

1.2 Node characteristics in ad-hoc wireless networks

A desirable feature in ad-hoc wireless nodes is self-manageability. As defined by IBM, the ad-hoc node has four major and four minor characteristics [9], [10]. The four major characteristics are:

- Self-configuration is the property of a node that enables it to implement specific strategies to change the relations among the components to guarantee either survivability in changing environments or a better performance.

- Self-healing enables nodes to detect (or predict) faults and automatically correct faults (events that cause the entire system or parts of it to malfunction).

- Self-optimisation enables nodes to monitor their components and fine-tune the resources automatically to optimise the performance.

- Self-protection is the property of node which allows it to anticipate. detect. identify. and protect itself from attacks in order to maintain overall integrity.

Additionally. the four minor characteristics are as follows:

- Self-awareness which means that a node knows itself (its components. resources. the relations among them. and the limits) in a detailed manner.

- Self-adaptation means automatically identifying the environment. generating strategies on how to interact with neighboring systems. and adapting the node's behaviour to a changing environment.

- Self-evolution means generating new strategies and implementing open standards.

- Self-anticipation means anticipating the requests for resources from the users without involving them in the complexity of its functionality.

Based on the characteristics of ad-hoc nodes, a self-organising wireless network will create its own connections. topology. transmission schedules. and routing patterns in a distributed manner. It may establish local hubs. a backbone network. gateways. and relays [11]. A wireless ad-hoc network has two main control and management mechanisms: discovery of routes between pairs of nodes and update of the current topology. by first detecting node or link failures and secondly by optimising the routes obtained through discovery.

1.3 Energy constraints in ad-hoc wireless networks

Due to their flexible structures and varied components. which include sensors. vehicles. laptops or PDAs (Personal Digital Assistances) all equipped with wireless cards. ad-hoc wireless networks have popular applications. such as environment monitoring. surveillance. military. and emergency aid. However. the degree of

survivability of these networks is limited by the level of energy or power consumption. Most of the nodes in ad-hoc wireless networks are battery powered, and unfortunately the energy density of batteries has shown little improvement recently compared to other technologies (e.g. memory, hard disk, computation speed). Furthermore, wireless ad-hoc devices have become smaller, which in turn has reduced the physical area available for batteries. Therefore, the limited energy capacity available to nodes has become the major constraint in the lifetime of both individual nodes and ad-hoc and sensor networks. On the other hand, it is costly and sometimes infeasible to recharge or replace the batteries of these devices such as in battle-fields or other dangerous scenarios. Therefore, it is necessary to properly manage the energy consumption of each node to reduce the energy consumption and prolong the network lifetime.

1.4 Definition of network lifetime

The network lifetime is defined as the time duration before 1) the first node dies [12], 2) the fraction of active nodes drops below a threshold [13] or 3) the aggregate delivery rate drops below a threshold [14]. These various definitions are appropriate in different scenarios. Therefore, in this work, the network lifetime is defined as the time duration before the first grid (cluster) dies in the topology management algorithms, and it is defined as the time duration before disconnection of the network in the Geographic Routing algorithms introduced.

1.5 Energy consumption states in ad-hoc wireless networks

There are various factors contributing to energy consumption in nodes in ad-hoc wireless networks. But as far as the energy consumed for network communication, the wireless nodes may be classified as being in one of four states: transmitting, receiving, listening and sleeping states. It is often assumed that the part of the total power consumed by nodes due to data exchange (transmitting and receiving)

is the dominant part in energy consumption. In fact, when one node sends packets to another node, all its neighbour nodes consume power even though the packet is not sent to them, and this is referred to as overhearing. Thus the listening state energy consumption is not negligible. Note that, the energy consumed in the sleeping state can be ignored compared to energy consumption in other states. In [15], the authors conducted some measurements on the power levels consumed during the different nodes states. Consequently, the ratios between the listening, receiving and transmitting states are described as: 1:1.05:1.4. In [14], the authors described the same ratios as: 1:1.2:1.7. Significant energy saving can be obtained by putting as many nodes as possible into the sleeping state. Some recent work on energy saving in ad-hoc networks has focused on this, and will be discussed and utilised as one of the main approaches of energy saving in this work. Note, however, that signal processing and node operation in a stand-by mode (listening) also consume non-negligible power. Many techniques that reduce the transmit power require a significant amount of signal processing, as shown in [16].

1.6 Transmission techniques used in ad-hoc wireless networks

Two transmission techniques are widely used by ad-hoc network nodes to communicate among themselves or send data to a destination point, such as a sink in sensor networks [6], [17–20]: single-hop communication (SHC) and multi-hop communication (MHC). While ad-hoc network nodes send or communicate directly with a destination in SHC, these nodes relay (forward) the message from one node to another until the information reaches the sink or destination in multi-hop communication. In single-hop communication, network nodes are able to cover the whole network, and thus consume energy according to the longest transmission distance. Hence, with this fixed transmission distance, extra energy is wasted even when nodes are close to each other.

In multi-hop communications, the total energy consumed for end-to-end communications increases as a function of both the number of relaying nodes and the

energy consumption in each individual hop. which is mainly determined by the transmission distance (d). Moreover, the energy consumed in each individual hop increases in a nonlinear fashion with transmission distance according to d^n (n is the signal propagation attenuation factor and is usually $2 \leq n \leq 4$) [3]. Therefore, if the number of hops is small (while the transmission distance is large), the energy consumed for one transmission increases nonlinearly. Alternately, if the hop's distance is short (for the same overall end-to-end distance). the energy consumption will be dominated by the electronic energy costs in the transceivers and therefore the total energy increases almost linearly as a function of the hop number (where the hop number is large). Apparently. there is a trade off between hop number and transmission distance of each hop to get the optimal energy efficiency, and the energy consumption may be reduced by selecting the proper transmission range (optimal transmission range). The optimal transmission range will be used as the second main approach in this work to achieve energy efficient performance in ad-hoc wireless networks.

1.7 Topology management and routing algorithms in ad-hoc wireless networks

In topology management protocols, all nodes are divided into groups or clusters according to their location information, and are then classified as head nodes and normal nodes. Therefore. the sleeping state can be simply managed and the communication routes are set up based on local information [21]. Routing is an important function in ad-hoc wireless networks and as part of its operation it can be used to set up communication paths and to manage the node states. In ad-hoc wireless networks, topology management and routing algorithms play important roles in managing the node states and establishing the optimal communication paths. Thus. with proper design of topology management or routing algorithms. the network energy consumption can be reduced and the network lifetime can be prolonged. As a third approach to achieve energy efficient performance in ad-hoc

wireless networks, topology management and routing algorithms may be utilised together with the other energy saving approaches.

Geographic Routing (GR), location/position-based routing, for communication in ad-hoc wireless networks has recently received much attention, especially in the energy saving area [22],[23]. In geographic routing, each node has knowledge of its own geographic information either via a Global Positioning System (GPS) or from network localisation algorithms, and broadcasts its location information to other nodes periodically. The next relay node is selected only based on the location of the source node, its neighbours and its ultimate destination (contained in the data packet). Therefore, GR is generally considered to be scalable and applicable to large networks. Furthermore, the energy consumption of each hop can be reduced if the next relay node is properly selected. In this thesis, an energy efficient GR approach is proposed.

1.8 Research objectives

The primary objectives of the work undertaken and presented in this thesis are:

1. To derive the optimal transmission range and the optimal location of relay nodes in ad-hoc wireless networks.

2. To analyse the energy efficiency in linear ad-hoc networks, when the optimal transmission range and topology managements are utilised.

3. To analyse the energy efficiency in rectangular ad-hoc networks, under the same condition as in objective 2.

4. To analyse the energy efficiency in the 2-D ad-hoc networks, where optimal transmission range and Geographic Routing algorithms are utilised.

5. To analyse energy efficiency in ad-hoc wireless networks when realistic physical layer models are considerd.

6. To evaluate energy efficiency in Vehicular Ad-hoc wireless networks.

1.9 List of contributions

The original contributions of this thesis are as follows:

1. the optimal transmission range and the optimal location of relay node in the ad-hoc wireless networks are derived .

2. an energy efficient Geographic Adaptive Fidelity (GAF) topology management protocol is proposed to achieve energy efficient performance in a linear ad-hoc wireless networks. In this protocol. multiple node states control is applied, and the size of the virtual grid in the GAF model is adjusted based on the optimal transmission range. The results show that around 12% energy can be saved using this energy efficient GAF protocol compared to the original GAF protocol.

3. an energy efficient GAF protocol in a rectangular ad-hoc wireless network is proposed, and it is shown that the network lifetime can be prolonged by using this protocol and node density control. The multiple node states control approach and the optimal transmission range are utilised in the protocol. The results show that the network energy consumption has been reduced and the network lifetime has been prolonged.

4. two energy efficient Geographic Routing algorithms, the Optimal Range Forward (ORF) and the Optimal Forward with Energy Balance (OFEB) algorithms. are proposed in a linear ad-hoc wireless network. Both are able to reduce the network energy consumption and prolong the network lifetime.

5. two new variants of the energy efficient Geographic Routing algorithms. ORF and OFEB, are proposed in a 2-D ad-hoc wireless networks. The network lifetime, the network throughput. the number of packets successfully received by the destination and the average energy cost for each successfully received packet are compared based on different node densities.

6. realistic physical layer models are considered and the energy efficiency of the approaches proposed so far under these realistic conditions is evaluated.

Signal attenuation, different values of the loss factor, and fading models (Rayleigh fading and Lognormal fading) are analysed.

7. the energy efficient GAF model is applied to a real Motorway traffic model, which is derived from the 'M4' road in the United Kingdom.

The original contributions are supported by the following publications:

Journals:

1. W. Feng, H. Alshaer and Jaafar M. H. Elmirghani, "Green ICT: Energy Efficiency in a Motorway Model", IET special issue on Vehicular Ad-hoc networks, 2010 [24]. The content of this journal paper will be discussed in Chapter 8.

2. W. Feng and Jaafar M. H. Elmirghani, "Lifetime Evaluation in Energy-efficient Rectangular Ad-hoc Wireless networks", International journal of communication systems [25]. The content of this journal paper will be discussed in Chapter 4.

Conferences:

3. W. Feng, H. Alshaer and Jaafar M. H. Elmirghani, "Evaluation of Energy Consumption and Network Lifetime in Rectangular Ad-hoc Wireless networks", Proceedings of IEEE 6th International Conference on Information Technology: New Generations (ITNG).Las Vegas, Nevada, USA, April 2009 [26]. The content of this paper relates to Chapter 4.

4. W. Feng, H. Alshaer and Jaafar M. H. Elmirghani, "Energy Efficiency: Optimal Transmission Range with Topology Management in Rectangular Ad-hoc Wireless networks", Proceedings of the IEEE 23rd International Conference on Advanced Information Networking and Applications (AINA-09), Bradford, UK, May, 2009 [27]. The content of this paper relates to Chapter 4.

5. W. Feng, H. Alshaer and Jaafar M. H. Elmirghani. "Energy Efficiency for Rectangular Ad-hoc Wireless Networks", the IEEE 5th International Wireless Communications and Mobile Computing Conference (IWCMC 2009), Leipzig, Germany, June 21-24. 2009 [28]. The content of this paper relates to Chapter 4.

6. W. Feng and Jaafar M. H. Elmirghani. "Optimization of energy consumption in linear ad-hoc wireless networks", 10th IEEE International Symposium on Communication Theory and Application, St. Martin's College, Ambleside, UK, 13th-17th July 2009 [29]. The content of this paper will be discussed in Chapter 3.

7. W. Feng, H.Alshaer and Jaafar M. H. Elmirghani, "Optimization of Energy Consumption in Rectangular Ad-hoc Wireless networks", IEEE ChinaCom. August, 2009 [30]. The content of this paper relates to Chapter 4.

8. W. Feng and Jaafar M. H. Elmirghani, "Green ICT: Energy Efficiency in a Motorway Model", IEEE Next Generation Mobile Applications. Services and Technologies, September. 2009 [31]. The content of this paper relates to Chapter 8.

9. W. Feng and Jaafar M. H. Elmirghani, "Energy-efficient Geographic routing in 2-D ad-hoc wireless networks", IEEE Next Generation Mobile Applications, Services and Technologies. September, 2009 [32]. The content of this paper will be discussed in Chapter 6.

10. W. Feng and Jaafar M. H. Elmirghani, "Energy Efficiency in Ad-hoc Wireless Networks With Two Realistic Physical Layer models". IEEE Next Generation Mobile Applications. Services and Technologies. September, 2009 [33]. The content of this paper will be discussed in Chapter 7.

11. W. Feng and Jaafar M. H. Elmirghani. "Energy Efficiency in the Cluster-based Linear Ad-hoc Wireless networks", IEEE Next Generation Mobile Applications. Services and Technologies. September, 2009 [34]. The content of this paper will be discussed in Chapter 5.

12. W. Feng, A. S. Koyamparambil Mammu and Jaafar M. H. Elmirghani. "Energy-Efficient Geographic Routing in Ad-hoc Wireless Networks". London Communications Symposium'09. September. 2009 [35]. The content of this relates to Chapter 6.

1.10   Thesis overview

In Chapter 2, the related literature is introduced, and most popular energy saving approaches are discussed and classified into three main categories.

In Chapter 3, an energy efficient GAF topology management protocol is proposed to achieve energy saving performance in a linear ad-hoc wireless network.

In Chapter 4, an energy efficient GAF protocol for rectangular ad-hoc wireless networks is proposed, and the network lifetime is prolonged by using this protocol and a node density control scheme.

In Chapter 5, energy efficient Geographic Routing algorithms are proposed in a linear ad-hoc wireless network.

In Chapter 6, energy efficient Geographic Routing algorithms for a 2-D ad-hoc wireless networks are proposed and evaluated.

In Chapter 7, realistic physical layer models are considered and are used to evaluate the performance of the proposed algorithms in realistic environments. Signal propagation attenuation, different values of loss factor, and fading models (Rayleigh fading and Lognormal fading) are employed.

In Chapter 8, the energy efficient GAF model is applied to a real Motorway traffic model, which is derived from the 'M4' motorway in the United Kingdom.

In Chapter 9, the thesis is concluded and the future work is outlined.

1.11   Summary

In this chapter, the communication networks, especially ad-hoc wireless networks are introduced. The network energy consumption, which is the motivation of this thesis, is discussed. Furthermore, the network lifetime is defined in different

12

manners. The main communication techniques. Single hop and Multi-hop communications. are introduced and discussed. The discussion was used to highlight the fact that an optimal transmission range should exist. Topology management and routing algorithms are introduced and discussed. which can be combined with optimal transmission range to achieve energy efficient performance. The chapter has outlined the objectives of this research work and the original contributions made.

Chapter 2

Power efficiency in ad-hoc networks

In battery-powered ad-hoc wireless networks, a critical issue is the efficient use of the available energy of a node while satisfying the Quality of Service (QoS) in the network [36],[37]. Most of the approaches used to achieve these goals can be classified into three main categories.

2.1 Multiple power consumption states

As mentioned in Chapter 1, different energy levels are consumed in different operating states (including transmitting, receiving, listening and sleeping states). The power consumed in the listening state is less than the power consumed in the transmitting and receiving states, but significantly greater than that in the sleeping state, the energy consumed in which can be ignored. Maximising the number of nodes in the sleeping state over all operating conditions minimises the network energy consumption.
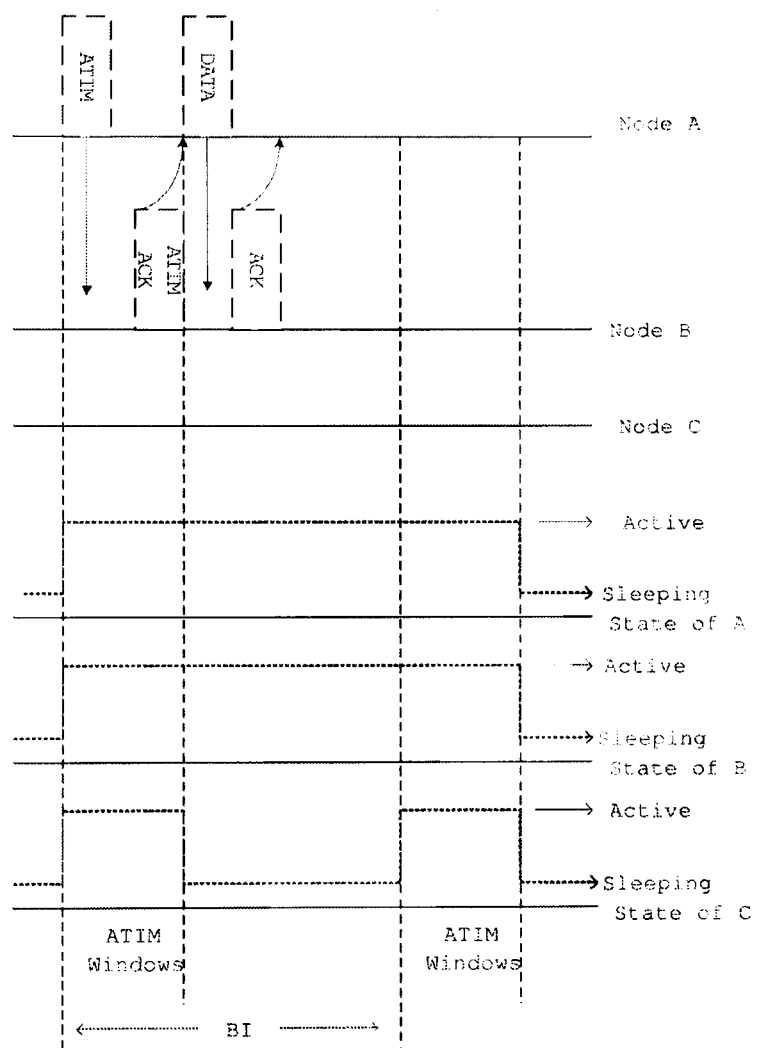
Figure 2.1: IEEE 802.11 ower Save Mode(PSM) [38]

2.1.1 Power save mechanism in IEEE 802.11

The IEEE 802.11 Power Save Mechanism (PSM) [38] is the foundation for other Multilevel States Power Saving (MSPS) protocol. All the nodes in the network are assumed to be synchronised and awake at the beginning of each Beacon Interval (BI). Then each node stays *on* during the Ad-hoc Traffic Indication Message (ATIM) window, which is a fixed duration of each BI. All nodes listen during the ATIM period, and a node which wants to transmits packets, sends an ATIM packet to the destination node. The destination node responds by sending an ATIM-ACK packet back. If the handshake is successful, both nodes stay in the transmitting/receiving state after the ATIM duration, and send/receive their data packets before the ATIM duration of the next BI. Other nodes, which do not send (and reply to) the ATIM packet, are put into the sleeping state after the ATIM duration until the next BI. As shown in Fig. 2.1, Node A sends an ATIM to node B during the ATIM period, and node B replies through ATIM-ACK, then they are put into the *ON* state and send/receive data packets after the ATIM until the next BI. Node C, not sending or receiving any ATIM packets, returns to the sleeping state till the next BI. Therefore, the power of node C is saved.

2.1.2 Delay Degradation in MSPS

MSPS approaches may induce a delay degradation in the network. The work in [39] analyses the impact of delay performance with on-demand routing in an ad-hoc Network Power Saving Mode (AHNPSM).

In [39], a probability model for nodes contending in the ATIM window was proposed. As shown in Fig. 2.2, N nodes contend to transmit ATIM packets during the ATIM window (W_A period, where W_A is the total period of ATIM window). Assuming the first successful transmission occurs at time slot m_1, then $N - 1$ nodes continue contending for the next successful transmission during the remaining $W_A - m_1 - T_{ATIM} + 1$ period, where T_{ATIM} is the size of ATIM packet. This contending procedure continues till the end of ATIM window. The numerical results given in [39] are summarised in Table. 2.1, and these have impact on the

Number of nodes	Increases
Successful RRP transmission rate	Decreases
Average end-to-end delay of RRP	Increases
Average successful route discovery time	Increases

Table 2.1: Impacts of Power Saving Mechanism (PSM)
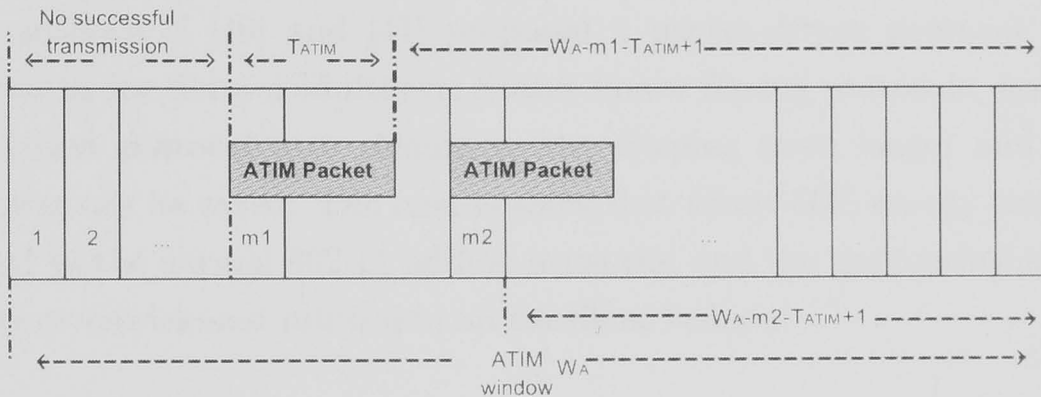
Figure 2.2: ATIM packets contending [39]

route discovery procedures thus degrading the delay performance, especially in large-scale ad-hoc networks.

2.1.3 Packet-driven Mechanism in MSPS

To get improved power saving performance based on MSPS protocols, both reducing the listening period and prolonging the sleeping period can be considered. Packet-driven mechanisms are among the approaches used to control these periods.

Two related concepts are introduced first [40]:

Time-driven mechanism: idle nodes remain in the sleeping state most of the time and wake up periodically to listen if there are packets waiting to send or receive.

Packet-driven mechanism: this mechanism drives all the irrelevant neighbouring nodes into a sleeping state when two nodes communicate and wakes them up

after the current data exchange has finished.

Most protocols based on IEEE 802.11 PSM implement the time-driven mechanism. This mechanism requires synchronisation for all the nodes to enable periodic wake up. This makes it difficult to use time driven mechanisms in large scale networks. The power saving performance becomes poor when there are many flows in the network [40]. Compared to the time-driven mechanism, the packet-driven mechanism does not need global synchronisation and the power saving performance is not a function of the number of flows in the network.

The authors of [40] and [41] proposed a packet-driven protocol for PSM. Compared to the normal Multilevel States Power Saving protocols, nodes in the Packet-driven protocol may remain in the sleeping state longer and therefore more power can be saved. The results show that about 60% energy can be saved compared to the normal 802.11 ad-hoc networks, and the approaches introduced can support on-demand routing in an excellent fashion.

2.1.4 Multiple Wake-up Frequency in MSPS

To keep nodes in the sleeping state longer to save power, nodes can employ a different wake up frequency, which is the key point discussed in this subsection. In [42], a k-frequency protocol was proposed, including a link layer protocol to provide k-frequency power saving levels and a routing protocol related to this link layer protocol. Different wake up frequencies impact the delay performance differently, thus this k-frequency protocol provides k different energy-delay tradeoffs and is classified as below:

PS0 consumes the most power with all the nodes always on, and has the lowest delay; PS1, which corresponds to the fundamental 802.11 PSM model, consumes less power than PS0 and nodes wake up for every ATIM window and sleep for the remainder of the beacon interval if they are not used. Its delay is higher than PS0. PS2 consumes less power than PS1 and nodes wake up every two ATIM windows and sleep for the remainder of the beacon intervals if not used, hence the delay is higher than PS1. Therefore the PS (k-1) level consumes the least amount of energy but has the highest delay. A four levels example shown in Fig. 2.3. This protocol is applied by considering an application-defined delay bound and trying
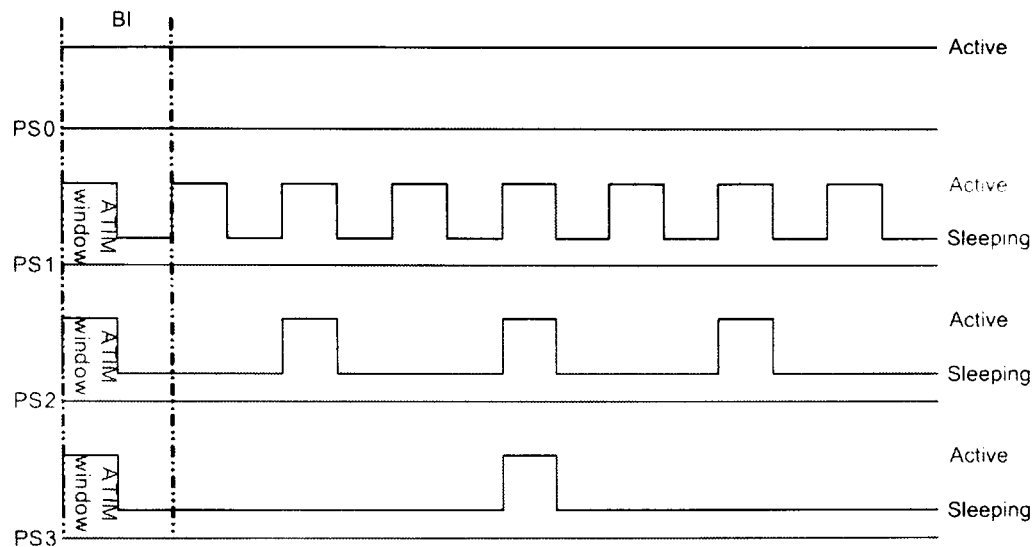
Figure 2.3: Four-level example

to find a route to achieve the delay bound and the power efficiency. A timer is set in the destination node after it receives the first RREQ which represents Route REQuest, and the timer expires after a specified delay time. All RREQs with the same sequence number from the source node are received and the destination node evaluates all the routes and then sends a RREP (which represents Route REPly) along the 'best' route according to the desired delay metric. For each route collected during the timer period at the destination node, the node whose energy consumption will decrease the most will be moved to the high power saving sate (or the node whose energy consumption will increase the least will be moved to the lower power saving state). This algorithm is iterated until the desired delay is obtained or all the nodes are not in any power saving state. The work in [42] uses an adaptive sleeping technique that allows nodes to adjust their sleeping interval in response to the desired delay of the data being forwarded.

2.1.5 Other work related to Multiple power consumption states control

The control of Multiple power consumption states is one of the key approaches for power saving in ad-hoc wireless networks, and the main concept behind this

approach is to put as many nodes as possible into a sleeping state for as long as possible.

As mentioned before, IEEE 802.11 PSM [38] is the foundation for the MSPS protocol. This work was extended in [39], [40–42]. The work in [39] proposed a routing protocol based on PSM to reduce the energy consumption and the transmission delay. In [40], [41] packet-driven mechanisms are introduced to induce sleep and wake-up modes in the nodes, which saved about 60% energy compared to the normal PSM. A multi-frequency wake-up mechanism is proposed in [42] where the nodes utilise different sleeping durations.

Furthermore, based on the fundamental work of IEEE 802.11 PSM [38], the research carried out in [43–48] analyses energy efficiency and related performance. A traffic shaping protocol to improve the performance of normal PSM is proposed in [43] where the sleeping state is prolonged by shaping the unexpected traffic packets (only few packets during a nearly empty duration). It is shown in [43] that about 83% energy can be saved by using the proposed traffic shaping protocol. The work in [44] and [45] try to avoid nodes being out of synchronisation and isolated. In [46–48], the PSM protocol is extended to fit multi-hop Mobile Ad-hoc Networks. There is other research work [49–61] based on PSM.

2.2 Transmission range adjustment

In ad-hoc wireless networks, to get an acceptable QoS (Quality of service), the SINR (signal-to-interference-plus-noise power ratio) at the receive end must be higher than a minimum threshold. In an end-to-end transmission, this acceptable SINR corresponds to an acceptable radio range of the source node. Furthermore, this acceptable radio range depends on the interference environment, the path loss factor, and the source node power. Unfortunately, in battery powered ad-hoc wireless networks, the batteries of nodes will be drained out quickly if the nodes always operate at a high power level, which corresponds to a large radio range. Thus, an adjustable radio range might be another approach to save power, which has been the focus of numerous studies.

For a multi-hop end-to-end transmission, the total energy consumed from a source node to a destination node increases as a function of both the number of relaying nodes and each individual node's radio range. Nodes consume energy in a nonlinear fashion with radio range (usually the attenuation exponent in d^n is $2 \leq n \leq 4$). Therefore, if the number of hops is small (i.e. each individual radio range (hop distance) is large), the energy consumed for one transmission increases nonlinearly. Alternately, if the hop distance is short (for the same overall end-to-end distance), the energy consumption will be dominated by the electronic energy cost in the transceivers and therefore the total energy increases almost linearly as a function of hop number (where the hop number is large). Clearly, there is a trade off between hop number and radio range of each hop to achieve optimal energy efficiency. Furthermore, for high-density deployment ad-hoc networks, if the radio range of a node increases, more nodes will be covered as neighbour nodes. Therefore, with multiple power consumption states control, more spare nodes can be turned into a sleeping state and the power associated with these nodes is saved.

2.2.1 Broadcasting protocols with transmission range adjustment

Broadcasting (flooding) is one of the basic communication methods in ad-hoc wireless networks, where a message from one source node is transmitted to every node of the networks through single-hop communication (if within radio range) or multi-hop communication. The easiest way for broadcasting is for every node to relay the message once to cover the whole network, which is called blind flooding. Clearly, nodes with blind flooding will generate a lot of extra packets, even when their neighbours have already received this message from other nodes, hence, a large amount of energy is wasted. A popular approach to solve this redundant relay problem is to choose a set of back bone nodes to cover the whole network, while the other remaining nodes just receive the broadcast message.

In [62], a network is divided into different numbers of homogenous hexagonal cells, where different cell sizes represent different node radio ranges. If the dis-

tance between two vertices of one hexagonal is r. which also represents the radio range of nodes. the number of cells can be calculated as

$$n_c = \frac{network\ area}{cell\ area} = \frac{A_n}{A_c} = \frac{A_n}{\frac{3}{2}r^2\sqrt{3}}. \tag{2.1}$$

To cover the whole network using a radio range r. 6 nodes. who act as a broadcasting relaying back bone, need to be set at the vertices of each cell. since each vertex is shared by three hexagonal cells, then the total number of back bone nodes in the network is [62]

$$n_b = \frac{6}{3}n_c = \frac{4A_n}{3r^2\sqrt{3}}. \tag{2.2}$$

In this model, the energy consumption for broadcasting is

$$E = n_b(r^n + c_t + c_r(d_r + 1)), \tag{2.3}$$

where n is the environment attenuation factor ($2 \leq n \leq 4$). c_t and c_r are constant energy consumption values for the transmitter/receiver electronics (including signal processing), d_r is the number of neighbour nodes who can receive the broadcasting message from each backbone node and $+1$ represents the message will be received by that backbone node, $d_r = d\pi r^2$. where λ is the node density of the network. Then the total energy consumption is

$$E = \frac{4A_n(r^n + c_t + c_r(\lambda\pi r^2 + 1))}{3r^2\sqrt{3}}. \tag{2.4}$$

To determine the radio range that results in the minimum energy consumption set the derivative of Equation 2.4 equal to zero, By computing. resulting in

$$r = \sqrt[n]{\frac{2c_t + 2c_r}{n - 2}}. \tag{2.5}$$

which identifies the optimal radio range for the nodes of this network to get the minimum energy consumption with this backbone broadcasting approach.
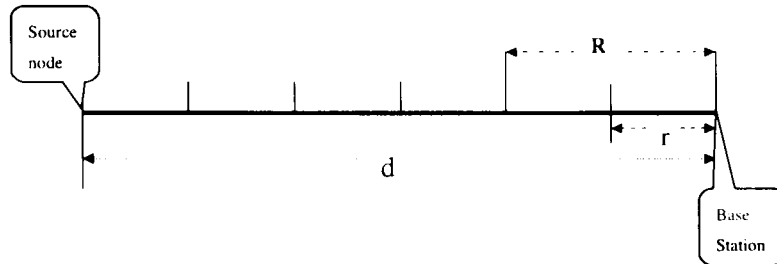
Figure 2.4: One dimensional network with fixed traffic

2.2.2 Linear Network with transmission range adjustment

A linear network was proposed in in [63]. Both equal grid and adjustable grid Geographic Adaptive Fidelity models were studied in [63]. Assuming the distance between the source node and the base station is L and the static traffic generated by the source node is A Erlang, which needs m hops to reach basestation (sink node), B is the channel bit rate. The power consumed by this communication is [63]

$$Power = \sum_{i=1}^{i=m}[c_r BA + c_e BA + c_a(2r_i)^n BA + cc_r(1 - 2A)B].\qquad(2.6)$$

By using the Jensen's Inequality, minimisation of $Power$ can be achieved when the grid sizes are equal $r_i = \frac{L}{m}$, which represents an equal grid linear network model, as shown in Fig. 2.4. Note that the transmission range R is $2 \times r$ (grid size), and the hop number $m = \frac{L}{r}$. Therefore,

$$Power = \frac{L}{r}[c_r BA + c_e BA + c_a(R)^n BA + cc_r(1 - 2A)B].\qquad(2.7)$$

The minimum of $Power$ can be determined when $\frac{\partial Power}{\partial r} = 0$, while the value of the optimal grid size r_{opt} can be determined as well. $\frac{\partial Power}{\partial r}$ and the r_{opt} are given below [63].

$$\frac{\partial Power}{\partial r} = Lc_a(n-1)2^n r^{n-2}BA - ((c_r + c_e)BA + cc_r(1 - 2A)B)Lr^{-2}.\qquad(2.8)$$

$$r_{opt} = \frac{R_{opt}}{2} = \sqrt[n]{\frac{(c_r + c_e)A + cc_r(1 - 2A)}{2^n A(n-1)c_a}}\qquad(2.9)$$

Clearly, there is a relationship between the optimal grid size r and static traffic (A). With typical values of all the parameters, where $c = 1$, $n = 2$, $e_t = 50 \times 10^{-9}$ J/bit, $e_r = 50 \times 10^{-9}$ J/bit, $\epsilon_a = 100 \times 10^{-12}$ J/bit/m^2 (when $n = 2$), and $B = 10kbit/s$ [64], the results in [63] shows the relationship between the network traffic and optimal radio range.

Assuming that the traffic is not static, but is generated by every node, and that all of the information data is to be relayed to the sink node, and if the nodes are uniformly distributed and the node density is λ and each node produces a Erlang traffic, then the traffic in the ith grid is [63]

$$A_{ti} = (L - (i-1)r)\lambda a$$
$$A_{ri} = (L - ir)\lambda\alpha. \tag{2.10}$$

Thus, with this network traffic and the same typical value of the parameters, the total energy consumption for the equal grid linear network model can be calculated as [63]

$$P = 4e_{t_a}L^3\lambda\alpha B[\frac{1}{2m} + \frac{a}{2m^2}] + me_r B. \tag{2.11}$$

Next, the work in [63] focus on the the adjustable grid linear network with the same variable network traffic scenario studied. According to the relationship between optimal grid size and network traffic (Equation 2.9), the optimal grid size will vary in response to the variable network traffic. According to this relationship and the network traffic in the 1st grid, which is shown in Fig. 2.5, the optimal radio range of nodes in this grid can be calculated, thus the optimal grid size can be determined ($r_1 = R_1$). Note that the traffic in the ith grid is [63]

$$A_{ti} = (L - r_1 - r_2... - r_{i-1})\lambda a$$
$$A_{ri} = (L - r_1 - r_2... - r_i)\lambda a. \tag{2.12}$$

By repeating the same procedure of calculating the optimal radio range in the 1st grid, the optimal radio range in the 2nd grid can be calculated. From the relationship between optimal radio range and optimal grid size in the ith grid, which is $R_i = r_i + r_{i-1}$, the optimal grid size of the 2nd grid can be calculated. Thus all of the optimal grid sizes can be calculated in a similar manner. As a
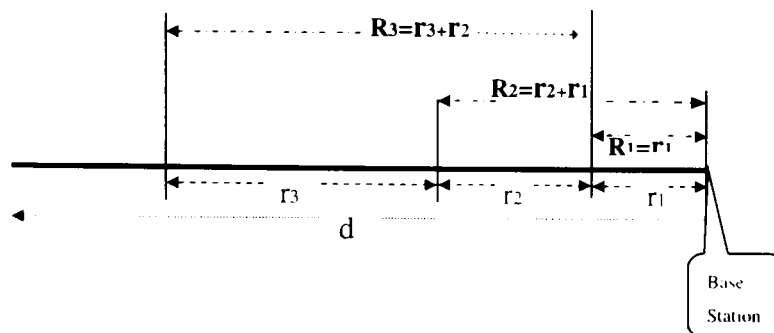
Figure 2.5: One dimensional network with variable traffic

result the total energy consumption in the adjustable grid linear network can be calculated. The results in [63] show that about 50% energy is saved by this adjustable grid model, compared to the minimum energy consumption of the equal grid model.

2.2.3 Clustering-based Model with transmission range adjustment

In ad-hoc wireless network, especially sensor ad-hoc wireless network, nodes can be clustered according to location information to save energy by keeping only cluster heads in active states. These cluster heads act as a backbone to relay the data for other nodes, while other nodes are turned into sleeping state to achieve energy efficient.

The authors of [65] proposed an LW rectangular network model, where the node density is λ $nodes/m^2$ and all nodes in the network use the same radio range r ($r < r_{max}$, r_{max} is the maximum radio range of nodes). This model considers a small time interval (T) scenario, and assume that all nodes are either in the active states (transmitting, receiving, and sleeping state) or in the sleeping state. The active nodes act as a communication backbone (cluster headers). Although these backbone nodes are rotated according their residual energy, however they are assumed not to change in the time T interval. It is also assumed that, in the T interval, every node in the sleeping state spends a fraction of time (s, $0 < s < 1$) in active states, which means these sleeping nodes will spend an sT interval in

active states. s represents how often a node is woken up from the sleeping state. and is determined by the MSPS protocol. In this model, nodes consume different energy when they are in these four different MSPS states. and the total energy consumption of the network is determined by the time distribution among these four states of all nodes in the network. which can be expressed as [65]:

$$T_t = \sum_{i=1}^{N} t_{t_i}, \quad T_r = \sum_{i=1}^{N} t_{r_i}$$

$$T_l = \sum_{i=1}^{N} t_{l_i}, \quad T_s = \sum_{i=1}^{N} t_{s_i}. \tag{2.13}$$

where i represents the ith node of the network and N is the number of nodes of the network ($N = WL\lambda$). Therefore the total energy consumption of the network is [65]

$$E = e_t T_t + e_r T_r + e_l T_l + e_s T_s, \tag{2.14}$$

where e_t, e_r, e_l, e_s respectively represent the energy consumption per unit time. and $e_t = e_e + e_a r^n$ ($2 \leq n \leq 4$), $e_r = e_e + e_p$. $e_l = e_e$, where e_e is the energy consumption for electronics of transceivers; e_a is the energy consumption of the amplifier; e_p is the energy consumption associated with the receive-processing: n is the attenuation factor. According to [66], e_s and e_p is very small (assume to be 0). Thus, $e_t = e_e + e_a r^n$ ($2 \leq n \leq 4$), $e_r = e_l = e_e$. $e_s = 0$. The number of active node (N_a) is a function of the network area (LW) and node radio range (r). $N_a = \frac{LW}{h\pi r^2}$, where h is a coefficient determined by the clustering algorithm. Therefore, $\frac{1}{h}$ represents the average number of neighbours of an active node. In particular, the optimal number of active nodes is $N_a = \frac{LW}{\sqrt{3}r^2}$. when the network area is divided into r sized hexagons and each active node covers $2/3$ of the hexagon area. The model in [65] uses some parameters to derive the network energy consumption. The time to transmit/receive a packet (t_p). $t_p = \frac{l}{R}$. where l is the packet length and R is the data transmission/reception rate. H is the average hops of a packet. λ is the average number of packets relayed by each active node. d is the estimated distance between source and destination node. N_p

is the number of packets passing through the network during the time interval T, and $P = \mu W T$, where μ is the traffic density per second per meter. Therefore

$$PH = N_a \lambda. \tag{2.15}$$

Assume

$$PHr = PJ\delta. \tag{2.16}$$

where $J\delta$ is the average path length between source and destination nodes, and δ is the coefficient determined by the clustering algorithm. Thus, the average number of packets relayed by each node (θ) is a function of the traffic and radio range, which is given below [65]

$$\theta = \frac{h\pi T J\delta W \mu r}{A}. \tag{2.17}$$

In this network model, the average time periods associated with each active node states are [65]

$$\bar{t}_{at} = \theta t_p$$
$$\bar{t}_{ar} = \frac{\theta}{h} t_p$$
$$\bar{t}_{al} = T - \theta t_p - \frac{\theta}{h} t_p$$
$$\bar{t}_{as} = 0, \tag{2.18}$$

where $\frac{\theta}{h}$ represents, for an active node, the average number of packets it receives from its neighbouring active nodes. Furthermore, for sleeping nodes, assume they only receive some overheard packets from the active nodes, during the sT time period. Then the average time periods of each state of the sleeping nodes are [65]

$$\bar{t}_{st} = 0$$
$$\bar{t}_{sr} = \frac{s\theta}{h} t_p$$
$$\bar{t}_{sl} = sT - \frac{s\theta}{h} t_p$$
$$\bar{t}_{ss} = T(1 - s). \tag{2.19}$$

Using the results above. the average energy consumption rate (energy per second per unit area) is [65]

$$E_r = \frac{E}{LWT} = \frac{e_a t_p \delta d}{L}\mu r^{n-1} + \frac{s e_p t_p \theta \pi \delta d}{L}\mu r + \frac{(1-s)\epsilon_p t_p \theta \pi \delta d}{hL}\mu r^{-1}$$
$$+ \frac{(1-s)(e_e - e_s)}{h\pi}r^{-2} + \epsilon_s \theta + f(\epsilon_e - \epsilon_s)\theta. \quad (2.20)$$

Therefore, to get the optimal r which corresponds to the minimum E_r. the derivative of E_r is set to 0. where the optimal radio range is a function of the traffic density (μ), which is given below

$$r_{opt} = \sqrt[1+\theta]{\frac{2L(1-s)(\epsilon_e - \epsilon_s)}{e_a(\theta-1)t_p dh\pi\delta}\frac{1}{\mu}}. \quad (2.21)$$

The work in [65] simulated this model. and the simulation results almost match the analytic results. This model shows us how to calculate the optimal radio range for energy efficiency, and the analysis results show that the optimal radio range is only a function of the traffic density (μ), and is not related to the node density (θ). The reason of this relates to the assumptions behind this model. ie the nodes in the network just receive or relay the traffic packets. In practice nodes also generate traffic in a real scenario, and in this case the optimal radio range will also be a function of node density (θ).

2.2.4 Transmission range adjustment

A Multipoint Relay Protocol has been proposed by the authors in [67] based on the optimal transmission range to reduce the number of transmissions. Optimised Link State Routing has been proposed in [68]. a Neighbour Elimination Scheme is independently proposed in [69] and [70], all result in reducing the quantity of transmission in ad-hoc networks.

Algorithms are proposed either for general topology control purposes [71]. [72] or for special tasks [73]. [74]. e.g. routing. data gathering. and broadcasting. The objective of energy saving is usually achieved by computing the best transmission range based on geographic information and the energy model. The work in

[75] proposes a quantitative analysis model for the optimal transmission range problem in this category. They use throughput and throughput per unit energy as the optimisation criteria and conclude that the optimal transmission power is determined by the network load, the number of nodes, and the network size.

The work in [71] and [76] studied the optimisation of radio transmission range in wireless networks. In [76], the optimal transmission range that maximises the expected packet progress in the desired direction was determined for different transmission protocols in a multihop packet radio network with randomly distributed terminals. The optimal transmission ranges were expressed in terms of the number of terminals in range. It is found that the optimal transmission radius for slotted ALOHA without capture capability covers on average eight nearest neighbours in the direction of the packet's final destination. The study attempted to improve the system throughput by limiting the transmission interference in a wireless network with heavy traffic load. A distributed position-based self-reconfigurable network protocol that minimises energy consumption was proposed in [71].

A similar assumption was made in [77], even though the node density was only considered in the analysis of the energy consumption of overhearing nodes. The work investigated the problem of selecting an energy-efficient transmission power to minimise the global energy consumption of ad-hoc networks. It was concluded that the average neighbourhood size is a useful parameter in finding the optimal balance point. The authors in [78] studied the optimal transmission radius that minimises the settling time for flooding in large-scale sensor networks. In the paper, the settling time was defined as the time when all the nodes in the network have forwarded the flooded packet. Regional contention and contention delay were then analysed. A bit-meter-per-joule metric for energy consumption in wireless ad-hoc sensor networks was investigated in [79]. The paper presented a system-level characterisation of energy consumption for sensor networks. The study assumed that the sensor network has a relay architecture, and all the traffic is sent from sensor nodes towards a distant basestation. Also, it was assumed that the source always chooses, among all relay neighbours, the one that has the lowest bit-meter-per-joule metric to relay its data packets. In the analysis, the power efficiency metric in terms of average watt per meter for each radio

transmission was first calculated, and was then extended to determine the global energy consumption. The analysis revealed how the overall energy consumption varies with transceiver characteristics. node density, data traffic distribution, and base-station location.

Based on the optimal transmission range, the authors in [80] proposed two energy efficient broadcasting protocols, with and without taking into account the energy consumed for reception. The work in [81] and [82] analysed the energy distribution and proposed a routing mechanism based on the location of nodes in linear wireless sensor networks. Note that, the network traffic is determined by the location of nodes in the models in these papers, therefore, the nature of the work in [81] and [82] is based on the relationship between the network traffic and the transmission radio range. The results show that the energy consumption can be balanced and that the bottleneck associated with the network lifetime can be relaxed. It was found in [83] that a higher throughput can be obtained by transmitting packets to the nearest neighbour in the forward direction. In [84], the authors evaluated the optimum transmission ranges in a packet radio network in the presence of signal fading and shadowing.

Although methods that can improve energy efficiency have been discussed, note that there are other performance metrics that should be considered at the same time, such as network connectivity, network capacity, and routing bounds. The work in [85] investigated the impact of these performance metrics in both fixed-range and variable-range ad-hoc networks and compared them. In fixed-range networks, high transmission power (long radio range) will increase the connectivity of the network and reduce the number of relay nodes between the source and destination nodes, which will benefit routing protocol by providing multiple routes and reducing the signalling overhead (contains the dynamic route information). Unfortunately, a high transmission power creates excessive environmental interference seen by other potential receivers, therefore, decrease the network capacity. For low transmission power, the network connectivity decreases and the number of relay nodes between the source and the destination nodes increases, thus the routing protocol is affected by reducing the number of routes and increasing the size of signalling overhead. Note that, the transmission power

must be higher than a threshold which guarantees no network partitions. Furthermore, a low transmission power will reduce the environmental interference to other receivers thus improves the network capacity. Energy efficient performance is a trade off between individual radio range and hop number, which has been discussed earlier.

2.3 Topology management and Routing algorithms

Topology management and routing protocols are an alternative (third) approach to save energy in ad-hoc wireless networks. The first two approaches can be utilised together in the topology management and routing algorithms.

2.3.1 Fundamental Routing Algorithms in Ad-hoc wireless networks

Unlike Internet routing, routing in ad-hoc wireless networks has its own specificities. First, most of the nodes in the network are battery powered, therefore the energy is limited. Second, the topology of ad-hoc networks are dynamically changing, therefore the information routes are dynamically changing. As mentioned before, single-hop communication is not energy efficient and has limited applications, while with multi-hop communication nodes can communicate with other nodes, even if they are out of transmission range, through intermediate nodes. Note that, most multi-hop routing protocols consider only minimum hop number in the selection of the shortest-path, but more and more attention is being paid to energy efficient multi-hop routing. Intuitively, energy efficient routing algorithms should focus on how to find the minimum energy cost routing paths. However, even when the minimum energy path is found, if the communication within the network always chooses this most energy efficient path, the relay nodes in this path will exhaust their energy rapidly, and therefore network partitioning might occur. Furthermore, if some important nodes are heavily selected for different routes by some routing algorithm, the energy of these nodes will be drained out quickly. The network lifetime can end prematurely if one or some

nodes are drained out. To avoid this problem, a threshold of remaining energy can be applied by the routing algorithm, where if the remaining energy of one node is under the threshold, this node is not selected as an intermediate node. Furthermore, this node may only process its own functions, such as collecting data, and operate its own transmission tasks. Thus, the network lifetime can be prolonged.

There are three main categories of multi-hop routing protocols in ad-hoc wireless networks: flooding, proactive routing and reactive routing. Flooding routing has the advantage of being highly robust to changing network topologies and requires little routing overhead. In fact, in highly mobile networks flooding may be the only feasible routing strategy. The obvious disadvantage is that redundant copies of the same packet are received and transmitted throughout the network, which wastes both network bandwidth and the power of the transmitting nodes. Therefore flooding routing is only suitable for very small networks, and its energy performance is not good. Proactive routing include both centralised routing and distributed routing. In centralised routing, information about channel conditions and network topology determined by each node is forwarded to a centralised node or a basestation that computes the routing tables for all nodes in the network. The optimal routes can be computed depending on the optimisation criterion, such as minimum average delay, minimum hops number, or minimum energy consumption. This minimum energy consumption can be the minimum energy consumption of the whole network, or can be defined according to the individual nodes, especially the important busy nodes. Obviously, this routing algorithm cannot adapt to rapid changes in the channel conditions or network topology. Thus, this algorithm is typically used in very small networks. Distributed route computation is the most common routing procedure used in ad-hoc wireless networks. In this protocol nodes send their connectivity information to neighbouring nodes, and then routes are computed from this local information.

Proactive routing requires fixed routing tables that must be updated at regular intervals, which is not suitable for large networks or rapidly changing-topology networks. Reactive (on-demand) routing does not need routing tables and it only creates routes at the request of a source node that has traffic to send to a given

destination. Therefore it is suitable for large scale networks and rapidly changing-topology networks. This eliminates the overhead of maintaining routing tables for routes not currently in use. Normally, reactive routing needs to discover routes first then maintain these routes until the transmission ends. The disadvantage is that reactive routing can result in significant delay since the route discovery process is initiated when there is data to send, but this data cannot be transmitted until the route discovery process has finished.

Ad-hoc wireless networks, especially sensor networks, usually have a high node density, a large scale and their topology changes rapidly, therefore reactive routing is widely applied in ad-hoc networks. Thw work in [86] discusses and compares the four most popular routing protocols in multi-hop wireless ad-hoc networks, which are Destination-Sequenced Distance Vector (DSDV), the Temporally-Ordered Routing Algorithm (TORA), Dynamic Source Routing (DSR), and Ad-hoc On-Demand Distance Vector (AODV).

2.3.2 Dynamic Source Routing (DSR) algorithms

Most traditional routing protocols use a 'minimum hop number' algorithm without considering the energy efficiency. The work in [87] proposed a DSR energy saving protocol, called ESDSR (Energy Saving DSR), to maximise the lifetime of an ad hoc network.

The DSR protocol includes two main procedures: route discovery and route maintenance, where the mechanism of route discovery is introduced in Algorithm 2.1. For route maintenance in DSR, each node relays DATA according to the routes table decided in the route discovery procedure, and each node receives an ACK from its next relay node after successfully transmitting a DATA to its next relay node. If a node cannot receive an ACK after transmitting DATA, a route BROKEN conclusion is reached. The source node then tries to find another route from its route cache. If no alternative route can be found in the route cache, the source node retries another route discovery procedure.

The ESDSR algorithm in [87] defined an 'expected life' parameter (N_l) for

RREQ: include SEQUENCE NO., NODE LIST

SEQUENCE NO.: unique number for each RREQ

NODE LIST: contain the routes information

RREP: NODE LIST

For different kind of nodes:

Source nodes

    IF (have task)

        broadcast the RREQ

    ELSE IF (receive RREP)

        send data packets with NODE LIST appended

Intermediate nodes

    IF (receive the first RREQ)

        add itself to NODE LIST

        rebroadcast RREQ

    ELSE IF (receive RREP)

        relay RREP according to NODE LIST

    ELSE IF (receive data packet)

        relay data packet according to NODE LIST

    ELSE

        ignore duplicated RREQ

Destination nodes

    IF (receive the first RREQ)

        generate RREP, whose NODE LIST is reversed from RREQ

        send RREP back to source along NODE LIST

    ELSE (receive data packet)

        store and processing

Algorithm 2.1: DSR route discovery mechanism [87]
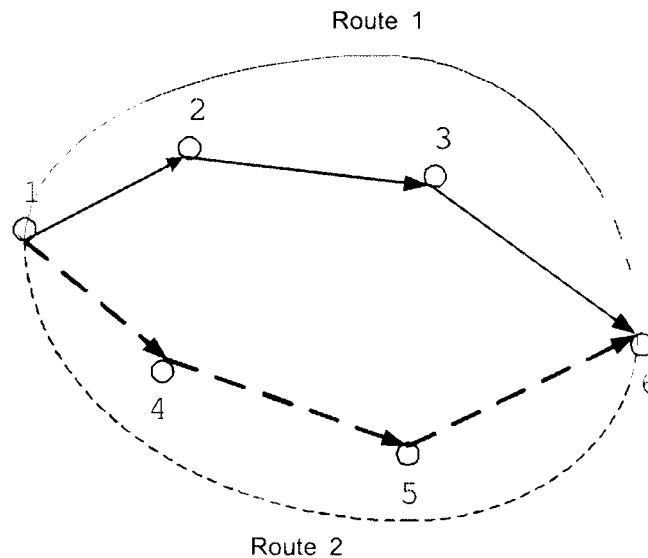
Figure 2.6: ESDSR route selection

every node, given by

$$N_{l_i} = \frac{E_i}{P_{t_i}}, \tag{2.22}$$

where E_i is the remaining energy of node i, and P_{t_i} is the transmit power of node i. The minimum value of N_{l_i} of every node, which supports one route, will determine the 'expected life' of this route (R_{l_j}, 'expected life' of route j). and the route with largest N_{l_i} value will be selected as the route to transmit DATA packets. For example, as shown in Fig. 2.6, assume there are two potential routes for future DATA transmission, and the remaining energy and transmit power of each node are known. thus the 'expected life' (N_{l_i}) can be calculated. Assume $N_{l_1} = 0.5$. $N_{l_2} = 0.4$. $N_{l_3} = 0.2$, then the 'expected life' of route 1 is 0.2. Furthermore, assume the 'expected life' of route 2 is 0.1. then route 1, whose 'expected life' value is larger. will be selected to transmit the DATA packets. This route discovery mechanism chooses the high energy life route to balance the lifetime of every route and thus prolong the lifetime of the network. ESDSR also proposed a mechanism to improve the energy saving performance during the route maintenance duration (DATA transmission duration). In general. the received power must be larger than a threshold value (P_{thr}) to ensure that the DATA has been successfully received. In ESDSR. during the first DATA transmission after the route has been determined. the transmitter or relay node attaches a transmit

power (P_t) value to the DATA packet and then transmits the DATA packet to the next relay node or destination node. The next relay node or the destination node attaches to the DATA packet a value when the packet has been received (P_r). The future minimum transmit power of the transmitter or the relay node can then be calculated.

$$P_{min} = P_t + P_{thr} - P_r. \tag{2.23}$$

To tolerate the environment induced fluctuations, a power margin (P_{tol}) is added to the minimum transmit power (P_{min}), which then becomes

$$P_{min} = P_t + P_{thr} - P_r + P_{tol}. \tag{2.24}$$

With this transmit power minimisation mechanism, the nodes energy along the route can be saved. The simulation results in [87] indicate that, compare to normal DSR with the same node battery capacity, about 20% more packets can be transmitted to the destination node.

2.3.3 Ad-hoc On-Demand Distance Vector (AODV) algorithms

An energy efficient route discovery mechanism based on the AODV routing protocol is proposed in [88]. It uses the characteristics of transceivers and channels to analyse the power saving performance of its model.

In this model, the received signal power is calculated as

$$P_r = \frac{P_t G_t G_r \lambda^2}{(4\pi)^2 d^2 L} . d \leq \frac{4\pi H_r H_t}{\lambda}$$
$$P_r = P_t G_t G_r \frac{H_r H_t}{d^2} . d > \frac{4\pi H_r H_t}{\lambda}. \tag{2.25}$$

where P_t is the transmit power, P_r is the receive power, G_t and G_r are the antenna gains at the transmitter and receiver, H_t and H_r are the heights of the antennas of the transmitter and receiver, L is the system loss factor, λ is the carrier wavelength, and d is the distance between transmitter and receiver.

The energy consumption of this algorithm is composed of energy consumed for route discovery (transmission of Rout REQuest (RREQ) and Route REPly

(RREP) packets) and data packets transmission. respectively. The two energy consumption terms between nodes i and j is

$$E_{i,j}^{data} = \frac{(P_t + P_r)L_{data}}{(1 - er)f_{data}}$$

$$E_{i,j}^{dis} = \frac{(P_t + P_r N_{area(i)})L_{dis}}{f_{dis}}. \tag{2.26}$$

where L_{data} and L_{dis} are the packet-lengths of data packets and route discovery packets, $N_{area(S)}$ is number of neighbour nodes within the coverage of transmit node i, f_{data} and f_{dis} are transmission bit rates of the data and the route discovery packets, er is the packet error rate over the link between these two nodes, which can be calculated as $er = 1 - (1 - BER)^l$. l is the packet size and BER is bit error rate from $BER \propto erfc(\sqrt{cSNR})$, $SNR = 10\log(\frac{P_r}{noise})$. Thus, the total energy cost between the source and destination nodes is

$$E_{sd}^{total} = \sum(E^{data} + E^{dis}). \tag{2.27}$$

Unlike normal AODV, the algorithm in [88] selects the route with minimum energy consumption (E_{sd}), and the simulation results show that about 12% energy has been saved compared to normal AODV.

2.3.4 Other Routing Algorithms

Cluster-based routing algorithms

As mentioned in Section 2.1, MSPS is the basic approach to save power by putting as many nodes as possible into the sleeping state. Clustering-based routing algorithms also achieve power saving performance by turning idle nodes in clusters into the sleeping state. while cluster head nodes act as a relay backbone to forward data on behalf of other normal nodes (non-cluster-head nodes). The work in [64] proposed a Low Energy Adaptive Clustering Hierarchy (LEACH) routing protocol. which is clustering-based. LEACH balances the energy consumption of every node by randomised rotation of cluster heads. which may result in an improper structure. for example a long distance between the head node and its

cluster member nodes, or too many nodes within one cluster. The Maximum Energy Cluster-Head (MECH) algorithm [89] improves the cluster structuring method and extends LEACH in some other aspects. Simulation results show that MECH lasts longer than LEACH before the first node dies.

Bionic routing algorithms

Some research groups have studied power saving routing algorithms based on biologically inspired concepts, such as Genetic algorithms [90], [91], Artificial Neural Networks [92], Immune Algorithms [93] and Ant Algorithms [94], to find the optimal energy saving mechanisms. The work in proposed a power saving routing algorithm, which is called Power Saving Ant Algorithm (PSAA), based on Ant Algorithm, and the simulation results show PSAA is more energy efficient especially when the network topology rapidly changes.

2.3.5 Geographic Routing

Traditional ad-hoc routing algorithms include global, on-demand and hybrid algorithms. Global routing strategies such as distance vector [95], [96] and link state [97], [98] routing protocols are suitable for smaller networks with low mobility, but do not scale well in larger dynamic environments due to the periodic and global dissemination of topology updates. On-demand routing protocols [99–104] use a query response mechanism to discover and maintain routes for individual sessions. However, flooding of route queries limits the performance under conditions of high mobility and high traffic loads. The hybrid approaches [105–108] use a cluster or hierarchical network structure to dynamically group nodes and then applies different routing strategies within and between groups.

Geographic Routing (GR), location/position-based routing, for communication in ad-hoc wireless networks has recently received increased attention, especially in the energy saving area [22], [23], [76], [109–114]. Compared to the non-Geographic routing algorithms, GR does not require maintenance of routing tables or route construction prior to or during the forwarding process. The forwarding process also allows a packet to adapt to changes in the topology by

selecting the next best choice of intermediate nodes. Other benefits include the ability to weight individual next hop choices according to additional metrics. Routes can be altered node by node and packet by packet simply by considering additional QoS related parameters relating to the next hop neighbours, such as delay or available bandwidth [115]. Furthermore, in this thesis, GR algorithms, which aim to reduce the network energy consumption and to prolong the network lifetime, are proposed and studied.

The authors in [116] proposed the Most Forward within Radius (MFR) algorithm to minimise the number of hops. MFR forwards a packet to the neighbour that is the farthest from the source in the direction of the destination within the transmission range. The work in [111] proposed a similar forwarding algorithm, the Greedy Routing Scheme (GRS), which selects the closest neighbour to the ultimate destination among the neighbours. In the above two forwarding algorithms, the transmission range is fixed, and the main goal is to minimise the transmission delay (hop numbers). When nodes have the ability to control the transmission range, additional features can be realised, for example the authors in [112] proposed the Nearest Forward Progress (NFP) algorithm to reduce energy consumption. NFP chooses the closest neighbour to the sender within the forward region. However, note that, with NFP, the energy consumption for each hop is minimised, but the number of hops may be large, which may lead to increasing the total energy consumption. The authors in [113] proposed compass routing, which selects the neighbour that has a minimum angle with respect to the line between the source and the destination. Distance Routing Effect Algorithm for Mobility (DREAM) [117] is another example of this idea. Unlike the most progress within radius scheme, however, a direction-based scheme like DREAM is not necessarily loop free.

In the forwarding algorithms proposed in this thesis, the best forwarding location is computed based on the optimal transmission range, and the node which is closest to the best location is selected as the next forwarding node. Therefore, the energy consumption for the total end-to-end communication is minimised.

Energy saving based on Geographic Routing algorithms has been proposed as well. The authors in [118] proposed the Geographic Power Efficient Routing (GPER) protocol to provide power efficient geographic routing in wireless sensor
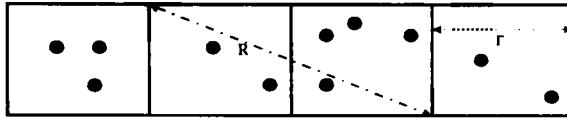
Figure 2.7: GAF virtual grids model

networks. The authors in [119] proposed the Energy-Efficient Geographic Routing (EEGR) protocol, which computes the optimal location of the next hop node and selects the next hop node based on the distance to the optimal location. The ORF forwarding algorithm in this thesis is similar to EEGR, however the best forwarding location of ORF is computed based on the optimal transmission range, and the node which is closest to the best location is selected to be the next forwarding node. Therefore, the energy consumption for the total end-to-end communication is minimised. The authors in [81] and [82] analyse the energy distribution and propose a routing mechanism based on the location of nodes in linear wireless sensor networks.

To prolong the network lifetime, not only the energy consumption should be reduced, but also the energy consumption among nodes should be balanced, which is achieved by balancing the traffic load of each node. The energy-proportional principle (EPP) is one that can achieve a balance under different traffic loads. It originates from the energy-proportional routing principle [120], [121].

2.3.6 Topology management protocols

In the topology management protocols, all nodes are classified into groups or clusters according to their location information, and therefore, the transition to the sleeping state is simple to manage and the communication routes are set up based on local information [21]. Topology management protocols in ad-hoc wireless networks provide a mechanism that can be utilised to achieve energy efficiency, if they are properly designed.

2.3.7 Geographic Adaptive Fidelity (GAF) protocol

In [13], [122], GAF (Geographical Adaptive Fidelity) assumes the nodes have
some location information and form virtual grids. The size of the grids is chosen
such that any two nodes in two adjacent grids are able to communicate with each
other, one GAF model is shown in Fig. 2.7, where R is the girds size and r is the
nodes transmission range. Within each grid, a protocol tries to ensure that most
of the time one node remains active to forward information while the rest enter
into the sleeping state. Therefore, the delay and energy cost will both be reduced,
but the number of hops will be determined by the gird size. In [13], the authors
analysed and simulated a GAF model based on both Ad-hoc On-demand Dis-
tance Vector (AODV) and Dynamic Source Routing (DSR) routing algorithms.
Compared to the normal AODV and DSR routing in ad-hoc wireless networks,
the GAF assisted ones reduce the energy consumption by 40% and 60%, respec-
tively [13]. Furthermore, their analysis shows that the network lifetime increases
when the node density increases. However, in [13], the GAF virtual grids are
the same size, and the optimal transmission radio range has not been considered.
In [63] the authors proposed a linear network (where the nodes are distributed
along a line) and, based on GAF topology management, analysed both equal and
adjustable grid models. In [63] a relationship between the optimal transmission
range and network traffic is derived in an equal-grid model, which is used to
calculate the grid-lengths and network energy consumption in an adjustable-grid
model. The results in [63] prove that the adjustable-grid model is more energy
efficient than the equal-grid model, but they assume that the energy cost in the
receiving state is only due to electronic consumption, where the energy consumed
for processing data in the receiving state is neglected. Furthermore [63] has not
considered the network lifetime (which is not entirely determined by energy sav-
ing): in the equal-grid model, the energy of nodes in the near-to-sink grids will
be drained much sooner than in the far-from-sink grids. Furthermore, this one-
dimensional linear network cannot represent most realistic ad-hoc networks (two
or three dimensional networks). These aspects are addressed in this thesis.

2.3.8 Other topology management protocols

Apart from GAF [13], [63], [122], [123] protocol introduced above, there are a number of topology management protocols, such as SPAN [14], ASCENT [66], CEC [124] and AFECA [125], STEM [126], TITAN [127] and TMPO [12]. The basic mechanism use in these protocols is that the state of nodes relies on geographic information, and energy is saved when nodes are turned into the sleeping state. Meanwhile, active nodes are selected as the communication backbone of the network. Other research in [128–131] focuses on topology management protocols.

2.4 Other energy saving methods

There are some other power saving methods which are not very connected to ad-hoc wireless networks and are more related to hardware techniques. For example, with directional antennas, data packets can be transmitted in a particular direction, and clearly power can be saved compared to omni-directional antennas. Another example is the better use of coding techniques to decrease the size (compression) of data packet to be transmitted, and/or the use of codes to allow operation at lower SNR levels, and therefore transmit power is saved.

2.4.1 Hybrid ad-hoc wireless networks

Furthermore, to improve energy efficiency in ad-hoc wireless networks, some nodes, which remain stationary and have a permanent power source, may be added to the network. These nodes act as the backbone nodes of the networks and are able to relay data, thus help enhance the network connectivity and power saving in other mobile battery-powered nodes. These networks are defined as semi-infrastructured networks in [132], or as hybrid networks in [133] and [134].

In [134], nodes in the network are classified as agents and clients. Clients are normal mobile ad-hoc nodes, and agents are nodes with permanent power sources. Agents do not generate or sink traffic but simply relay packets from clients. Agents are not randomly distributed, but carefully located for network metrics performance, such as network capacity, network connectivity and network

energy efficiency. Agents can act like a virtual infrastructure that carries the user data across the network. The presence of agents helps clients reduce their transmission power consumption, especially with agent-aware routing methods. The work in [134] also shows that the use of agent-aware routing techniques might cause some throughput degradation, especially for lower agent densities. The work in [135] combines cellular structures and mesh networks to form the backbone of a large sensor network. The sensor network is divided into many equal cells and each cell has a local controller with enough resources at the centre to collect the data and to form the mesh network backbone. The results show that the power consumption in the individual cells is evenly distributed and no areas in the cells run out of energy prematurely.

Although routing algorithms in ad-hoc networks have been classified into three main approaches, these approaches can be combined, usually referred to as hybrid routing algorithms. Some research groups have studied these hybrid routing algorithms to improve the energy efficiency. The authors in [136] proposed a Dynamic Leader Set Generation (DLSG) algorithm, which is a hybrid routing algorithm. DLSG uses leader nodes as the communication backbone of the network and other local nodes communicate with the network through their own leader nodes. In this local communication between a leader node and its normal nodes, DLSG uses proactive routing for local routing. For global routing, DLSG selects leader nodes through the use of reactive routing algorithms. Furthermore, in DLSG, the leader nodes are determined based on the remaining energy, and the leader nodes de-select themselves if their remaining energy falls below some threshold level. Therefore, the energy of every node can be balanced and the lifetime of the network can be prolonged. The results in [136] show that DLSG can prolong the network lifetime by $20 - 50\%$. The work in [137-140] also concentrates on energy saving in hybrid ad-hoc wireless networks.

2.5   Summary

This chapter surveyed the energy saving approaches used in ad-hoc wireless networks. Most of these approaches are classified into three main categories: mul-

tiple power consumption states. transmission range adjustment. and topology management and routing algorithms. In each main energy saving approach. the fundamental concepts have been described. and work related to each approach has been introduced and evaluated. These three main approaches can be combined together to reduce the network energy consumption and prolong the network lifetime. Furthermore, other energy saving methods. such as hybrid ad-hoc wireless network have been discussed.

Chapter 3

Energy Efficient GAF Protocol in Linear Ad-hoc Wireless Networks

3.1 Introduction

The Geographic Adaptive Fidelity (GAF) protocol is one of the topology management protocols use in ad-hoc wireless networks. Based on the nodes' position information, the GAF model divides the network topology into small virtual grids, where any node in each grid can communicate with any node in its adjacent grid. Note that, the GAF model ensures that there should always be one or an optimal set of active nodes in each grid to act as the communication backbone of the network while the remaining nodes enter into the sleeping state to save energy. In this chapter, an energy efficient Geographic Adaptive Fidelity (GAF) protocol is proposed to reduce the energy consumption of a linear ad-hoc wireless network, which is shown in Fig. 3.1, where the grid size is derived based on the optimal transmission range. Furthermore, another adjustable-grid GAF model is derived based on Genetic Algorithms (GA) to improve energy efficiency in linear ad-hoc wireless networks. In this chapter, and in a linear ad-hoc wireless network, network energy consumption models are proposed considering the energy consumed for processing data at the receiver, while a new adjustable-grid model is designed
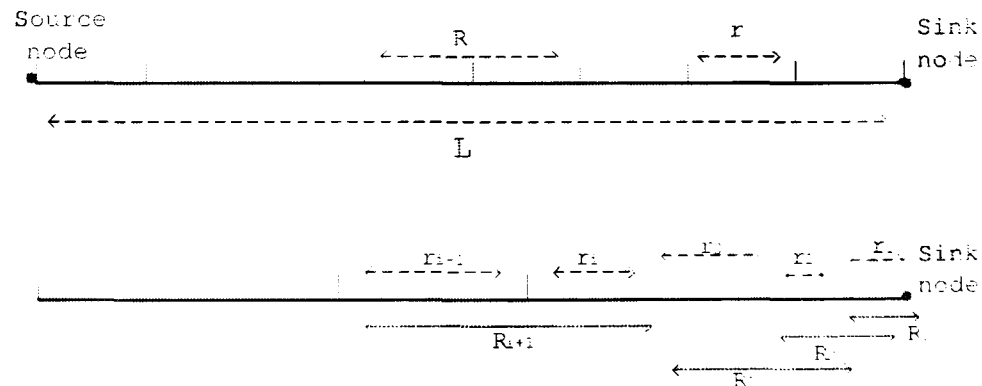
Figure 3.1: Equal-grid and adjustable-grid linear GAF models using Genetic Algorithms.

3.2 Energy consumption model

The energy consumed by ad-hoc wireless network nodes is the sum of the energy consumed for transmitting, receiving and listening. Based on [141] the energy consumed per second by a node in these three states can be respectively calculated as follows:

$$
\begin{aligned}
E_t &= (e_c + e_a R^n) D_t \\
E_r &= (e_e + e_p) D_r \\
E_l &= e_l T_l = e_l (1 - T_t - T_r),
\end{aligned}
\tag{3.1}
$$

where R is the node transmission range; D_t and D_r are the transmitted and received traffic data bits respectively; T_t and T_r denote respectively the time for transmitting and receiving the traffic data of a grid, which can be expressed as follows:

$$
\begin{aligned}
T_t &= D_t / d_R \\
T_r &= D_r / d_R.
\end{aligned}
\tag{3.2}
$$

where d_R is the transmit or receive data bit rate ($bit/second$) of each network node; T_l, which denotes the time spent listening to the radio environment in one second, is: $T_l = 1 - T_t - T_r$, where $0 \leq T_l \leq 1$, thus $0 \leq (1 - D_t/d_R - D_r/d_R) \leq 1$.

For the transceiver design parameters: e_e is the energy/bit consumed by the transceivers electronics, and e_a is the energy/bit consumed in the transmitter RF amplifier, and e_p is the energy/bit consumed for processing in receivers and e_l is the energy/second consumed for listening to the radio environment: e_e, e_a, e_p and e_l are determined by the design characteristics of the transceivers. Based on [64] and [65], the typical values of these parameters are: $e_e = 3.32 \times 10^{-7}$ J/bit, $e_p = 6.8 \times 10^{-8}$ J/bit, $e_a = 8 \times 10^{-11}$ J/bit/m^2 for $n = 2$. where n is the power index of the channel path loss, which is typically between 2 and 4. Since the energy consumption for listening is attributed only to the transceivers electronics.

$$e_l = e_e d_R. \tag{3.3}$$

Note that, the energy consumption model used in this chapter considers the energy consumed for listening. which is not considered in Chapter 3.

3.3 Equal-grid GAF model

As mentioned before, the normal GAF protocol divides the entire network into equal-size grids, which will be discussed in this section as the Equal-grid GAF model. As shown in Fig. 3.1, the nodes are uniformly distributed along the linear network, the length of each grid is r, and the transmission range of nodes. which are uniformly distributed along the network, is R.

3.3.1 Optimal transmission range

To derive the optimal transmission range. the static traffic is considered to be deployed in the equal-grid GAF model. Static traffic refers to a scenario in which the traffic rate flowing along the network is constant. This occurs typically when a source node is outside the network. as shown in Fig. 3.1. where static traffic. denoted by D. is transmitted from a source node to a sink node. In the equal-grid GAF model. L represents the length of the network: r and R represent the grid length and the transmission range of nodes in each grid. respectively. Therefore.

the number of grids, m, is:

$$m = \frac{L}{r} \tag{3.4}$$

and the transmission range (R_i) of nodes in the ith grid is determined by the GAF mechanism (any node in one grid is able to transmit data to any node of its neighbour grid):

$$R_1 = 2r. \tag{3.5}$$

Since the head node forwards the traffic through the network, while other nodes remain in the sleeping state to save energy, the total energy consumed in the ith grid, E_i, is the sum of the energy consumed by the head node in the listening, transmitting and receiving states. Thus, based on equations 3.1, 3.2 and 3.3, the energy consumed in the ith grid is:

$$
\begin{aligned}
E_i &= E_t + E_r + E_l \\
&= (e_e + e_a R^n)D_t + (e_e + e_p)D_r + e_e d_R(1 - \frac{D_t}{d_R} - \frac{D_r}{d_R}) \\
&= e_p D + e_e d_R + e_a R_i^n D. \tag{3.6}
\end{aligned}
$$

Therefore, based on equations 3.4, 3.5 and 3.6, the energy consumed in the entire network can be expressed as follows:

$$E_{total} = mE_i = \frac{L}{r}[e_p D + e_e d_R + e_a(2r)^n D]. \tag{3.7}$$

To compute the minimum energy consumption of the network nodes, we take the first derivative of E_{total} in terms of grid-length, r, and let $\partial E_{total}/\partial r = 0$:

$$\partial E_{total}/\partial r = L[(-e_p D - e_e d_R)r^{-2} + (n-1)2^n e_a D r^{n-2}] = 0. \tag{3.8}$$

Solving equation 3.8 for r gives:

$$
\begin{aligned}
r^n &= \frac{e_p D + e_e d_R}{(n-1)2^n e_a D} \\
r^* &= \sqrt[n]{\frac{e_p D + e_e d_R}{(n-1)2^n e_a D}}. \tag{3.9}
\end{aligned}
$$

where r^* is the optimal grid length. Based on equation 3.5, the optimal transmission range, R^*, can be described as follows:

$$R^* = 2\sqrt[n]{\frac{e_p D + e_e d_R}{(n-1)2^n e_a D}}. \tag{3.10}$$

Equation 3.10 shows that the optimal transmission radio range. R^*. relates to the network traffic (D), the attenuation loss factor (n). and the data bit rate (d_R).

3.3.2 Energy consumption in equal-grid model

A second scenario that approaches (more) the reality of ad-hoc wireless networks will be discussed in this section. In this scenario, the network traffic is uniformly distributed among the entire network. and all traffic is accumulated and relayed to the sink node. The energy consumption of the network is derived as follows.

In the ith grid the traffic received from the $(i + 1)^{th}$ grid, the traffic to be transmitted to the $(i - 1)^{th}$ grid, and the listening time duration can be described as follows:

$$D_{ti} = (L - (i - 1)r)\lambda$$
$$D_{ri} = (L - ir)\lambda$$
$$T_{li} = 1 - T_{ti} - T_{ri} = 1 - \frac{D_{ti} + D_{ri}}{d_R}. \tag{3.11}$$

where λ denotes the traffic intensity per metre $(bits/m)$. By using equations 3.5. 3.6 and 3.11, the energy consumed in the ith grid is

$$E_i = e_p(L - ir)\lambda + e_e d_R + e_a(2r)^n(L - (i - 1)r)\lambda. \tag{3.12}$$

The total energy consumption of the network is

$$E_{total} = \sum_{i=1}^{m} E_i. \tag{3.13}$$

Based on equation 3.4. $r = \frac{L}{m}$. Therefore the total energy consumption is determined as follow:

$$E_{total} = m\left\{ e_p L\lambda + e_e d_R + e_a\left(L + \frac{L}{m}\right)\lambda\left(2\frac{L}{m}\right)^n \right]$$
$$- \frac{m + 1}{2}L\lambda[e_p + e_a\left(2\frac{L}{m}\right)^n\right\}. \tag{3.14}$$

3.4 Adjustable-grid GAF model

In a dynamic traffic scenario, nodes near the sink will relay more traffic than nodes at the other end of the network. Therefore, to optimise their energy consumption according to the relationship between the optimal transmission range (optimal grid length) and traffic using equations 3.9 and 3.10, the nodes near a sink should have a smaller radio range. An adjustable-grid GAF model, as shown in Fig. 3.1, can lead to lower energy consumption compared to the equal-grid GAF model, if properly designed. Therefore, in this section, two adjustable-grid GAF models, the first based on the optimal transmission range (equation 3.10) and the second based on Genetic Algorithms (GA), are proposed.

3.4.1 Optimal Transmission Range (OTR) based energy minimisation

As illustrated in Fig. 3.1, the adjustable-grid linear GAF model divides the network into m variable-length grids, where the length of each grid is determined according to equation 3.9.

To derive the total energy consumed in the ith adjustable-grid, let us assume $r_0 = 0$. Then, based on equation 3.11 the transmitted and received traffic and listening time period in the ith grid can be described as follows:

$$D_{ti} = (L - r_1 - r_2... - r_{i-1})\lambda$$
$$D_{ri} = (L - r_1 - r_2... - r_i)\lambda$$
$$T_{li} = 1 - T_{ti} - T_{ri} = 1 - \frac{D_{ti} + D_{ri}}{d_R}. \tag{3.15}$$

The radio transmission range R_i (in the ith grid) is

$$R_i = r_i + r_{i-1}. \tag{3.16}$$

Therefore, based on equations 3.12, 3.19 and 3.20, the energy consumed in the ith grid is derived as:

$$E_i = c_p(L - r_1 - r_2... - r_i)\lambda + c_e d_R$$
$$+ c_a(r_i + r_{i-1})^n(L - r_1 - r_2... - r_i)\lambda. \tag{3.17}$$

and the total energy consumption of the entire network is

$$E_{total} = \sum_{i=1}^{m} E_i.$$

(3.18)

Given fixed values of the attenuation loss factor (n) and data bit rate (d_R), based on equation 3.9 the optimal grid length (r^*) is a function of network traffic (D), which is a function of grid length (r). Therefore, the optimal grid length can be computed, and then the network energy consumption can be computed as well.

3.4.2 Genetic Algorithms based energy minimisation

Genetic Algorithms (GA) [90], [91] are optimisation and search techniques based on the principles of genetics and natural selections. A GA is applied to search the minimum value of a fitness function, and the variables are processed by three main GA operators, which are defined as follows:

- Selection: This operator selects chromosomes in the population for reproduction, and a fitter chromosome has a higher probability of being selected to reproduce.

- Crossover: This operator chooses a locus and exchanges or crosses over two chromosomes to create two offspring.

- Mutation: This operator randomly flips some bits in a chromosome.

Each variable is considered as a chromosome which evolves through the iterations (generations). The chromosomes of the next generation are created by merging or modifying the chromosomes in the current population, where the Crossover and Mutation operators are applied in the process. In each generation, the chromosomes are selected according to their selection probabilities, which are determined by the selection operators.

In our GA model, the fitness function is:

$$E_f = \sum_{i=1}^{m} E_i.$$

(3.19)

where

$$E_i = e_p(L - r_1 - r_2... - r_i)\lambda + e_l$$
$$+ e_a(r_i + r_{i-1})^n (L - r_1 - r_2... - r_i)\lambda. \tag{3.20}$$

which is constrained by the set:

$$\bigvee = \{(r_1, r_2, ...r_m) : 0 < r_i < L. \sum_{i=1}^{m} r_i = L\}, \tag{3.21}$$

where the r_is represent the chromosomes in the GA algorithm based on which new chromosomes are produced in each generation. Given enough generations (about 20000 generations in our simulations), the minimum of the fitness function (minimum energy consumption) is determined. The result will be discussed in Section 3.5.

3.5 Numerical results

3.5.1 Optimal transmission range

The optimal transmission range (3.10) is a function of the network traffic (D), the attenuation loss factor (n), the data bit rate (d_R), and the transceiver parameters $(e_e, e_a, and e_p)$, which are determined by the design of transceivers. Note that, the length of the entire network (L) does not effect the optimal transmission range. Given a fixed value of attenuation loss factor $(n = 2)$, the relationship between the optimal transmission range. the network traffic and data bit rate is shown in Fig. 3.2. In this figure. for higher data bit rate. the optimal transmission range decreases sharply when the network traffic increases: for lower data bit rates. the optimal transmission range slowly decreases when the network traffic increases.

Given a fixed value of data bit rate $(d_R = 2.5 \times 10^7 \ bits/s$ is the maximum data process rate of transceiver. and will be utilised in the remainder of this thesis). the relationship between the optimal transmission range and the network traffic & attenuation loss factor is shown in Fig. 3.3. In this figure. the optimal
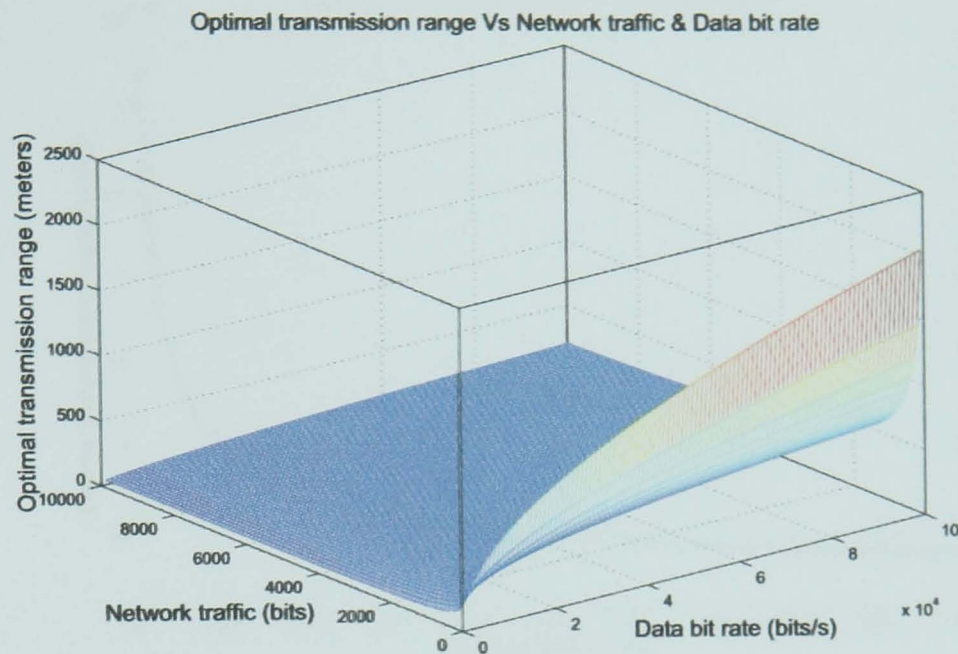
Figure 3.2: Optimal transmission range versus network traffic & Data bit rate $(n = 2)$
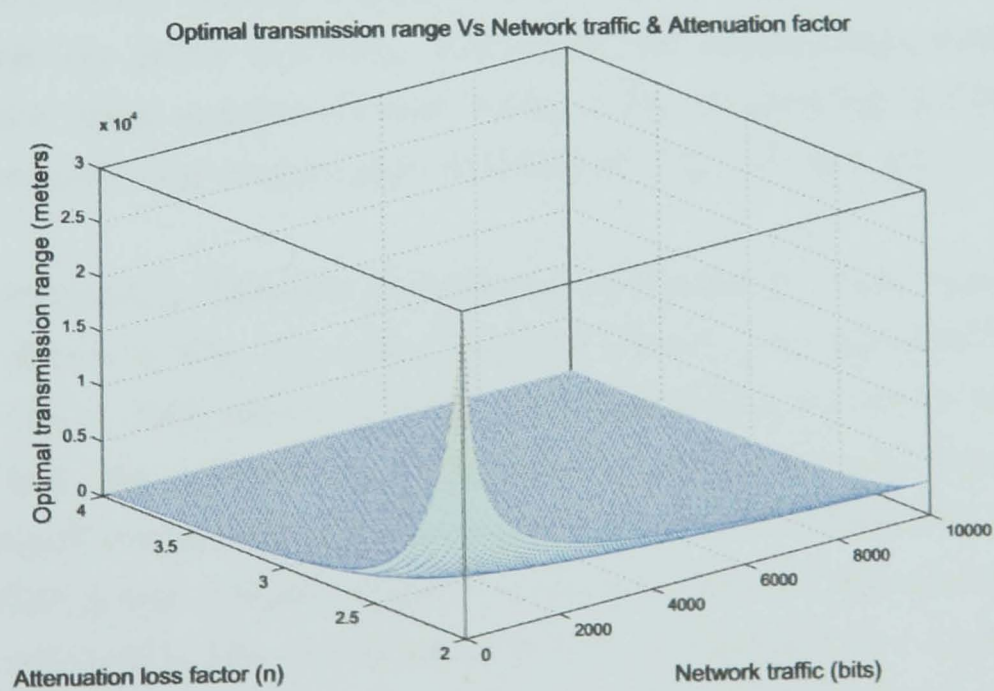
Figure 3.3: Optimal transmission range versus network traffic and attenuation factor $(d_R = 1000 \ bits/s)$
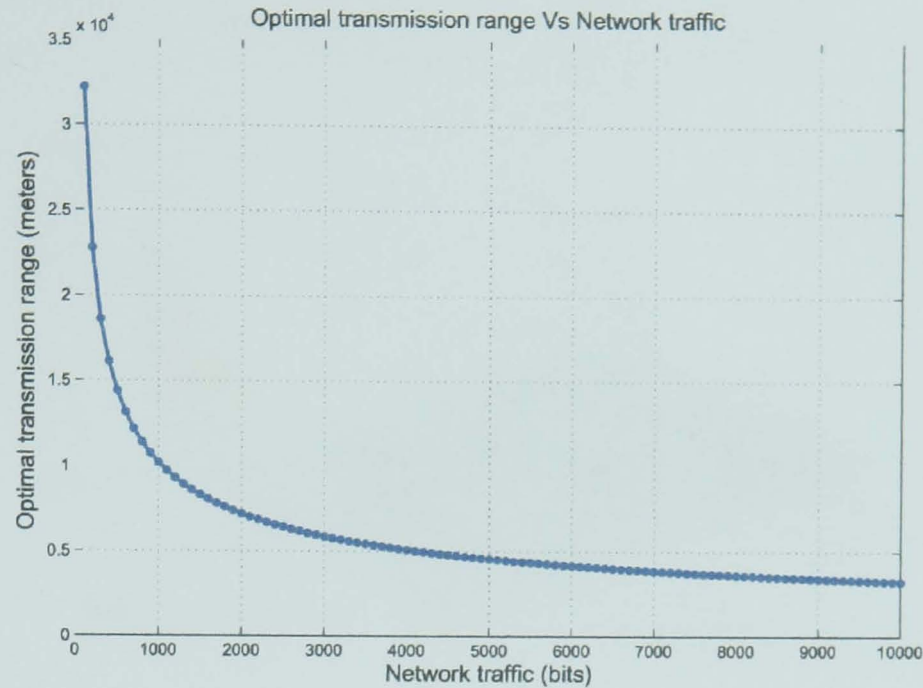
Figure 3.4: Optimal transmission range versus network traffic ($d_R = 1000 \; bits/s$, $n = 2$)

transmission range sharply decreases when the network traffic increases or the attenuation loss factor increases. Note that, the relationships between optimal transmission range and the network traffic in Fig. 3.2 and Fig. 3.3 have the same trend, moreover, this relationship is shown in Fig. 3.4 and will be discussed in detail.

The relationship between the optimal transmission range and the network traffic is shown in Fig. 3.4 when the data bit rate and attenuation loss factor are fixed ($d_R = 1000 \; bits/s$, $n = 2$). As a result, Fig. 3.4 shows two important points: First, the optimal radio transmission range increases sharply when the traffic through the network is low, where the number of transmissions is small and therefore the global network energy can be minimised by minimising the number of nodes involved in the transmission, which corresponds to a large node range. The analysis agrees with this observation and predicts this trend, where a large number of nodes are in the sleeping state and therefore the transmission range is large. The majority of the network is in the sleeping state when the transmitted traffic is less than 2000 *bits* in this example. Second, when the network traffic
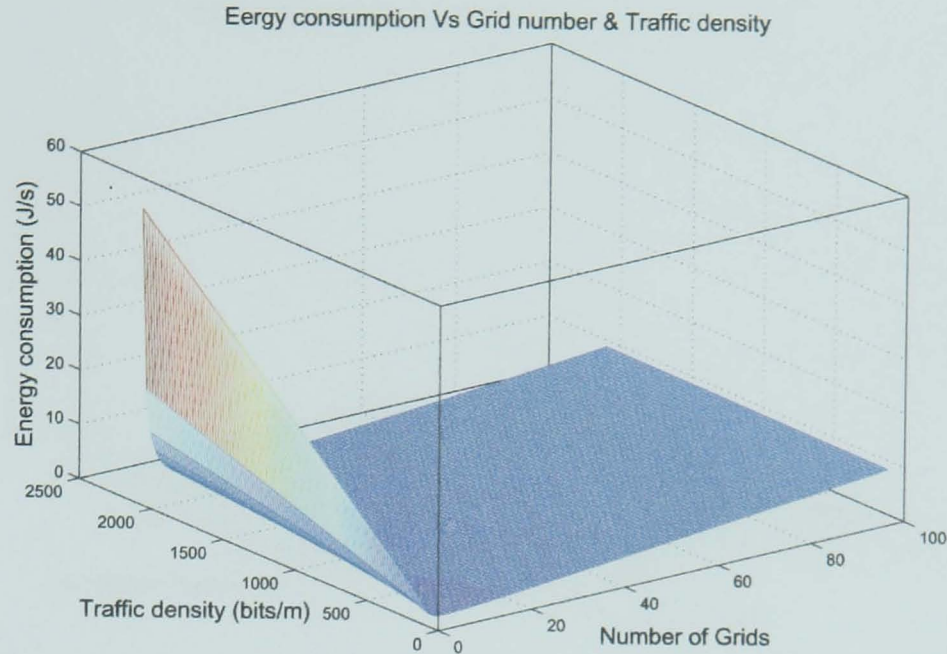
Figure 3.5: Network energy consumption versus traffic density & no. of grids $(n = 2)$

is large, the optimal transmission range takes smaller values and therefore the optimal grid length becomes smaller, hence, there will be more relaying nodes (more grids) involved in the transmission.

3.5.2 Comparison of energy consumption

As shown in equation 3.14, the network energy consumption is a function of the number of grids (m), network traffic density (λ), attenuation factor (n), data bit rate $(d_R = 1000 \ bits/s)$, network length (L) $(L = 2000m)$, and transceiver parameters. Given a fixed value of attenuation factor $(n = 2)$, the relationship between network energy consumption and the network traffic density & number of grids is shown in Fig. 3.5. In this figure, when the number of grids is small, the energy consumption increases when the traffic density increases, which correspondences to a high network traffic.

Given a fixed value of the network traffic density $(\lambda = 1000 \ bits/m)$, the relationship between the network energy consumption and the attenuation loss factor
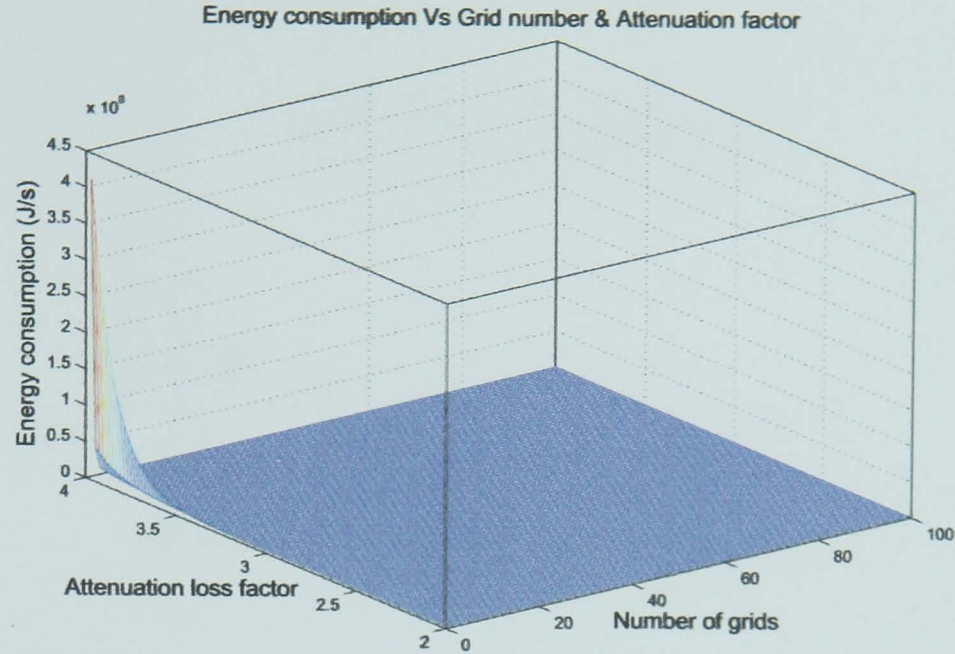
Figure 3.6: Network energy consumption versus attenuation factor & no. of grids $(d_R = 1000 \ bits/s)$

& number of grids is shown in Fig. 3.6. In this figure, the energy consumption increases when the number of grids decreases or the attenuation loss factor increase. The energy consumption is large when the attenuation loss factor is large and the number of grids is small. The relationship between energy consumption and number of grids is depicted in Fig. 3.7.

To compare the network energy consumption in the equal-grid and the adjustable-grid GAF models in the same scenario, the parameters of the network model used are: $L = 2000m$, $d_R = 1000 \ bits/s$, $n = 2$, and $\lambda = 1000 \ bits/m$. Based on equation 3.14, the network energy consumption of the equal-grid model in terms of the number of grids (m) is shown in Fig. 3.7. In Fig. 3.7, the minimum energy consumption $(E_{total} = 2.1475J)$ is achieved when $m = 13$. When the number of grids is small, the length of the grid is large, therefore the d^n propagation loss component dominates the energy consumption, and the energy consumption decreases sharply for $m < 13$ with increase in the number of grids. However, when the number of grids is large, the length of each grid is small and the d^n propagation loss component becomes smaller, where the transmitter and receiver
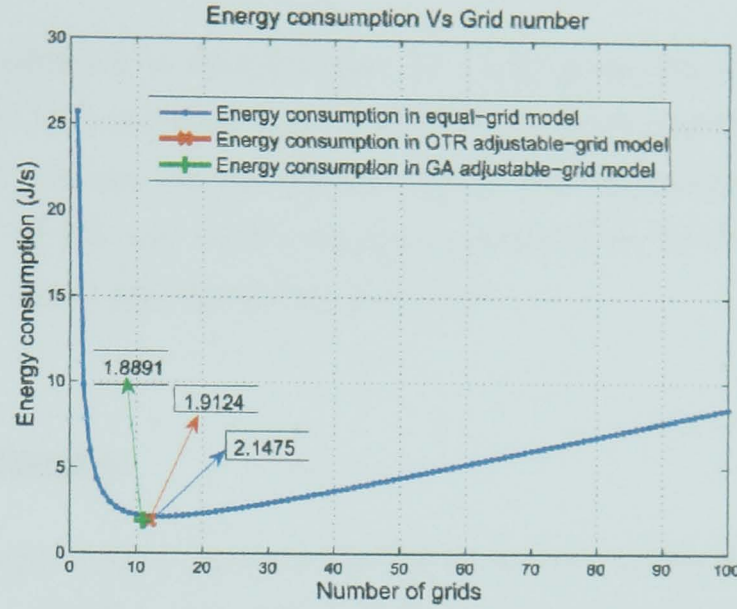
Figure 3.7: Network energy consumption in three models ($d_R = 1000\ bits/s$, $n = 2$)

electronics energy consumption per bit become large and therefore the energy consumption increases linearly with the number of grids, as shown in Fig. 3.7, for $m > 13$.

To compare the total network energy consumption in equal-grid and adjustable-grid linear GAF models, the author calculated the optimal grid lengths for 12 adjustable grids based on the optimal transmission range (OTR), equation 3.9, where the traffic in each grid is calculated using equation 3.19. Therefore, the total energy consumed by the OTR adjustable-grid model can be calculated from equation 3.19, equation 3.17 and equation 3.18: $E_{total} = 1.9124J$, and it occurs when the network is divided into 12 adjustable grids. Also, by using Genetic Algorithms (GA), the energy consumption of GA adjustable-grid model is computed: $E_{total} = 1.8891J$, and it occurs when the network is divided into 11 adjustable grids.

Fig. 3.7 gives a comparison of the network energy consumption among all the models. The X mark in this figure represents the total energy consumption in OTR adjustable-grid model and the $+$ mark represents the total energy consumption in GA adjustable-grid model, and they are both smaller than the minimum value of the energy consumption in equal-grid model, which is 2.1475 J/s and

occur when the network is divided into 13 equal grids ($m = 13$). This means that the GA and OTR adjustable-grid models are more energy efficient than the equal-grid model. Based on the results, these two adjustable-grid models can respectively save 12.0% and 10.9% energy in comparison to the minimum energy consumed in the equal-grid Model in this case.

3.6   Summary

In this chapter, the author proposed a linear ad-hoc wireless network based on GAF mechanism. Firstly, the author derived the optimal transmission range in terms of the network traffic, the attenuation loss factor, and the data bit rate. Secondly, the author derived the network energy consumption of the equal-grid GAF model in terms of the number of grids, network traffic density, and attenuation loss factor. Thirdly, the author proposed two adjustable-grid GAF models respectively based on the optimal transmission range equation and Genetic Algorithms, and computed the energy consumption of both models. The author then compared the network consumption of the above three models. The results show that, compared to the minimum energy consumption of the equal-grid model, GA and OTR adjustable-grid models respectively save energy by 12.0% and 10.9% under the set of network and transceiver parameters assumed. Note that, the energy consumption model considers the energy consumed in the listening states, which has been neglected in previous work in the literature.

Chapter 4

Energy Efficient GAF Protocol in Rectangular Ad-hoc Wireless Networks

4.1 Introduction

In this chapter, the energy efficient Geographic Adaptive Fidelity (GAF) protocol is studied in the context of rectangular ad-hoc wireless networks shown in Fig. 4.1. The optimal transmission range (optimal grid length) is derived, and the energy consumption in both equal and adjustable grids models are compared. The network lifetime of both models are compared, and node density control is used to prolong the network lifetime. Furthermore, to approach a real network environment, the propagation attenuation function, different values of the loss factor, and Rayleigh fading are considered. In this chapter, in a rectangular ad-hoc wireless network, new network energy consumption models are proposed considering the energy consumed for processing data at the receiver, and an adjustable-grid model is proposed for rectangular network based on Genetic Algorithms. The network lifetime is studied for the first time in rectangular GAF models, and

59
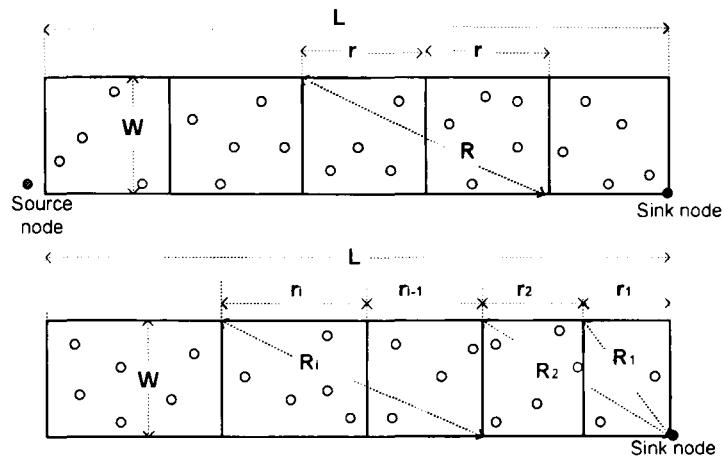
Figure 4.1: Equal-grid and adjustable-grid rectangular GAF model.

node density control is proposed to prolong the network lifetime. Furthermore, the new contributor in this chapter include the consideration of physical layer impairments including attenuation and fading.

4.2 Energy consumption model

The energy consumed by ad-hoc wireless network nodes is the sum of energy consumed for transmitting, receiving and listening. Considering a transmission from a transmitter to a receiver, where the distance between them is R, the received signal power can be expressed as [3]:

$$p_r(R) = \frac{p_t G_t G_r \lambda^2}{(4\pi)^2 R^n Loss}.$$ (4.1)

where G_t and G_r are respectively the gains of the transmitter and receiver. The carrier wavelength is λ and $Loss$ represents any additional losses in the transmission. The propagation loss factor, n is typically between 2 and 4. Thus, with $G_t = G_r = 1$, and $Loss = 1$, the received signal power is

$$p_r(R) = \frac{p_t \lambda^2}{(4\pi)^2 R^n}.$$ (4.2)

To be successfully received by the receiver, the received signal power must be above a certain threshold power (p_{thr}). Therefore, the signal power at the

transmitter must be above $\frac{p_{thr}(4\pi)^2 d^n}{\lambda^2}$.

$$E_t = (e_e + \frac{p_{thr}(4\pi)^2 R^n}{\lambda^2 d_R})Packet = (e_e + e_a R^n)Packet. \qquad (4.3)$$

where e_e is the energy/bit consumed in the transmitter electronics and $e_a =$ $\frac{p_{thr}(4\pi)^2}{\lambda^2 d_R}$, which can be considered as the energy/bit consumed in the transmitter RF amplifier, d_R is the transmit or receive data rate ($bit/second$) of each network node, and *Packet* is the number of bits in the packet. Therefore, based on [141] the energy consumed per second by a node in these three states can be respectively calculated as follows:

$$E_t = (e_e + e_a R^n)D_t$$
$$E_r = (e_e + e_p)D_r$$
$$E_l = e_l T_l = e_l(1 - T_t - T_r). \qquad (4.4)$$

where R is the node transmission range; D_t and D_r are the transmitted and received traffic data bits respectively; T_t and T_r denote respectively the time for transmitting and receiving the traffic data of a grid. which can be expressed as follows:

$$T_t = D_t/d_R$$
$$T_r = D_r/d_R. \qquad (4.5)$$

where T_l, which denotes the time spent listening to the radio environment in one second, is: $T_l = 1 - T_t - T_r$, $(0 \le T_l \le 1)$, thus $0 \le (1 - D_t/d_R - D_r/d_R) \le 1$. For the static traffic data scenario, where $D_t = D_r = D$. the range of D can be described as follows:

$$0 \le D \le \frac{1}{2} \times d_R \times 1 second. \qquad (4.6)$$

Consequently. the maximum traffic data that can be forwarded in each grid in one second is $\frac{1}{2} \times d_R$ *bits*, which occurs when nodes in this grid spend $\frac{1}{2}$ second for receiving data and $\frac{1}{2}$ second for transmitting data and do not listen to the radio environment. Throughout this chapter our analysis will be based on $d_R = 2.5 \times 10^5$ *bps* [65], and hence. based on equation 4.6. the maximum traffic data (D) which can be forwarded in the network is $1.25 \times 10^5 bits$ in one second.

For the other transceiver design parameters: e_p is the energy/bit consumed for processing in receivers and e_l is the energy/second consumed for listening to the radio environment: e_e, e_a, e_p and e_l are determined by the design characteristics of the transceivers. Based on [64] and [65], the typical values of these parameters are: $e_e = 3.32 \times 10^{-7}$ J/bit, $e_p = 6.8 \times 10^{-8}$ J/bit. Furthermore, given $p_{thr} = 2 \times 10^{-9}$ w, $d_R = 2.5 \times 10^5$ bps, and $f = 2.4 \times 10^9$ Hz (which is an unlicensed frequency band and one of the most popular in radio based networking), e_a is computed as: $e_a \approx 8 \times 10^{-11}$ $J/bit/m^n$. Since the energy consumption for listening is only consumed by the transceivers electronics,

$$e_l = e_e d_R. \tag{4.7}$$

Note that, the energy consumption model has been improved by adding the propagation attenuation function, compared to the energy models used in the previous chapters.

4.2.1 Static traffic in equal-grid model

Static traffic refers to a scenario in which the traffic rate flowing along the network is constant. This occurs typically when a source node is outside the rectangular network, as shown in Fig. 4.1, where static traffic, denoted by D, is transmitted from a source node to a sink node. In the equal-grid rectangular model, L and W represent the length and width of the network, respectively, while r and R represent the grid length and the transmission range of nodes in each grid, respectively. Therefore, the number of grids, m, is:

$$m = \frac{L}{r} \tag{4.8}$$

and the transmission range (R_i) of nodes in the ith grid is derived based on GAF mechanism as follows:

$$R_1 = \sqrt{r^2 + W^2}, \quad R_i = \sqrt{(2r)^2 + W^2}, \quad i \neq 1. \tag{4.9}$$

Since the head node (active node) forwards the traffic data through the network, and the other nodes remain in the sleeping state to save energy, the total
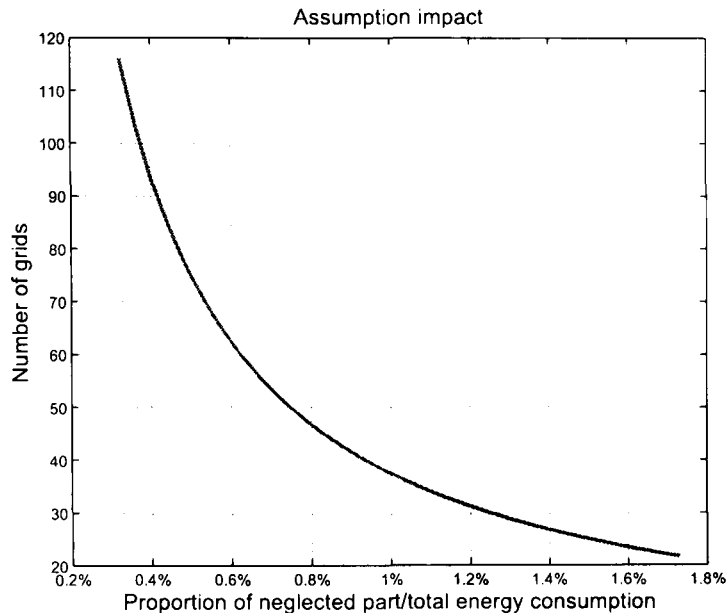
Figure 4.2: Impact of neglecting part of energy.

energy consumed in the ith grid, E_i. is the sum of the energy consumed by the head node in the listening, transmitting and receiving states. Thus, based on equations 4.4, 4.5 and 4.7, the energy consumed in the ith grid is:

$$E_i = E_t + E_r + E_l$$
$$= (e_e + e_a R^n)D_t + (e_e + e_p)D_r + e_e d_R(1 - \frac{D_t}{d_R} - \frac{D_r}{d_R})$$
$$= e_p D + e_l + e_a R_i^n D. \tag{4.10}$$

Therefore, based on equations 4.8, 4.9 and 4.10, the energy consumed in the entire network can be expressed as follows:

$$E_{total} = mE_i$$
$$= \frac{L}{r}[e_p D + e_l + e_a(\sqrt{(2r)^2 + W^2})^n D] - 3e_a r^2 D. \tag{4.11}$$

To determine the minimum energy consumption of the network nodes, we take the first derivative of E_{total} in terms of grid-length. r. and let $\partial E_{total}/\partial r = 0$. The solution of equation 4.11 has two complex roots, which cannot be applied in the model. Fig. 4.2 shows the impact of the term $3e_a r^2 D$ in equation 4.11. The value of the term $3e_a r^2 D$ is only about 1.2% of equation 4.11 when the number of grids is 30, and the proportion is even smaller when the number of network grids is

large. As an alternative, we assume that the transmission range of nodes in the 1st grid is equal to that of other nodes in other grids, thus the term $3e_a r^2 D$ can be ignored and the total energy consumed in the whole network can be derived as:

$$E_{total} = mE_i$$
$$\simeq \frac{L}{r}[e_p D + e_l + e_a(\sqrt{(2r)^2 + W^2})^n D]. \tag{4.12}$$

To compute the minimum energy consumption of the network nodes, we take the first derivative of E_{total} in terms of grid-length, r, and let $\partial E_{total}/\partial r = 0$. Two cases ($n = 2$ and $n = 4$) are discussed below.

Assuming $n = 2$:

$$\partial E_{total}/\partial r = (-e_p D - e_l - W^2 e_a D)Lr^{-2} + 4Le_a D = 0. \tag{4.13}$$

The range can be evaluated as:

$$r^2 = \frac{e_p D + e_l + W^2 e_a D}{4e_a D}$$
$$r^* = \sqrt{\frac{e_p D + e_l + W^2 e_a D}{4e_a D}}. \tag{4.14}$$

where r^* is the optimal grid length. Based on equation 4.9, the optimal transmission range, R^*, can be described as follows:

$$R^* = \sqrt{\frac{e_p D + e_l + 2W^2 e_a D}{e_a D}}. \tag{4.15}$$

Equation 4.15 shows that the optimal transmission radio range, R^*, relates to the static network traffic data, D, and width W.

Following a similar procedure and assuming $n = 4$, and the optimal grid length is derived as:

$$r^* = \frac{1}{2\sqrt{3}}\sqrt{\sqrt{\frac{3e_p D + 3e_l + 4e_a DW^4}{e_a D}} - W^2}. \tag{4.16}$$

which shows that the optimal grid length is a function of the network traffic (D) and network width (W).

4.2.2 Dynamic traffic in equal-grid model

Here a more realistic scenario is considered where the traffic has variable intensities. In the ith grid, the traffic received from the $(i + 1)^{th}$ grid, the traffic to be transmitted to the $(i - 1)^{th}$ grid, and the listening time duration can be described as follows:

$$D_{ti} = (L - (i - 1)r)W\lambda$$
$$D_{ri} = (L - ir)W\lambda$$
$$T_{li} = 1 - T_{ti} - T_{ri} = 1 - \frac{D_{ti} + D_{ri}}{d_R}. \tag{4.17}$$

where λ denotes the traffic data (bits) intensity per metre^2 (m^2). By using equations 4.8, 4.9 and 4.10, the energy consumed in the ith grid is

$$E_1 = e_p D_{r1} + e_l + e_a(\sqrt{r^2 + W^2})^n D_{t1}$$
$$E_i = e_p D_{ri} + e_l + e_a(\sqrt{(2r)^2 + W^2})^n D_{ti}, \quad i \neq 1. \tag{4.18}$$

The total energy consumption of the network is

$$E_{total} = \sum_{i=1}^{m} E_i. \tag{4.19}$$

Based on equation 4.8, $r = \frac{L}{m}$. Therefore the total energy consumption can be expressed as:

$$E_{total} = e_a L^3 W\lambda(-m^{-2} + m^{-1}) - \frac{1}{2}e_p LW\lambda$$
$$+ \frac{1}{2}e_a LW^3\lambda + (\frac{1}{2}e_a LW^3\lambda + e_l + \frac{1}{2}e_p LW\lambda)m. \tag{4.20}$$

4.2.3 Dynamic traffic in adjustable-grid model

For the dynamic traffic scenario, nodes near the sink will relay more traffic than nodes at the other end of the network. Therefore, to optimise their energy consumption according to the relationship between optimal radio range (optimal grid length) and traffic using equations 4.14 and 4.15, the nodes near a sink should have a smaller radio range. An adjustable-grid rectangular GAF model can lead

to lower energy consumption compared to the equal-grid GAF model. if properly designed. As illustrated in Fig. 4.1, the adjustable-grid rectangular GAF model divides the network into m variable-length grids, where the length of each grid is determined according to equation 4.14.

To derive the total energy consumed in the ith adjustable-grid. let us assume $r_0 = 0$. Then, based on equation 4.17 the transmitted and received traffic and listening time period in the ith grid can be described as follows:

$$D_{ti} = (L - r_1 - r_2... - r_{i-1})W\lambda$$
$$D_{ri} = (L - r_1 - r_2... - r_i)W\lambda$$
$$T_{li} = 1 - T_{ti} - T_{ri} = 1 - \frac{D_{ti} + D_{ri}}{d_R}. \tag{1.21}$$

The radio transmission range R_i (in the ith grid) is

$$R_i = \sqrt{(r_i + r_{i-1})^2 + W^2}. \tag{4.22}$$

Therefore, based on equations 4.18 and 4.22. the energy consumed in the ith grid is:

$$E_1 = e_p D_{r1} + e_l + e_a(\sqrt{r_1^2 + W^2})^n D_{t1}$$
$$E_i = e_p D_{ri} + e_l + e_a(\sqrt{(r_i + r_{i-1})^2 + W^2})^n D_{ti}, i \neq 1, \tag{4.23}$$

and the total energy consumption of the entire network is

$$E_{total} = \sum_{i=1}^{m} E_i. \tag{4.24}$$

4.2.4 Realistic physical layer: Rayleigh fading

To approach a realistic networking environment, a realistic physical layer (Rayleigh fading model) is utilised with the energy consumption model to derive the optimal grid length and to calculate the network energy consumption in both equal/adjustable-grid models.

Based on the propagation attenuation equation 4.1 and the Rayleigh fading model. the probability $(P(R))$ of the signal being successfully received at R (distance between the sender and the receiver) is derived as

$$P(R) = exp(-\frac{p_{thr}(4\pi)^2 R^2 f^2}{p_t c^2}), \tag{4.25}$$
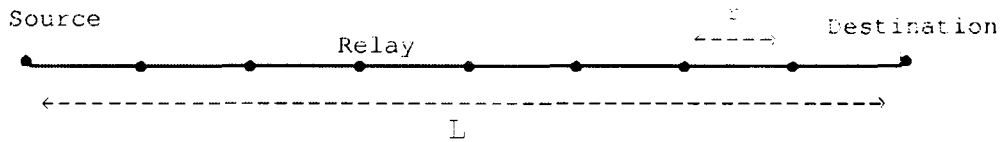
Figure 4.3: End-to-end multi equal hop transmission.

where R can be expressed as

$$R^2 = -\frac{p_t c^2 ln[P(R)]}{p_{thr}(4\pi)^2 f^2}.$$

(4.26)

Furthermore, in a linear multi equal-hop end-to-end transmission as shown in Fig. 4.3, the expected number of transmissions from the source node to the destination node is

$$u_t = v \times \frac{1}{P(R)},$$

(4.27)

where v ($v = L/R$) is the number of hops and $\frac{1}{P(R)}$ is the expected number of transmissions for one hop. Therefore, based on equations 4.26, equation 4.27 can be expressed as

$$u_t = \frac{L}{R} \times \frac{1}{P(R)} = \frac{L}{\sqrt{-\frac{p_t c^2 ln[P(R)]}{p_{thr}(4\pi)^2 f^2}}} \times \frac{1}{P(R)}$$

$$= \frac{L}{\sqrt{\frac{p_t c^2}{p_{thr}(4\pi)^2 f^2}}} \times \frac{1}{P(R)\sqrt{-ln[P(R)]}}.$$

(4.28)

The minimum value of u_t corresponds to the minimum value of the term $\frac{1}{P(R)\sqrt{-ln[P(R)]}}$. Taking the first derivative of the term and equaling it to zero, gives the following relation:

$$P(R)^{-2}[-ln[P(R)]]^{-0.5} = -\frac{1}{2}P(R)^{-2}[-ln[P(R)]]^{-1.5}.$$

(4.29)

By solving equation 4.29, $P(R) = e^{-0.5} \approx 60.7\%$. This shows that the minimum expected number of hops occurs when the optimal probability of the data being successfully received in each hop is 60.7% ($P(R)_{opt} = 60.7\%$).

In the static traffic equal-grid GAF model, by using $P(R)_{opt}$, the total network energy consumption is $E_{total} = mE_i \times \frac{1}{P(R)_{opt}}$.
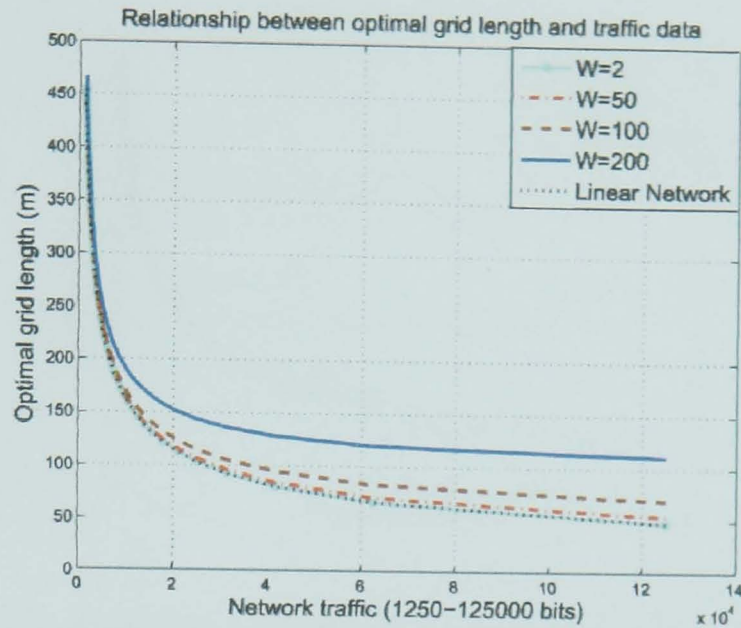
Figure 4.4: Optimal grid length versus network traffic (n=2).

Furthermore, in the dynamic traffic equal/adjustable-grid GAF networks, there ia a probability of a packet being successfully received between each grid $(P(R) = 60.7\%)$ compared to the model without a physical layer. By consider this in the simulation, the network energy consumption is evaluated to compare the results to those obtained without physical layer consideration.

4.2.5 Numerical results

Simulations were carried out using MATLAB to compare the proposed rectangular GAF model with the linear GAF model [63]. Furthermore, as shown in Fig. 4.4, to understand the effect of network width W on optimal grid length (r^*), r^* was calculated from equation 4.14 with different values of W at $L = 2000m$. As a result, Fig. 4.4 shows three important points: Firstly, the optimal grid length (or optimal radio transmission range) increases sharply when the traffic data through the network is low, where the number of transmissions is small and therefore the global network energy can be minimised by minimising the number of nodes involved in the transmission, which corresponds to a large node range. The analysis agrees with this observation and predicts this trend, where a large number of nodes are in the sleeping state and therefore the transmission range is
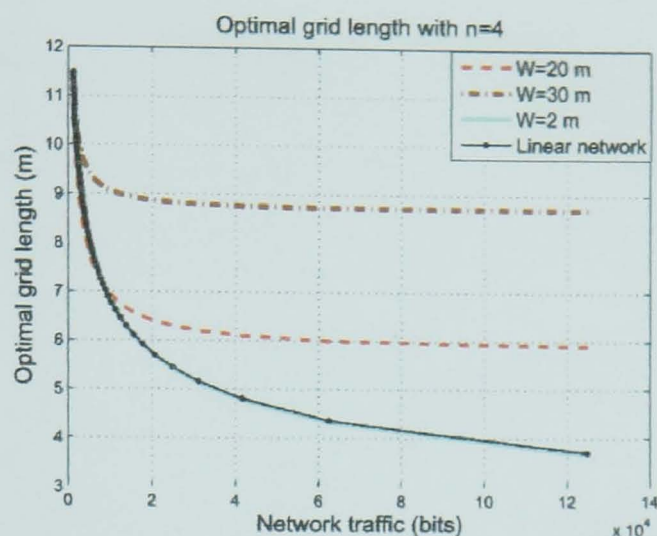
Figure 4.5: Optimal grid length versus network traffic (n=4).

large. The majority of the network is in the sleeping state when the transmitted traffic data is less than 2×10^4 *bits* per second in this case. Secondly, when the network traffic is large, the optimal transmission range, R^*, takes smaller values and therefore the optimal grid length becomes smaller, and hence, there will be more relaying nodes (more grids). Thirdly, in Fig. 4.4 it should be observed that this two dimensional network analysis contains the linear network as a special case when W/L is very small, eg. at $W = 2m$ and $L = 2000m$ where the curves overlap. Furthermore, when W increases (Linear network, $W = 2m$, $W = 50m$, $W = 100m$, $W = 200m$), the optimal grid length (r^*) also increases (R^* increases as well). Note that the traffic data range is between 0 and 1.25×10^5, which is determined by equation 4.6.

In Fig. 4.5, where the propagation attenuation factor (n) is 4, similar trends to Fig. 4.4 are observed, where $n = 2$. Note that, the optimal grid length when $n = 4$ is much smaller than the optimal grid length when $n = 2$, which is a reflection of the highly non-linear (in d) propagation environment and where the losses increase sharply with d.

To evaluate the total network energy consumption with dynamic traffic in the rectangular equal-grid GAF model, the total energy consumption was evaluated in terms of the number of network grids, m, based on equation 4.20. The nodes are uniformly distributed in the network grids, where the node density is n_d per m^2, and the traffic to be forwarded is uniformly distributed, where the traffic
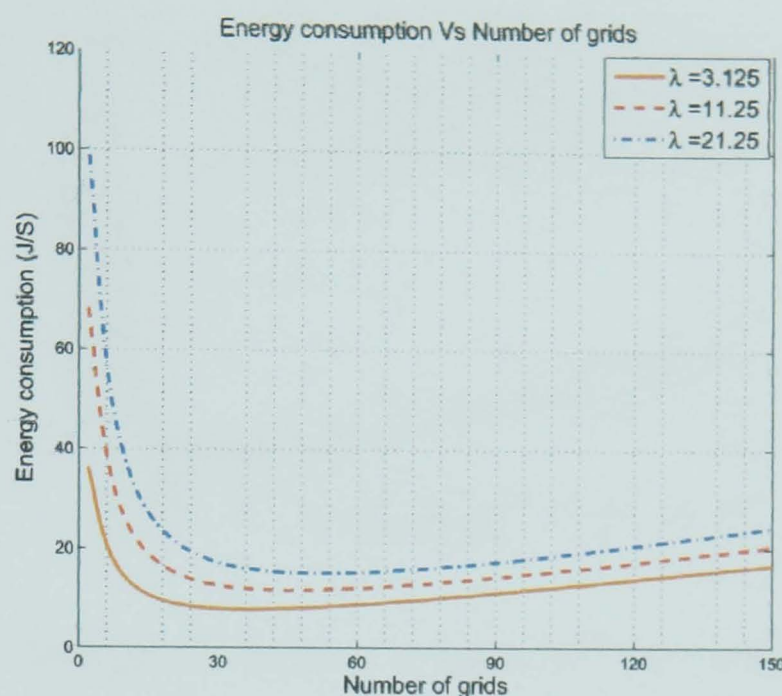
Figure 4.6: Energy consumption versus number of grids

data density is λ. With $W = 2$ ($metres$), based on different values of λ, the relationships between E_{total} and m are shown in Fig. 4.6. Obviously, larger λ means more network traffic, which calls for higher energy levels to transmit the traffic to the sink node. However, the curve shapes with different λ are similar, thus, the author only considered one λ to compare and analyse the energy consumptions of the qual-grid and adjustable-grid models, where $\lambda = 3.125$ $bits/m^2$ is selected. To analyse the energy consumption of the equal-grid model, the '*Energy consumption of equal-grid model*' in Fig. 4.7 is discussed, where the minimum energy consumption is achieved when $m = 30$. When the number of grids is small, the length of the grid is large, therefore the d^n ($n = 2$) propagation loss component dominates the energy consumption, and the energy consumption decreases sharply for $m < 30$ with increase in the number of grids. However, when the number of grids is large, the length of each grid is small and the d^n (for free space propagation $n = 2$) propagation loss component becomes smaller, and here the transmitter and receiver electronics energy consumption per bit becomes large and therefore the energy consumption increases linearly with the number of grids, as shown in Fig. 4.7, for $m > 30$.
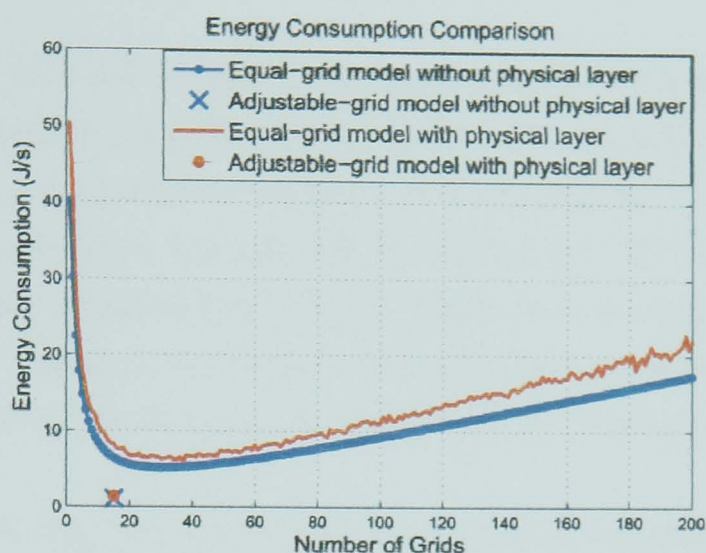
Figure 4.7: Energy consumption of equal and adjustable-grid models

Table 4.1: Calculated optimal grid-lengths

r_1	98.5040m	r_2	101.022m	r_3	103.815m
r_4	106.942m	r_5	110.478m	r_6	114.526m
r_7	119.232m	r_8	124.804m	r_9	131.565m
r_{10}	140.035m	r_{11}	151.132m	r_{12}	166.680m
r_{13}	191.019m	r_{14}	238.627m	r_{15}	436.167m

To compare the total network energy consumption in equal-grid and adjustable-grid rectangular GAF models, the author calculated the optimal grid lengths for 15 adjustable grids based on equation 4.14, where the traffic in each grid is calculated from equation 4.21. Table 4.1 illustrates the values of the optimal grid lengths which correspond to the optimal transmission ranges of these grids. Based on Table 4.1, the total energy consumed by the network can be calculated from equation 4.21, equation 4.23 and equation 4.24, which is 1.129 J/s and occurs when the network is divided into 15 adjustable grids. Fig. 4.7 gives a comparison of the entire network energy consumption in the adjustable-grid and the equal-grid rectangular GAF Models.

Note that, the X mark in this figure represents the total energy consumption in the adjustable-grid rectangular GAF model. and it is smaller than the minimum value of the energy consumption in equal-grid rectangular GAF model. which is 5.166 J/s and occurs when the network is divided into 30 equal grids ($m = 30$). This means that the adjustable-grid GAF model is more energy efficient than the equal-grid model. Based on our resluts. the adjustable-grid model can save up to 78.1% energy in comparison to the minimum energy consumed in the equal-grid model.

Furthermore, in Fig. 4.7, the energy consumption considering a real physical layer (Rayleigh fading model) in both equal and adjustable grids models are compared to the results without physical layer. Firstly. in the adjustable-grid model, the network energy consumption is about 1.417 J. which consumes about 25.5% more than the adjustable-grid model without physical layer. Secondly. the minimum energy consumption in the equal-grid model with physical layer impairments is 6.019 J and it occurs when $m = 32$. Note that. the minimum energy consumption of the equal-grid model without physical layer occurs when $m = 30$, which is different from that of the equal-grid model with physical layer. By comparison, the equal-grid model with physical layer impairments consumes 16.5% more energy than the case without physical layer impairments. Thirdly. there is fluctuation in the curve of equal-grid model with physical layer. which is caused by the random probability of the packet being successfully received.

4.3 Network Lifetime Model

Only considering energy saving in wireless ad-hoc networks cannot guarantee a longer network lifetime. energy balance must be considered as well. For example. in the GAF model. if a particular node of one grid is always selected as the active node of this grid to forward the traffic data of other grids. the energy of this node will be drained out fast, and thus the local information provided by this node (sensing application) cannot be retrieved. which means that the function of this network is not complete any more. As such our proposed protocol ensures that the active nodes of each grid are automatically rotated based on their residual

battery-capacities. Furthermore, not only the loads associated with nodes in each grid, but the energy consumption of each grid should be balanced to prolong the network lifetime. Obviously, grids near the sink node relay much more traffic data than the grids at the other end of the network. This section proposes network lifetime models which can be incorporated in equal and adjustable-grid rectangular GAF models to prolong the network lifetime. The idea behind these models is to balance the lifetime of each grid, referred to here as grid-lifetime, in order to avoid an energy bottleneck in the network and consequently increase the entire network lifetime. Based on the derived energy consumption models, the author derived network lifetime models which enable energy efficient ad-hoc networks to manage their bottleneck grid-lifetime and hence increase the network lifetime. In what follows, we discuss the network lifetime models in equal and adjustable-grid rectangular GAF models. Note that, the physical layer is not considered in the network lifetime models introduced. This can form the basis for future work in this area.

4.3.1 Network lifetime in equal-grid rectangular GAF model

Network lifetime estimation

As was assumed before, the nodes in each grid will be rotated and will take turn as the active node of that grid based on their residual energy, which means the battery-capacities of nodes in each grid of the rectangular GAF model will be drained out at a comparable rate. Therefore the energy capacity of each grid is determined by the energy capacity of each node and the number of nodes in each grid, where the number of nodes in each grid of the equal-grid model is the same. Based on the energy consumption models, the energy consumed in the ith grid is E_i, therefore the grid-lifetime of the ith grid (G_{li}) can be defined as the time taken for all nodes in the ith grid to drain out their energy capacities, where the grids dies. Let C_e denote the node energy capacity and N_{gi} denote the number of nodes in a grid (N_{gi} are the same in the equal-grid model), then G_{li} can be calculated as follows:

$$G_{li} = \frac{N_{gi} \times C_e}{E_i}.$$ (4.30)

where E_i can be calculated from equation 4.18.

Fig. 4.7 shows that. for an equal-grid model. the network consumes the minimum energy when it is partitioned into 30 grids ($m = 30$). To study the relationship between the energy efficiency and network lifetime. the author has carried out simulations using MATLAB on a network partitioned into 30 grids where 30 nodes are distributed in each of the 30 grids (node density $n_d = 0.225\ nodes/m^2$) and each node has $20J$ energy capacity. As a result. the curve *without node density control* in Fig. 4.8 shows that the the minimum grid-lifetime in equal-grid rectangular GAF model is 2250 seconds, which means the entire network lifetime is 2250 seconds. As the traffic is generated along the network uniformly and forwarded by each grid to the sink node. the traffic will accumulate when the nodes are close to the sink node. Therefore. the energy consumption of each grid increases if the grid is close to the sink (the grid-lifetime decreases when close to the sink). The grid-lifetime of the grid nearest to the sink is significantly higher than that of the adjacent grid because its radio transmission range is $\sqrt{r^2 + H^2}$ (not $\sqrt{(2r)^2 + H^2}$ as in the other grids). At the same time. the grid next to the sink (*the* 1st *grid*) and the one immediately before ((*the* $2^{nd}grid$)) relay almost comparable amount of traffic. Note that this lifetime is only before the network re-configuration: the equal-grid GAF network will be re-configured to a new equal-grid network with larger grid lengths when the grid with the lowest grid-lifetime drains out.

Network lifetime with node density control

In the equal-grid rectangular GAF model, the network lifetime can be extended by equalising the grid-lifetimes of each grid, which can be implemented by grid energy capacity control (controlling the node density in each grid). Thus. as shown in Fig. 4.8. the values of the low grid-lifetimes (including the threshold grid-lifetime) are extended. while other grid-lifetimes with high values are reduced. which prolongs the entire network lifetime. To this end. the grid-lifetimes are made equal by properly re-distributing the nodes in the network. Based on equation 4.30. the target grid-lifetime ($G_{l_{tg}}$) can be expressed as
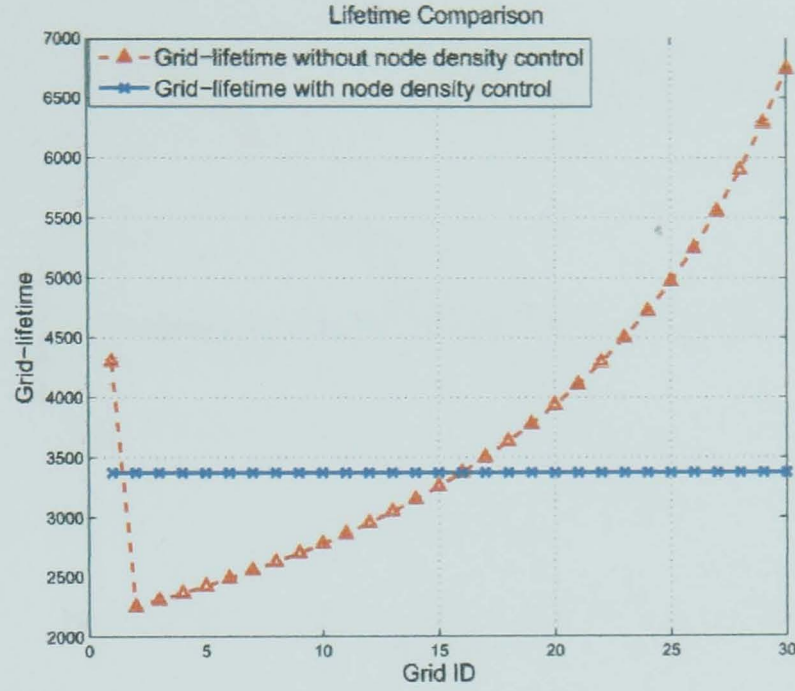
Figure 4.8: Lifetime comparison in equal-grid model (30 grids)

$$G_{li} = G_{l_{tg}}$$

$$\frac{N_{gi} \times C_e}{E_i} = G_{l_{tg}}$$

$$N_{gi} = \frac{G_{l_{tg}} \times E_i}{C_e}, \tag{4.31}$$

where $G_{l_{tg}}$ is constant. Note that, the total number of nodes in the network is not changed after nodes re-distribution, which means $\sum_{i=1}^{30} N_{gi} = 900$. Therefore,

$$\sum_{i=1}^{30} \frac{G_{l_{tg}} \times E_i}{C_e} = 900. \tag{4.32}$$

This equation can be solved based on equation 4.18, where the new grid-lifetime is 3398 seconds. Thus, according to equation 4.18 and 4.31, the number of nodes in each grid can be calculated, see Fig. 4.9.

With these new numbers of nodes, based on equation 4.30, the new grid-lifetimes can be computed, which are shown in Fig. 4.8. As a result, these new grid-lifetimes have the same value, which avoids constraining the entire network
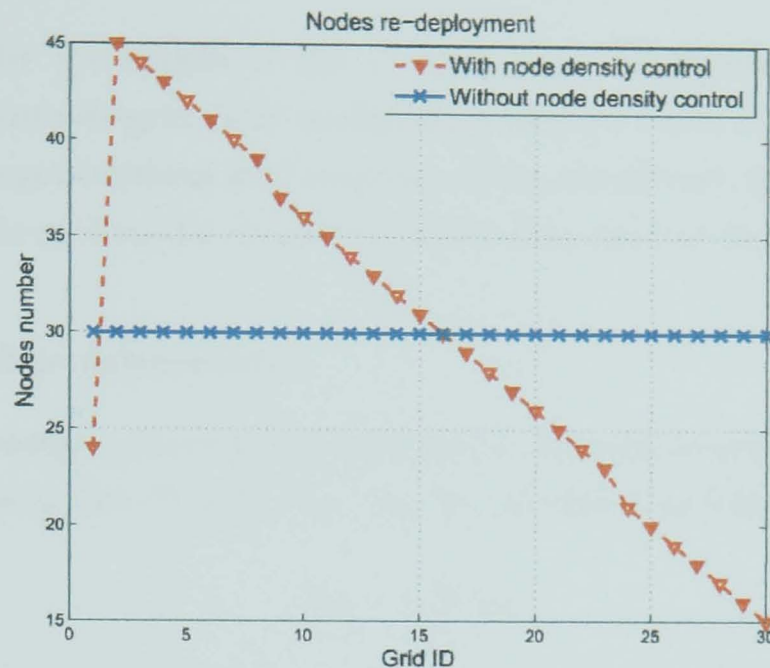
Figure 4.9: Nodes number comparison in each grid (30 grids)

lifetime by some bottleneck grid-lifetime. Furthermore, as shown in Fig. 4.8, the entire network lifetime with node density control is about 3398 seconds. Consequently this network node density control approach prolongs the entire network lifetime by 51.0% compared to the original equal-grid model, where the network lifetime is 2250 seconds.

Nevertheless, network nodes redeployment is not a practical approach once the network has been initially configured. However, the nodes can be deployed according to these results before the network is initialised to prolong the network lifetime. For existing networks, where the node density is fixed, the grid-lifetimes can be balanced by using an adjustable-grid model, which will be introduced in the next section.

4.3.2 Network lifetime extension in adjustable-grid model

According to equation 4.30, the grid-lifetimes can be balanced by changing N_{gi}, E_i or both of them, where only N_{gi} is changed in the node density control approach. Note that, if the node density is fixed, N_{gi} is determined by the coverage of the ith grid, where in the rectangular GAF model, the coverage of the ith grid

is determined by the length of the ith grid (r_i). Furthermore, based on the rectangular adjustable-grid GAF model, E_i is derived based on the optimal node transmission ranges (optimal grid lengths). Thus, intuitively, the network lifetime of the adjustable-grid model should be better than that of the equal-grid model.

Network lifetime estimation

Based on the energy consumption rectangular adjustable-grid GAF model, the number of nodes in the ith grid, N_{gi}, can be calculated as follows:

$$N_{gi} = r_i W n_d,$$
(4.33)

where $n_d = 0.225\ nodes/m^2$, which is the same as in the equal-grid model. Based on equation 4.30 the ith grid-lifetime can be calculated as follows:

$$
\begin{aligned}
G_{li} &= \frac{N_{gi} \times C_e}{E_i} \\
&= \frac{r_i W n_d \times C_e}{E_i}.
\end{aligned}
$$
(4.34)

As a result, Fig. 4.10 shows that the grid-lifetime with the minimum value (11719.5 seconds) in the second grid is the threshold grid-lifetime, which determines the entire network lifetime. In comparison to the network lifetime in equal-grid GAF model, using an adjustable-grid GAF model prolongs the network lifetime up to 420% and the node density control approach has not been used as yet.

Node density control in adjustable-grid model

Following the same simulations in the equal-grid model, the grid-lifetimes can be balanced by node density control in the adjustable-grid model. To realise node re-distribution, the same procedure was followed as in the equal-grid model. Based on equations 4.23, 4.31 and 4.32, the target grid-lifetime after nodes re-distribution is 15940 seconds. Thus, according to equations 4.23 and 4.31, the number of nodes in each grid of the new networks can be calculated. As a result Fig. 4.11 gives a comparison between the network lifetime before and after
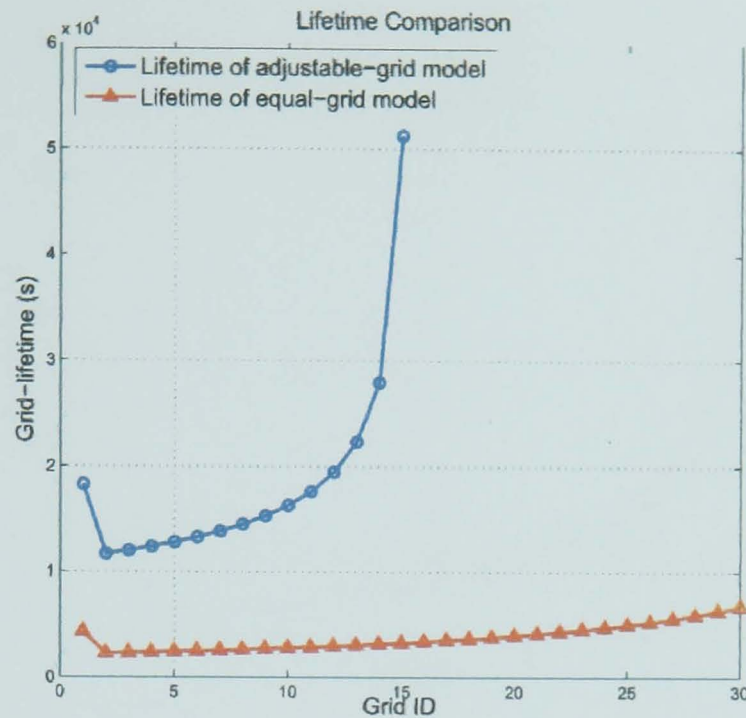
Figure 4.10: Lifetime comparison of equal (30 grids) and adjustable-grid (15 grids) models

nodes redeployment which shows that the entire network lifetime can be prolonged by 36.0% by node density control compared to the adjustable-grid model before nodes re-distribution. Furthermore, comparing this adjustable-grid model with node density control to equal-grid model without node density control, the lifetime can be significantly prolonged by 608.4%.

4.4 Summary

Compared to linear networks, where all network nodes lie on one line, the rectangular model is closer to real networks, such as Vehicular Ad-hoc NETworks (VANET) topologies configured on motorways, or Wireless Ad-hoc Sensor NETworks (WASNET) rectangular (or square) topologies. In this chapter, the author has derived the relationship between the optimal grid length (optimal transmission radio range) and network traffic.

The author has derived the relationship between network energy consumption and number of grids, and derived the minimum energy consumption based on
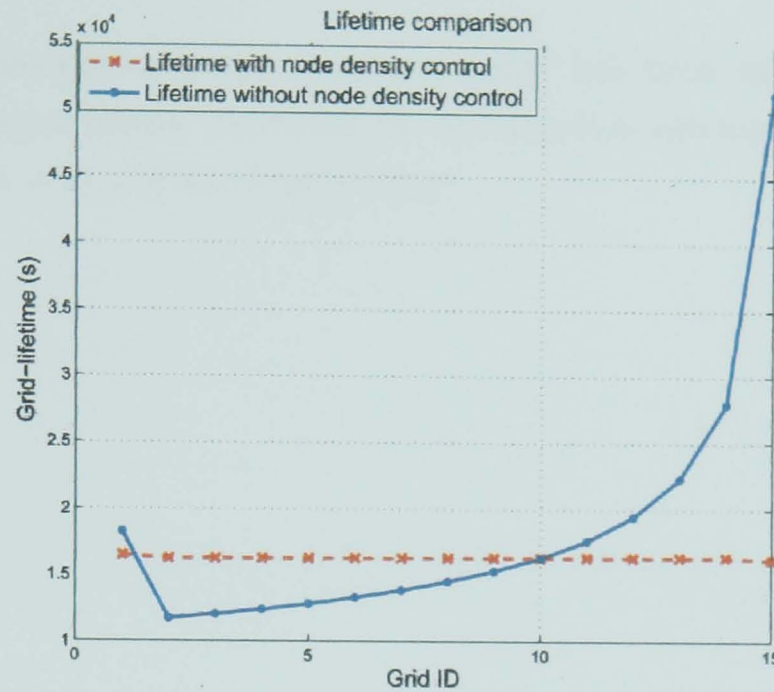
Figure 4.11: Lifetime comparison in adjustable-grid model (15 grids)

this relationship. The author has calculated the optimal grid lengths of the adjustable-grid model and calculated the network energy consumption based on this optimal adjustable-grid model. The results show that about 78.1% energy is saved by using the adjustable-grid model compared to the minimum energy consumption in the equal-grid model. Furthermore, the author has evaluated the entire network lifetime based on a new grid-lifetime concept in both equal-grid and adjustable-grid models, and the results show that the adjustable-grid model can prolong the network lifetime by 420% compared to the equal-grid model. Also, with the node density control approach, the network lifetime can be prolonged. Note that, the node density control approach in this chapter is only used to analyse the relationship between the node density and the network lifetime, where normally the node density is determined by other factors (not network lifetime), such as sensing coverage in sensor network. Furthermore, for non-uniformly distributed network nodes (which is determined by other factors), the sink node can be re-deployed to the location with the highest node density to prolong the network lifetime.

Compared to the energy consumption models used in the previous chapters,

the energy consumption model in this chapter has been improved by adding transmission impairments, including the propagation attenuation function. loss factor ($n = 2, n = 4$) and Rayleigh fading.

Chapter 5

Energy Efficient Geographic Routing in Linear Ad-hoc Wireless Networks

5.1 Introduction

Geographic routing algorithms in ad-hoc wireless networks have recently gained increased interest, and energy saving is of particular interest. In this chapter, the Optimal Range Forward (ORF) algorithm is proposed and is based on the optimal transmission range, which minimises the total energy consumption of the transmission (summation of energy consumption of all hops) in a linear network. Furthermore, based on ORF, the Optimal Forward with Energy Balance (OFEB) algorithm is proposed, in which the next-hop node is selected according to the remaining energy of each neighbour node and the distance between each neighbour node and the best neighbour location, the latter is determined by the optimal transmission range. In the OFEB algorithm, the total energy consumption of the transmission and the residual energy of each node are both considered to prolong the network lifetime. The network lifetime resulting from all the algorithms
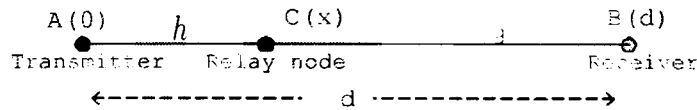
Figure 5.1: Locating relay node

above are compared in our simulation, and it is shown that the performance of the OFEB algorithm is significantly better than the others.

Also, in this chapter the author introduces a method to locate relay nodes, and derive the range of relay node locations that results in energy saving. The optimal node transmission range is derived in terms of the propagation loss factor. The energy consumption of a multihop ad-hoc wireless network has been computed based on both optimal transmission range and under direct transmission where the source and destination communicate directly. Multihop routing with optimal transmission range saves 90.1% energy compared to direct transmission. The trade-off between energy consumption and delay time has been analysed to achieve a balanced performance in terms of both energy consumption and delay time, and the results show that with modest increase in delay (13%), the trade-off scheme saves energy by 89.2% compared to direct transmission. In a dynamic traffic scenario, the author proposes cluster based energy consumption models taking into account both equal hop and adjustable hop approaches, where the adjustable-range model is based on a Genetic Algorithm. The results show that the adjustable-range model is more energy efficient than the equal-range model.

5.2   Energy consumption model

Considering the simple model shown in Fig. 5.1, node A, located at (0), is the transmitter and node B, located at (d), is the receiver. When A transmits a packet (with P bits) directly to the receiver (B), the energy consumed for transmission (E_t) and reception (E_r) can be calculated as follows:

$$E_t = (\epsilon_c + \epsilon_a R^n)D$$

$$E_r = \epsilon_c D, \tag{5.1}$$
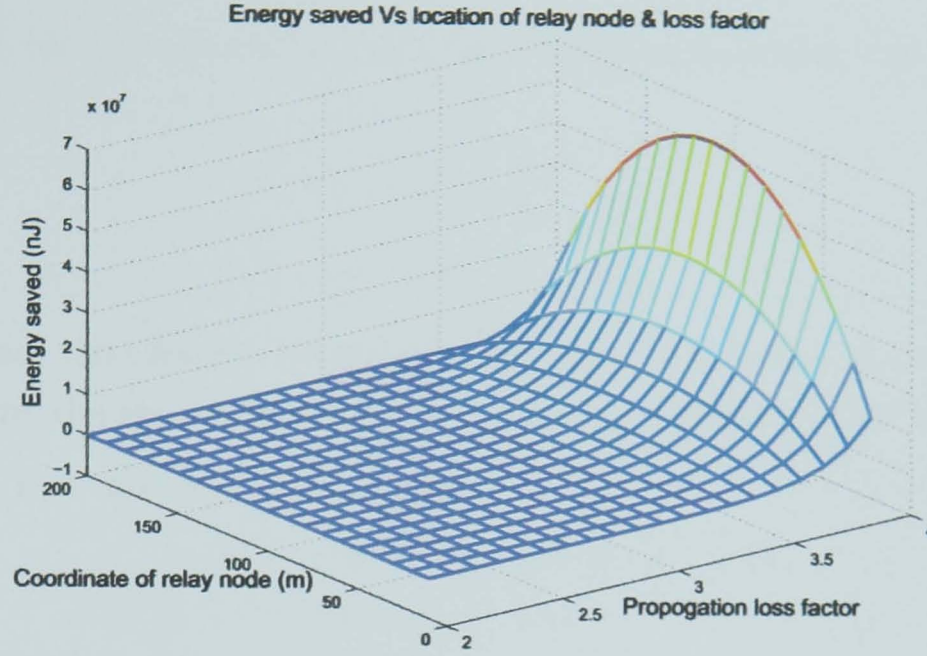
Figure 5.2: Energy saved versus location of forward node & loss factor

where e_e is the energy consumed by the transceivers electronics per bit, and e_a is the energy consumed in the transmitter RF amplifier per bit. e_e and e_a are determined by the design characteristics of the transceivers. Based on [64] and [65], the typical values of these parameters are: $e_e = 3.32 \times 10^{-7}$ J/bit and $e_a = 8 \times 10^{-11}$ $J/bit/m^2$ for $n = 2$, where n is the power index of the propagation path loss, which is typically between 2 and 4; R is the node transmission range, which can be set to be equal to the distance between the two nodes $(R = d)$.

5.2.1 Relay node location

As shown in Fig. 5.1, the relay node is node C at location (x), where the distance between A and C is h, and the distance between B and C is g. To achieve energy efficiency, the energy consumption when the relay node is involved must be smaller than the energy consumption without the relay node, leading to:

$$(e_e + e_a d^n) + e_e >$$
$$(e_e + e_a h^n) + [e_e + (e_e + e_a g^n)] + e_e. \qquad (5.2)$$

Introducing the coordinates of each node. the above inequality can be expressed as:

$$h^n + g^n < d^n - \frac{2e_c}{e_a}$$

$$x^n + (d-x)^n < d^n - \frac{2e_c}{e_a}, \tag{5.3}$$

which defines the effective energy efficient range of locations of the relay node. Furthermore, the energy saved (E_s) per packet by using the relay node is:

$$\begin{aligned} E_s &= \{(e_c + e_a d^n) + e_c - \\ &\quad (e_e + e_a h^n) - [e_e + (e_e + e_a g^n)] - e_e\} \times D \\ &= \{e_a[d^n - h^n - g^n] - 2e_e\} \times D \\ &= \{e_a[d^n - x^n - (d-x)^n] - 2e_e\}D, \tag{5.4} \end{aligned}$$

where D is the data packet transmitted from transmitter (A) to receiver (B). Given $D = 1$ *bit* and $d = 200$ *metres*, the relationship between the energy saved by utilizing the relay node, the location of the relay node and propagation loss factor is shown in Fig. 5.2. In Fig. 5.2. the energy saved increases when the relay node moves to the middle between the transmitter and the receiver (relay node's coordinate x=100). The energy saved when $n = 4$ is much more than the case when $n = 2$. According to the energy consumption model (equation 5.1). the energy consumption is much more sensitive to the transmission range when $n = 4$. compared to $n = 2$: much more energy will be consumed when the node transmission range increases for large n. It is noted that. energy saving includes both positive and negative values. which respectively mean less and more energy consumption compared to the energy consumption of direct transmission from the transmitter to the receiver. The positive and negative energy savings can be seen more clearly in Fig. 5.3. which shows the relationship between the energy saved by utilizing the relay node and the effective energy efficient zone of locations of relay node when $n = 2$. The zone of positive values (energy efficient zone) can be derived from equation 5.3 as follows:

$$(x - \frac{d}{2})^2 < \frac{d^2}{4} - \frac{e_c}{e_a}$$

$$\frac{d}{2} - \sqrt{\frac{d^2}{4} - \frac{e_c}{e_a}} < x < \frac{d}{2} + \sqrt{\frac{d^2}{4} - \frac{e_c}{e_a}}. \tag{5.5}$$
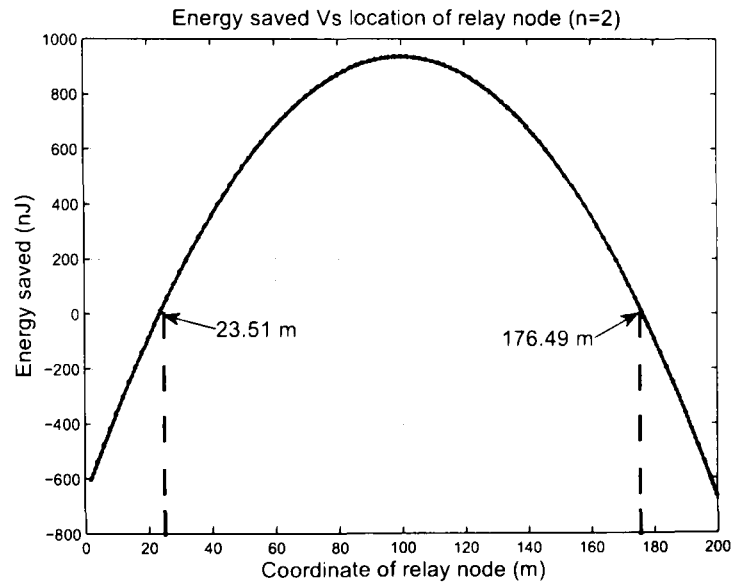
Figure 5.3: Energy saved versus location of forward node (n=2)

With $d = 200$, equation 5.5 was solved for $23.51 < x < 176.49$, which shows that the energy consumption is reduced by utilizing the relay node if the location of the relay node is within the above range. To meet the condition in equation 5.5, $\frac{d^2}{4} - \frac{e_c}{e_a} \geq 0$ must be satisfied, which can be solved resulting in:

$$d \geq 2\sqrt{\frac{e_c}{e_a}}. \tag{5.6}$$

where for the specific transceiver parameters in this chapter, $d \geq 128.8$. This means that energy consumption with a relay node does not achieve energy saving when the distance between the transmitter and the receiver is smaller than 128.4 metres, which is a function of the transceiver design parameters (e_c and e_a) and propagation coefficient.

5.2.2 Optimal transmission range

For an end-to-end multihop transmission, as shown in Fig. 5.4, the data packet is forwarded from the source node to the destination node, where the distance separating them is L. Assume that the range of each hop is r, the number of hops is derived as

$$m = \frac{L}{r}. \tag{5.7}$$
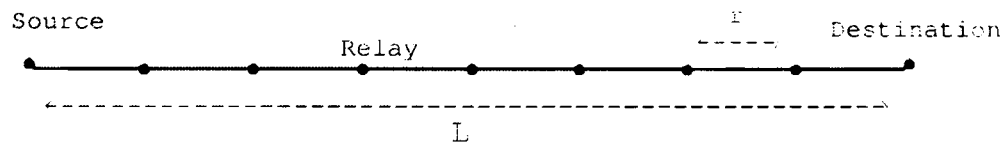
Figure 5.4: End-to-end multihop transmission
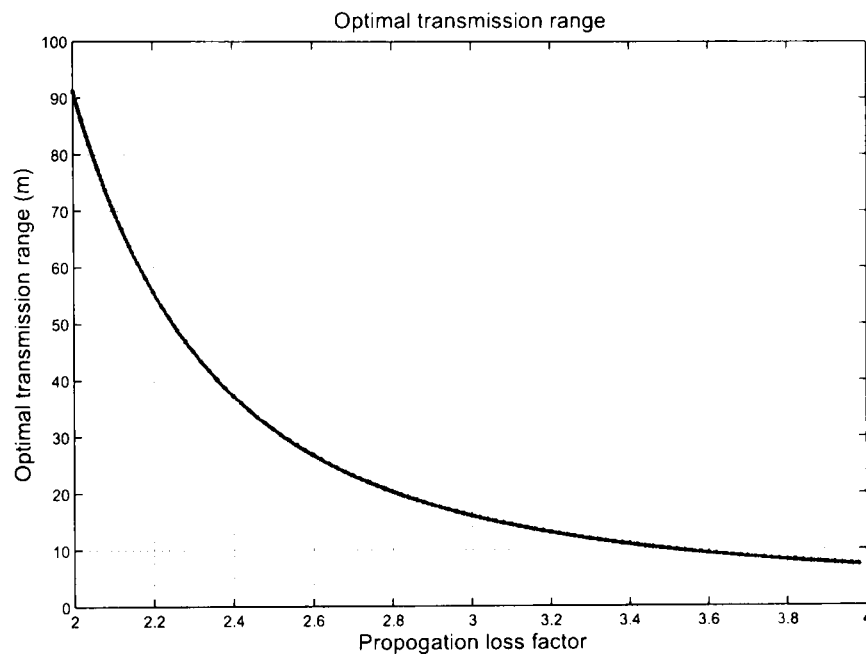
Figure 5.5: Optimal transmission range

Based on the energy consumption model mentioned before, the energy consumption of the end-to-end transmission is:

$$E_t = m \times \{[(e_e + e_a r^n)D] + (e_e D)\}$$
$$= \frac{L}{r} \times \{(2e_e + e_a r^n)D\}. \qquad (5.8)$$

To compute the minimum energy consumption, the first derivative of E_t with respect to the grid-length, r. $\partial E_t/\partial r = 0$:

$$\partial E_t/\partial r = LD[(n-1)e_a r^{n-2} - 2e_e r^{-2}] = 0. \qquad (5.9)$$

Solving equation 5.9 for r gives the optimal transmission range as:

$$r^n = \frac{2e_e}{(n-1)e_a}$$

$$r^* = \sqrt[n]{\frac{2e_e}{(n-1)e_a}}.$$

(5.10)

With specific transceiver parameters. equation 5.10 shows that the optimal transmission radio range, r^*, relates only to the propagation loss factor (n). and the relationship is shown in Fig. 5.5. In Fig. 5.5, the optimal transmission range decreases when the propagation loss factor (n) increases. As mentioned before. there is a trade off between the energy consumed in each hop and the number of hops. Based on equation 5.8, when the number of hops (m) is large. the transmission range of each hop (r) becomes small, and the fixed energy consumption of each hop (energy consumed for transceiver electronics) dominates the energy consumption. When the number of hops is small, the transmission range of each hop becomes large, and the energy consumed in the transmitter amplifier of each hop increases rapidly and dominates the energy consumption. When n is large. the energy consumed in the transmitter amplifier becomes relatively more important than the fixed energy consumption. and vice versa. Specifically, the optimal transmission range is 90.1 m when $n = 2$, with the transmitter and receiver parameters assumed.

5.2.3 Energy consumption of the multihop transmission model

Based on equation 5.8, the energy consumption for the multihop transmission model, shown in Fig. 5.4. is plotted in Fig. 5.6, where $L = 2000$ and $n = 2$. As have calculated in Section 5.2.2 the optimal transmission range is $r_{opt} = 90.1$ m. which corresponds to a number of hops $m = 23$ and the energy consumption of the multihop model $E_t = 29.16$ μJ. If the data packet is transmitted directly from the transmitter to the receiver, the energy consumption $E_t = 320.66$ μJ and the transmission range is 2000 m. Note that. the transmission delay time. which corresponds to the number of hops (m). is another important parameter essential in wireless and wired communications. The optimisation of energy consumption only may not satisfy the requirements of delay time. Therefore. the trade-off between total energy consumption (E_t) and delay was to be evaluated. The delay
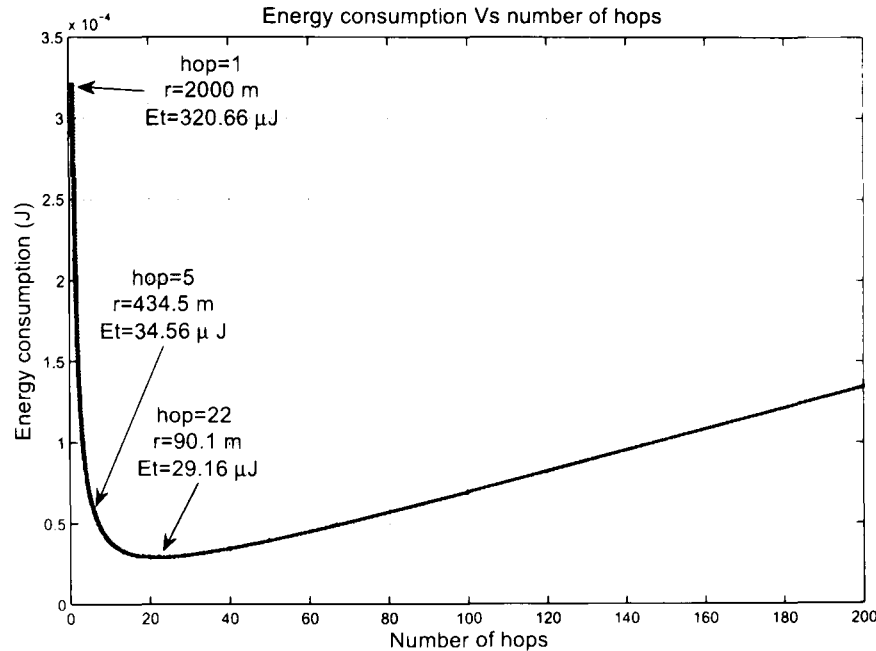
Figure 5.6: Energy consumption of multihop model

between transmitter and receiver is made up of the signal flight time between transmitter and receiver, and in the case of multihop transmission an additional processing delay is incurred at each intermediate relay node. The relay nodes can implement an 'amplify and forward' or a 'decode and forward' strategy. In either case an additional delay is incurred at each intermediate relay node. The end-to-end flight time is fixed regardless of the number of intermediate stops. The processing time increases as a linear function of the number of relay nodes (hops). Here the author use m as a measure of the processing time end-to-end. Since E_t and m use different units, they need to be normalised in advance and the following function should be minimised to achieve the optimal performance given these two parameters.

$$f(E_t, m) = \theta E_{t_{normalised}} + (1 - \theta)m_{normalised}. \qquad (5.11)$$

where $f(E_t, m)$ is the function to be minimised, and θ is the weight index of total energy consumption. E_t is normalised using the energy consumption of the direct transmission from transmitter to receiver ($E_{t_{direct}} = 320.66\ \mu J$) $E_{t_{normalised}}$. The delay time index (m) is normalised by reference to the number of hops where

the minimum energy consumption is achieved in Fig. 5.6 at $m_{min} = 23$ and this is used to define $m_{normalised}$. Thus, the function to be minimised is given by:

$$f(E_t, m) = \theta \frac{E_t}{E_{t_{direct}}} + (1 - \theta) \frac{m}{m_{min}}. \tag{5.12}$$

With $\theta = 0.5$, the minimum value of $f(E_t, m)$ is 0.2178, at which point $E_t = 34.56 \ \mu J$, $r = 434.5 \ m$ and $m = 5$. Compared to the energy consumption of direct transmission $(E_{t_{direct}})$, the energy consumption with the optimal transmission range and the energy consumption under the range dictated by the trade-off between energy consumption & delay time result in energy saving by 90.1% and 89.2%, respectively. Under single hop transmission, the delay incurred over the 2000-metre link span is 6.7 μs. The delay parameters associated with a 9.2 Mb/s Decode-and-Forward relay node that processes a 1296-bit packet are: transmission delay of 140 μs, detection latency 10 μs, decoding latency 80 μs, re-encoding latency 10 μs, resulting in a total processing delay of 240 μs for 1296 bits and a processing delay of 0.185 μs per bit [142]. Under the optimal transmission range, m=23 results in processing delay of 4.2 μs and total delay of 10.9 μs. The increase in delay is 62% compared to the delay associated with direct transmission. Under the delay-energy tradeoff scheme introduced, m=5, the additional delay is 0.9 μs, and total delay is 7.6 μs. The increase in delay is 13% compared to direct transmission. Note that the energy saving under the two schemes were 90.1% and 89.2% respectively and given the modest increase in delay (13%) under scheme 2 (energy-delay tradeoff), this is the better scheme.

5.2.4 Effect of dynamic data traffic

The analysis above is based on a static data traffic model, in which only one packet is transmitted from the source to the destination node. Therefore, the packet forwarded through the linear network has the same size. Here we will discuss and analyse the impact of dynamic data traffic. In the linear network, the nodes, which are uniformly distributed along the network, are clustered and data traffic is transmitted (consider nodes as sensors) to the head node of each cluster, and then the data is relayed to the sink node by each head node. As
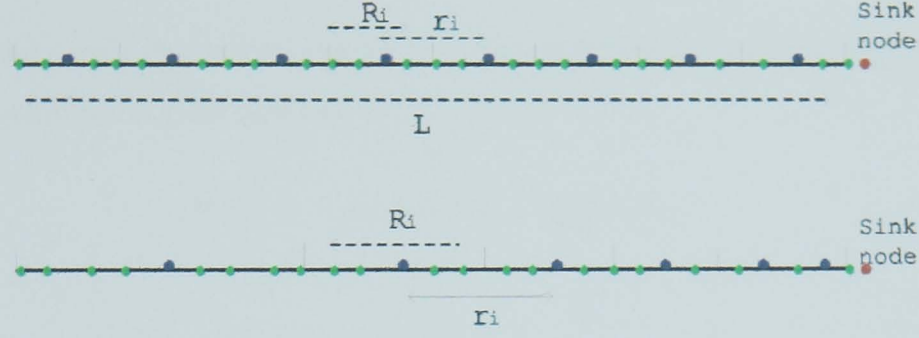
Figure 5.7: Equal-range and adjustable-range models

shown in Fig. 5.7 , each head node gathers data from the normal nodes of its cluster (the ith node gathering data from the ith cluster). R_i is the size of the ith cluster and r_i is the transmission range of the ith head node, where

$$R_i = \frac{r_i + r_{(i+1)}}{2}. \tag{5.13}$$

As shown in Fig. 5.7, the energy consumption of both equal-range and adjustable-range models are analysed here.

Equal-range model

Similar to the equal hop multihop model discussed above, in the equal-range model, the range of each hop is equal and the coverage of each cluster is equal. Based on equation 5.13, $R_i = r_i$ in the equal-range model. According to the experimental results of [143], the energy consumed for sensing temperature or light by each node occupies less than 0.1% of the total energy consumption of the node, which can be neglected. Furthermore, to calculate the energy consumption of the linear network, the nodes are classified as normal nodes (N_n) and head nodes (N_h).

The energy consumed by the normal nodes is only for transmitting, which can be derived based on equations 5.1:

$$E_{N_n} = [e_e + e_a(\frac{R_i}{2})^n]D_{unit}. \tag{5.14}$$

where D_{unit} represents the data gathered by each normal node. With a transmission range of $\frac{R_i}{2}$, any normal node in the ith cluster is able to transmit data

to the ith head node, no matter where their location is. The energy consumed by the i_{th} head nodes can be derived as:

$$E_{N_h i} = e_e D_{ri} + [e_e + \epsilon_a r_i^n] D_{ti}.$$ (5.15)

where

$$D_{ti} = (L - (i-1)R)\lambda$$
$$D_{ri} = (L - iR)\lambda.$$ (5.16)

where R is the transmission range of each head node and λ denotes the traffic data (bits) intensity per metre ($bits/m$).

By using equations 5.14, 5.15 and 5.16, the energy consumption of the entire network is:

$$E_{total} = \sum_{i=1}^{m} E_{N_h i} + (N - m) \times E_{N_n}.$$ (5.17)

where N is the number of nodes in the linear network and m is the number of head nodes (number of hops).

Adjustable-range model based on Genetic Algorithms

Nodes near the sink will relay more traffic than nodes at the other end of the network and their energy will be drained out much sooner than the nodes far from the sink. Therefore, to balance the energy consumption of each node, the nodes near to the sink should have a smaller transmission range to reduce the energy consumption. Here, we compare the energy consumption of the equal-range and the adjustable-range models, where a Genetic Algorithm is used to set up the adjustable-grid model.

Based on the adjustable-range linear model, as illustrated in Fig. 5.7, the fitness function in the Genetic Algorithm is:

$$E_{total} = \sum_{i=1}^{m} E_{N_h i} + (N - m) \times E_{N_n}.$$ (5.18)

where E_{N_n} and $E_{N_h i}$ respectively represent the energy consumed by the normal nodes and the ith head nodes:

$$E_{N_n} = [e_e + e_a(\frac{R_{normal_i}}{2})^n]D_{unit}. \qquad (5.19)$$

where D_{unit} represents the data gathered by each normal node and R_{normal_i} is determined by equation 5.13;

$$E_{N_h i} = e_e D_{ri} + (e_e + e_a r_i)^n D_{ti}. \qquad (5.20)$$

where

$$D_{ti} = (L - r_1 - r_2... - r_{i-1})\lambda$$
$$D_{ri} = (L - r_1 - r_2... - r_i)\lambda. \qquad (5.21)$$

r_i ($1 \leq i \leq m$) represent the chromosomes in the GA algorithm based on which new chromosomes are reproduced in each generation.

To compare the energy consumption in the two models, the parameters utilised are: $n = 2$, $N = 100$, $L = 2000\ m$, $\lambda = 1\ bits/m$, and $D_{unit} = \frac{L \times \lambda}{N} = 20\ bits$. Given enough generations (about 20000 generations) in the GA adjustable-range model, the minimum of the fitness function (minimum energy consumption) is computed: $E_t = 0.0291 J$, where $m = 22$.

With the same parameters listed above. in the equal-range model. the relationship between energy consumption and the number of hops is plotted in Fig. 5.8. The minimum energy consumption is 0.0317 J and it occurs when there are 25 hops. By comparing the minimum energy consumption of equal-range to the energy consumption of the adjustable-range models, as shown in Fig. 5.8. the adjustable-range model saves energy by about 8.5%. Note that. in the adjustable-range model, the energy consumption of each head node is much more balanced than that of the equal-range model.

5.3 Energy-efficient geographic routing

An energy-efficient geographic routing algorithm is proposed for a linear ad-hoc wireless network, where N nodes are randomly distributed along a linear network
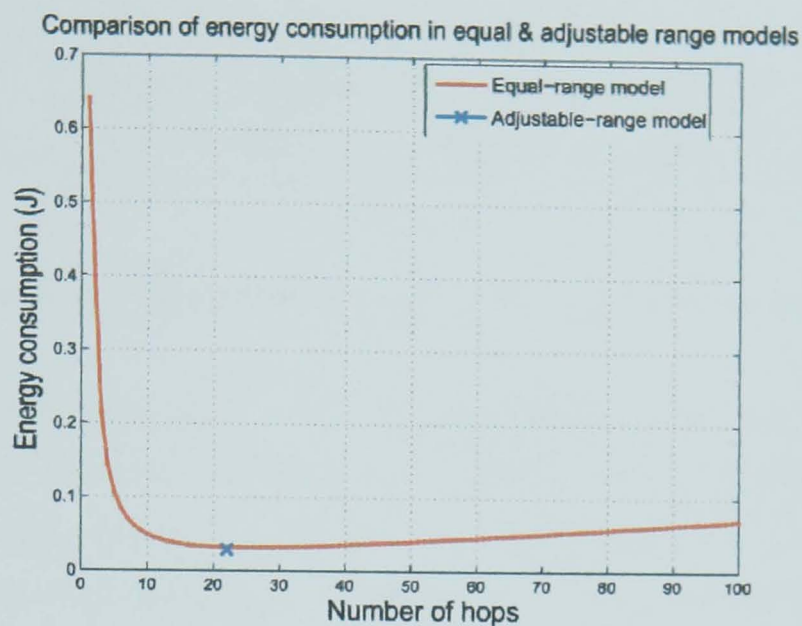
Figure 5.8: Energy consumption comparison of equal and adjustable-range models

of length L, as shown in Fig. 5.9. The coordinates of the transmitter and the receiver nodes are (0) and (L); r_{opt}, which determines the best location of the next hop node, is the optimal transmission range computed based on equation 5.10 ($r_{opt} = 90.1$ m for $n = 2$); Δd is the distance between the best location and the neighbour node; In the simulation, each node is equipped with the same radio transceiver that enables a maximum transmission range r_{max}. The location information (coordinate) of each node is obtained by using GPS and is shared with its neighbours through periodic broadcasting. The location information of the source and the destination nodes is included in the transmitted packet. Note that, in this simulation, the author only considers one packet transmitted from the source node to the destination node, forwarded by the relay nodes. Therefore, in the forwarding scheme of each relay node, the next hop node can be selected according to the local geographic information and the location of the destination node.

To achieve energy efficiency, the next hop node can be selected based on the new Optimal Range Forward (ORF) algorithm, where the next hop node is selected based on the optimal transmission range. Furthermore, considering the balance of residual energy of every node, the author proposes the Optimal Forward with Energy Balance (OFEB) algorithm, in which both energy consumption
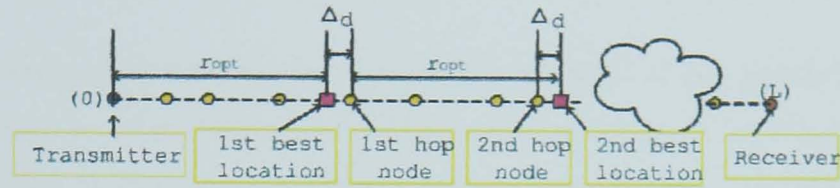
Figure 5.9: Forwarding scheme (next hop node selection)

and the energy balance of each node are considered. ORF and OFEB are com-
pared to the Most Forward within Radius (MFR) algorithm, see algorithm 1.1.
In OFEB, the weight indexes (α and $(1-\alpha)$) are assigned to Δd, which relates to
the energy consumption, and E_{res}, which is the residual energy of the neighbours
and relates to the energy balance. Intuitively, without considering the energy
balance, some nodes may be frequently selected as the relay nodes, and their
energy may be drained out much sooner compared to other nodes. The network
will then be partitioned. Since E_{res} and Δd use different units, they need to be
normalised first. E_{res} is normalised with respect to the default energy capacity
of each node (E_{cap}) to define $E_{res_{normalised}}$ ($E_{cap} = 10\ mJ$ in the simulation); Δd
is normalised with respect to the optimal transmission range ($r_{opt} = 90.1\ m$) to
define $\Delta d_{normalised}$. Thus, the function to be minimised is:

$$f(E_{res}, \Delta d) = \alpha \frac{\Delta d}{r_{opt}} - (1 - \alpha) \frac{E_{res}}{E_{cap}}, \qquad (5.22)$$

which is utilised as the criterion for locating the next hop node in OFEB. With
reference to the four algorithms 5.1 to 5.4, note that the two existing algorithms,
MFR and NFP perform as follows. MFR selects as the next hop node the node
nearest to the maximum range allowed in the system. NFP selects the node
nearest to the sender. Therefore both algorithms do not make use of the optimal
range that minimises the energy consumption as derived in this chapter. The
optimal range includes the d^n loss effect and the multihop forwarding losses as in
equation 5.10. The new ORF algorithm selects as the next hop the node nearest
to the optimal transmission range (so long as it is within the max allowed range)
and therefore minimises the energy consumption. The new OFEB algorithm
selects the next hop node as the node (within the maximum transmission range)
that minimises equation 5.22. This is a node that uses the best combination

of energy reserves and needs the minimum energy to be reached. The weight factor α determines the relative significance placed on these two requirements. Therefore, OFEB is superior in concept and performance as will be seen. Note that, in ORF and OFEB forwarding algorithms and based on equation 5.6, the relay node is needed only when the distance between the source node and the destination node is larger than $2\sqrt{\frac{e_e}{e_a}}$ metres.

For sender node:

Search the neighbour farthest from the sender

     and within the maximum transmission range

Node(i) is selected as the relay node

Node(i) becomes the new sender node

Repeat the above procedure

......

Algorithm 5.1: The forwarding algorithms of MFR

For sender node:

Search the neighbour nearest to the sender

     and within the maximum transmission range

Node(i) is selected as the relay node

Node(i) becomes the new sender node

Repeat the above procedure

......

Algorithm 5.2: The forwarding algorithms of NFP

5.3.1 Simulation results

Using the geographic routing algorithm, the simulation of a linear ad-hoc wireless network (Fig. 5.9) is carried out, and the parameters used in the simulation are listed in Table 5.1.

For sender node:

Compute the best location of the next neighbour node

Compare Δd of each neighbour

and within the maximum transmission range

Node(i) with the smallest Δd is selected as the relay node

Node(i) becomes the new sender node

Repeat the above procedure

......

Algorithm 5.3: The forwarding algorithms of ORF

For sender node:

Compute the best location of the next neighbour node

Compare $[\alpha \frac{\Delta d}{r_{opt}} - (1 - \alpha)\frac{E_{res}}{E_{cap}}]$ of each neighbour

and within the maximum transmission range

Node(i) with minimum value is selected as the relay node

Node(i) becomes the new sender node

Repeat the above procedure

......

Algorithm 5.4: The forwarding algorithms of OFEB

Propagation factor (n)	2
Network length	2000 m
Number of nodes (N)	500
Running time (t)	0.1 sec
Node energy capacity (E_{cap})	0.001 J
Optimal transmission range (r_{opt})	90.1 m
Maximum transmission range (r_{max})	250 m

Table 5.1: Simulation parameters
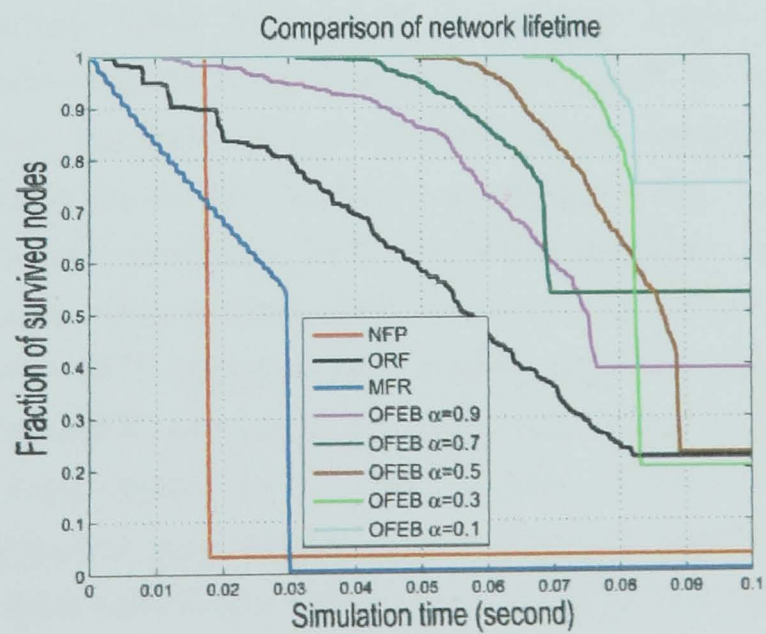
Figure 5.10: Comparison of network lifetime

In Fig. 5.10, the author simulates the network lifetime in a linear ad-hoc wireless network based on different forwarding algorithms: MFR, NFP, ORF and OFEB (different weight indexes are applied). In Fig. 5.10, the horizontal line of each algorithm which represents the number of surviving nodes indicates that there is no transmission in the network (network disconnection). Thus the ratio of the network lifetimes of each algorithm is shown below: $MFR : NFP : ORF : OFEB(\alpha = 0.9) : OFEB(\alpha = 0.7) : OFEB(\alpha = 0.5) : OFEB(\alpha = 0.3) : OFEB(\alpha = 0.1) = 0.20 : 0.34 : 0.91 : 0.85 : 0.79 : 1 : 0.92 : 0.92$. It shows that the OFEB algorithm (especially with $\alpha = 0.5$) has better network lifetime performance compared to the other algorithms. Furthermore, both the delays associated with transmission and processing of each hop are considered. The transmission delay is determined by the transmission distance and the electromagnetic wave speed. The processing delay of each hop is 0.185 μs per bit [142], as mentioned in Section 5.2.3. With the constraint of computer memory, the simulation time chosen in Fig. 5.10 is 0.1 second, which demands about 10^6 loops in the simulation.

Since MFR selects the Most Forward node within Radius to be the next hop node, the delay time (number of hops) of one transmission is smaller than the other algorithms; while NFP selects the nearest neighbour to be the next node, which means that the delay time (number of hops) is larger than the other algorithms. Thus, the data packets received by the destination node of these different algorithms should be compared, as shown in Fig. 5.11. It shows that, before the network disconnection, with the OFEB algorithm, the destination node received much more data packets than the other algorithms. In Fig. 5.11, the received data with MFR increases more rapidly than the other algorithms. The reason is that the MFR selects the next hop node as far as possible, therefore, the number of hops needed for the data packets transmitted from the source node to the destination node is smaller than the other algorithms. Based on the real simulation time calculation mentioned, the simulation time needed for data transmitted from the source node to the destination node is less than the other algorithms. Since NFP selects the next hop node as near as possible, therefore the delay time for data transmitted from the source node to the destination node
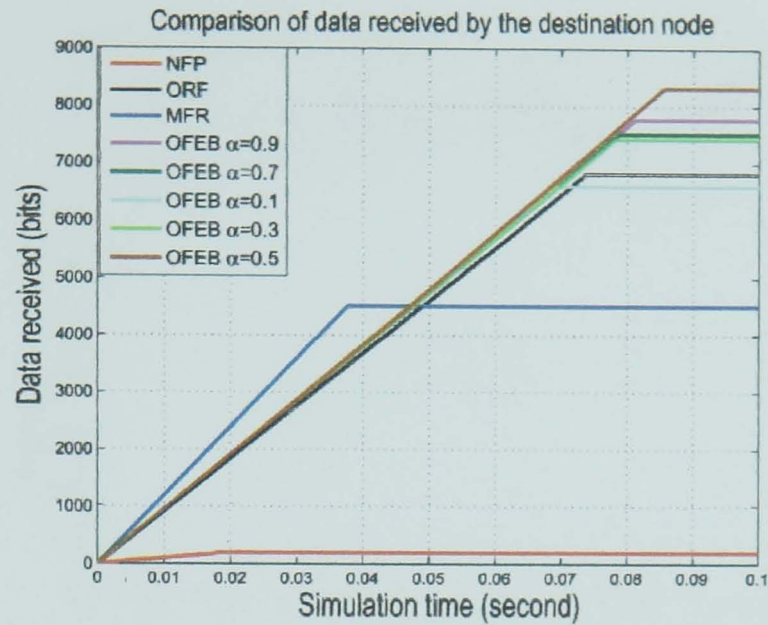
Figure 5.11: Comparison of data (packets) received by the destination node

is more than the other algorithms. Thus the slope of the NFP curve is smaller than the others.

Furthermore, the energy consumption of each packet successfully received by the destination node based on different algorithms are compared, where the ratio of energy consumption of each packet are: $MFR : NFP : ORF : OFEB(\alpha = 0.9) : OFEB(\alpha = 0.7) : OFEB(\alpha = 0.5) : OFEB(\alpha = 0.3) : OFEB(\alpha = 0.1) = 0.0541 : 1 : 0.0234 : 0.0251 : 0.0280 : 0.0211 : 0.0230 : 0.0224$. This shows that the OFEB and the ORF algorithms have better performance than the others, and that the NFP algorithm demands the most energy consumption for one packet successfully received by the destination node.

Furthermore, in Fig. 5.12, the remaining energy of nodes in both ORF and OFEB ($\alpha = 0.5$) are compared, where $*$ represents the ORF algorithm and o represents the OFEB algorithm. The nodes selected in ORF are used until they are out of energy, while the energy consumed at each node of OFEB is more balanced. Therefore, based on the network lifetime definition of "time duration before the first node dies", OFEB is much better than ORF.
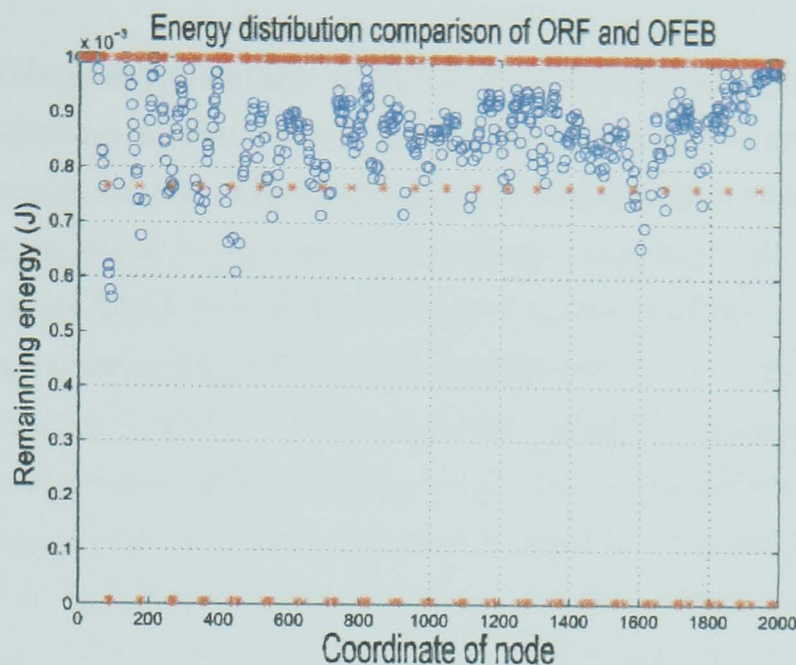
Figure 5.12: Comparison of remaining energy of nodes

5.4 Summary

In this chapter, the author proposed energy-efficient geographic routing algorithms to prolong the network lifetime. Among existing geographic routing algorithms, MFR selects as the next hop node the node nearest to the maximum range allowed in the system. NFP selects the node nearest to the sender to be the next hop node. Both algorithms do not make use of the optimal transmission range that minimises the energy consumption as derived in this chapter. Our new ORF algorithm selects as the next hop node the node nearest to the optimal transmission range (within the maximum range) and therefore minimises the energy consumption. Our new OFEB algorithm selects the next hop node as the node (within the maximum range) that minimises the value of $[\alpha\frac{\Delta d}{r_{opt}} - (1-\alpha)\frac{E_{res}}{E_{cap}}]$. This is a node that has the best combination of energy reserves and needs the minimum energy to be reached. The weight factor α determines the relative significance placed on these two requirements. The simulation results show that the OFEB algorithm has the best performance in terms of network lifetime and amount of data received by the destination node. Note that, among OFEB algorithms, selection of (α)'s value need to be considered based on different nodes distribution to achieve the optimal performance.

100

Also, in this chapter the author introduced a method that can be used to select the optimum locations of relay nodes, and derived the range of relay node location that result in energy saving. The optimal node transmission range was derived in terms of the propagation loss factor. The energy consumption of a multihop ad-hoc wireless network has been computed based on the optimal transmission range and has also been computed under direct transmission where the source and destination communicate directly. Multihop with optimal transmission range saves 90.1% energy compared to direct transmission. The trade-off between energy consumption and delay time has been analysed to achieve a balanced performance in terms of energy consumption and delay time, and the results show with modest increase in delay (13%), the trade-off scheme saves energy by 89.2% compared to direct transmission. In a dynamic traffic scenario, the author proposed cluster based energy consumption models taking into account both equal hop and adjustable hop scenarios, where the adjustable-range model is based on a Genetic Algorithm. The results show that the adjustable-range (GA) model is more energy efficient than the equal-range model.

Chapter 6

Energy Efficient Geographic Routing in 2-D Ad-hoc Wireless Networks

6.1 Introduction

To evaluate the impact of a realistic ad-hoc wireless network scenario, the proposed energy efficient Geographic Routing algorithms are studied for the first time in a 2-D ad-hoc wireless network scenario.

In this chapter, the Optimal Range Forward (ORF) algorithm, in which the next hop node is selected based on the optimal transmission range, is proposed to minimise the total energy consumption associated with data transmission (summation of energy consumption of all hops) in 2-dimensional networks. Furthermore, based on ORF, the Optimal Forward with Energy Balance (OFEB) algorithm, in which the next-hop node is selected not only according to the optimal transmission range but also the remaining energy of each neighbour node, is proposed to prolong the network lifetime. In the OFEB algorithm, the total energy consumption associated with the transmission and the residual energy of each

node are both considered to prolong the network lifetime. The network lifetime and the data received by the destination node. resulting from all the algorithms above. are compared in our simulation. and it is shown that the performance of the OFEB algorithm is significantly better than the others. In this chapter. the network lifetime, the network throughput. the number of packets success-fully received by the destination and the average energy cost of each successfully received packet, resulting from all the algorithms above. are compared based on different node densities. It is shown that the performance of the OFEB algorithm is significantly better than the others. Also, in a 2-D ad-hoc wireless network. the method for locating relay node is analysed, and the range of relay node locations that result in energy saving is derived.

6.2 Energy consumption model

The energy consumed by ad-hoc wireless network nodes is the sum of energy consumed for transmitting, receiving and listening. Considering a transmission from a transmitter to a receiver. where the distance between them is R. the received signal power can be expressed as [3]:

$$p_r(R) = \frac{p_t G_t G_r \lambda^2}{(4\pi)^2 R^n Loss}.$$ (6.1)

where G_t and G_r are respectively the gains of the transmitter and receiver. The carrier wavelength is λ and $Loss$ represents any additional losses in the transmis-sion, n is the propagation loss factor. which is typically between 2 and 4. Thus, with $G_t = G_r = 1$. and $Loss = 1$, the received signal power is

$$p_r(R) = \frac{p_t \lambda^2}{(4\pi)^2 R^n}.$$ (6.2)

To be successfully received by the receiver. the received signal power must be above a certain threshold power (p_{thr}). Therefore, the signal power at the transmitter must be above $\frac{p_{thr}(4\pi)^2 R^n}{\lambda^2}$. Assuming one signal represents one bit data information, the energy consumed for transmitting is

$$E_t = (c_c + \frac{p_{thr}(4\pi)^2 R^n}{\lambda^2}) \times D$$
$$= (c_c + c_a R^n) \times D.$$ (6.3)
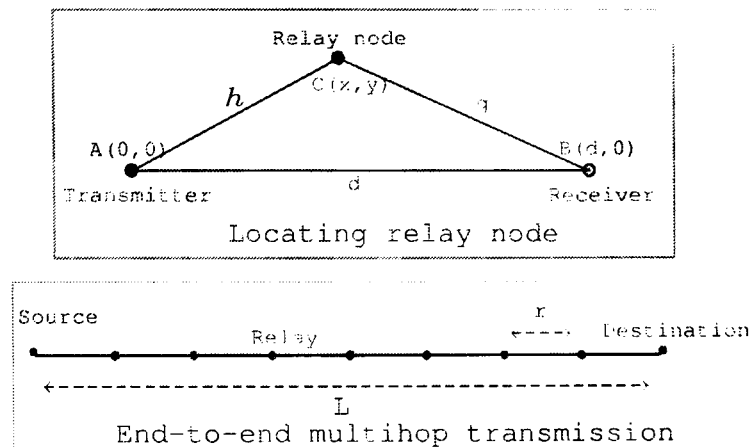
Figure 6.1: Locating relay node and end-to-end multihop transmission

where, D represents traffic data bits, e_e is the energy/bit consumed in the transmitter electronics, and $e_a = \frac{p_{thr}(4\pi)^2}{\lambda^2}$, which can be considered as the energy/bit consumed in the transmitter RF amplifier. Furthermore, the energy cost at the receiver is considered to be only consumed for electronics, thus the energy consumption model utilised in this chapter is:

$$E_t = (e_e + e_a R^n)D$$

$$E_r = e_e D, \qquad (6.1)$$

Based on [64] and [65], the typical value of e_e is: $e_e = 3.32 \times 10^{-7}\ J/bit$. Given $p_{thr} = 8 * 10^{-15}\ w$ and with a carrier frequency $f = 2.4 * 10^9\ Hz$ (which is an unlicensed frequency band and one of the most popular in radio based networking). e_a is computed as: $e_a \approx 8 \times 10^{-11}\ J/bit/m^n$.

6.2.1 Relay node location

Considering the simple model shown in Fig. 6.1. node A. located at $(0, 0)$. is the transmitter and node B, located at $(d, 0)$, is the receiver. As shown in Fig. 6.1. the relay node is set to be node C at location (x, y), where the distance between A and C is h, and the distance between B and C is g. To achieve energy efficiency. the energy consumption when the relay node is involved must be smaller than the energy consumption without the relay node. leading to:

$$(e_e + e_a d^n) + e_e > (e_e + e_a h^n) + [e_e + (e_e + e_a g^n)] + e_e \qquad (6.5)$$

Introducing the coordinates of each node, the above inequality can be expressed as:

$$h^n + g^n < d^n - \frac{2e_e}{e_a}$$

$$[x^2 + y^2]^{\frac{n}{2}} + [(d-x)^2 + y^2]^{\frac{n}{2}} < d^n - \frac{2e_e}{e_a}. \tag{6.6}$$

which defines the effective energy efficient zone of locations of the relay node. Furthermore, the energy saved (E_s) per packet by using the relay node is:

$$
\begin{aligned}
E_s &= \{(e_e + e_a d^n) + e_e - \\
&\quad (e_e + e_a h^n) - [e_e + (e_e + e_a g^n)] - e_e\} \times D \\
&= \{e_a[d^n - f^n - g^n] - 2e_e\} \times D \\
&= \{e_a[d^n - [x^2 + y^2]^{\frac{n}{2}} - [(d-x)^2 + y^2]^{\frac{n}{2}}] - 2e_e\}D, \tag{6.7}
\end{aligned}
$$

where D is the data packet transmitted from transmitter (A) to receiver (B). Given $D = 1$ *bit* and $d = 200$ *metres*, the relationship between the energy saved by utilizing the relay node and the location of the relay node is shown in Figs. 6.2 and 6.3 for $n = 2$ and $n = 4$ respectively. In both Fig. 6.2 and Fig. 6.3. the energy saved increases when the relay node moves to the middle between the transmitter and the receiver ((100,0)). By comparing these two figures. the energy saved when $n = 4$ is much more than the case when $n = 2$. According to the energy consumption model (equation 6.4), the energy consumption is much more sensitive to the transmission range when $n = 4$, compared to $n = 2$: much more energy will be consumed when the node transmission range increases for large n. It is noted that. energy saving includes both positive and negative values. which respectively mean less and more energy consumption compared to the energy consumption of direct transmission from the transmitter to the receiver.

Specifically. for the case of $n = 2$. the zone of positive values (energy efficient zone) can be derived from equation 6.6 as follows:

$$\left(x - \frac{d}{2}\right)^2 + y^2 < \frac{d^2}{4} - \frac{e_e}{e_a}. \tag{6.8}$$
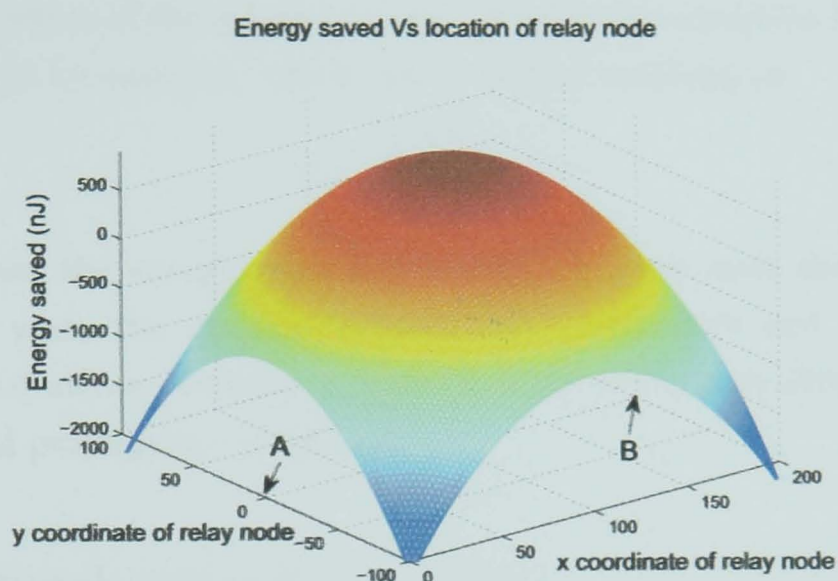
Figure 6.2: Energy saved versus location of relay node (n=2)
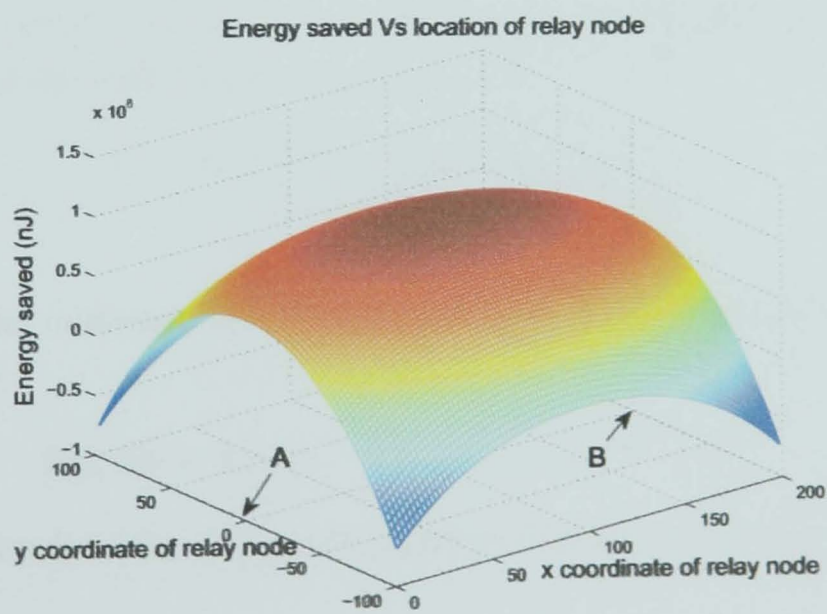
Figure 6.3: Energy saved versus location of relay node (n=4)

Thus, the relay node must be located in a sphere to achieve energy saving performance and the centre of the sphere is $(\frac{d}{2}, 0)$. To meet the condition in equation 6.8, $\frac{d^2}{4} - \frac{e_c}{e_a} \geq 0$ must be satisfied, which can be solved resulting in:

$$d \geq 2\sqrt{\frac{e_e}{e_a}}. \tag{6.9}$$

This means that the energy consumption with a relay node does not achieve energy saving when the distance between the transmitter and the receiver is small than 128.4 metres, which is a function of the transceiver design parameters (e_e and e_a) and propagation coefficient.

6.2.2 Optimal transmission range

For an end-to-end multihop transmission, as shown in Fig. 6.1, the data packet is forwarded from the source node to the destination node, where the distance separating them is L. Assume that the range of each hop is r, the number of hops is derived as

$$m = \frac{L}{r}. \tag{6.10}$$

Based on the energy consumption model mentioned in Section 6.2, the energy consumption of the end-to-end transmission is:

$$\begin{aligned} E_t &= m \times \{[(e_e + e_a r^n)D] + (e_e D)\} \\ &= \frac{L}{r} \times \{(2e_e + e_a r^n)D\}. \end{aligned} \tag{6.11}$$

To compute the minimum energy consumption, with respect to the grid-length, r, $\partial E_t/\partial r = 0$:

$$\partial E_t/\partial r = LD[(n-1)e_a r^{n-2} - 2e_e r^{-2}] = 0. \tag{6.12}$$

Solving equation 6.12 for r gives the optimal transmission range as:

$$r^n = \frac{2e_e}{(n-1)e_a}$$

$$r^\star = \sqrt[n]{\frac{2e_e}{(n-1)e_a}}. \tag{6.13}$$
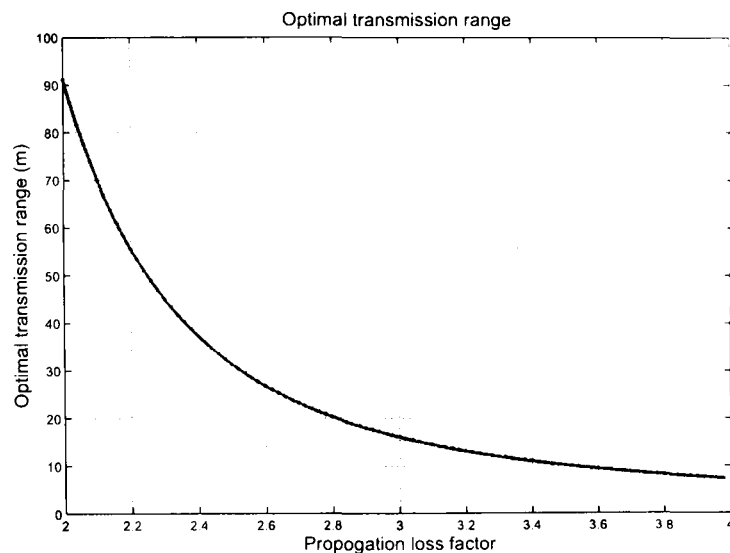
Figure 6.4: Optimal transmission range

With specific transceiver parameters, equation 6.13 shows that the optimal transmission radio range, r^*, relates only to the propagation loss factor (n), and the relationship is shown in Fig. 6.4. In Fig. 6.4, the optimal transmission range decreases when the propagation loss factor (n) increases. As mentioned, there is a trade off between the energy consumed in each hop and the number of hops. Based on equation 6.11, when the number of hops (m) is large, the transmission range of each hop (r) becomes small, and here the fixed energy consumption for each hop (energy consumed for transceiver electronics) dominates the energy consumption. When the number of hops is small, the transmission range of each hop becomes large, and the energy consumed in the transmitter amplifier of each hop increases rapidly and dominates the energy consumption. When n is large, the energy consumed in the transmitter amplifier becomes relatively more important than the fixed energy consumption, and vice versa. Specifically, the optimal transmission range is 90.1 m when $n = 2$, with the transmitter and receiver parameters assumed.

For current source node:

If $(d_{CD} < 2\sqrt{\frac{\epsilon_c}{\epsilon_a}})$

directly communicate to the destination node.

Else

relay node needed.

For current source node:

  Search the neighbour nearest to destination

      and within the maximum transmission range

  Node(i) is selected as the relay node

  Node(i) becomes the new current source node

  Repeat the procedure above

......

Algorithm 6.1: The forwarding algorithms of MFR

For current source node:

If $(d_{CD} < 2\sqrt{\frac{\epsilon_c}{\epsilon_a}})$

directly communicate to the destination node.

Else

relay node needed.

For the current source node:

  Search the neighbour nearest to the sender

      and within the maximum transmission range

  Node(i) is selected as the relay node

  Node(i) becomes the new current source node

  Repeat the procedure above

......

Algorithm 6.2: The forwarding algorithms of NFP

For current source node:

If $(d_{CD} < 2\sqrt{\frac{e_c}{e_a}})$

  directly communicate to the destination node.

Else

  relay node needed.

  For the current source node:

  Compute the best location of the next hop node

   Compare Δd of each neighbour

     and within the maximum transmission range

  Node(i) with smallest Δd is selected as the relay node

  Node(i) becomes the new current source node

  Repeat the procedure above

  ......

Algorithm 6.3: The forwarding algorithms of ORF
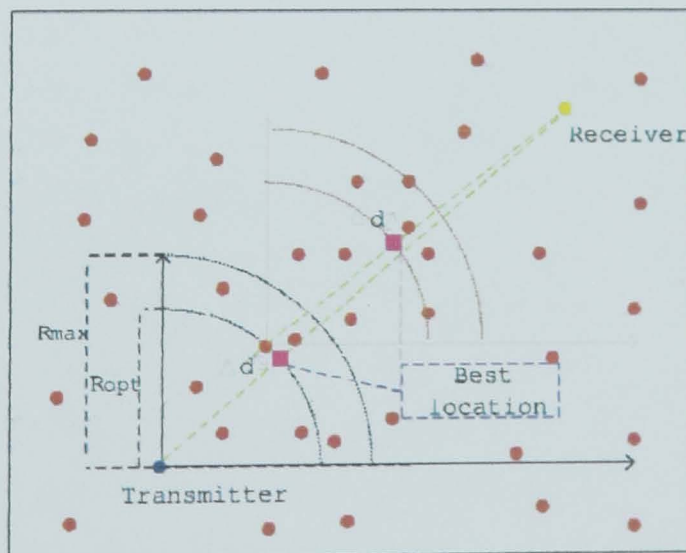
Figure 6.5: Forwarding scheme (next hop node selection)

For current source node:

If $\left(d_{CD} < 2\sqrt{\frac{e_c}{e_a}}\right)$

directly communicate to the destination node.

Else

relay node needed.

For current source node:

Compute the best location of the next hop node

Compare $\left[\alpha \frac{\Delta d}{r_{opt}} - (1 - \alpha)\frac{E_{res}}{E_{cap}}\right]$ of each neighbour

and within the maximum transmission range

Node(i) with minimum value is selected as the relay node

Node(i) becomes the new current source node

Repeat the procedure above

Algorithm 6.4: The forwarding algorithms of OFEB

6.3 Energy-efficient geographic routing algorithms

Based on the optimal transmission range, two energy-efficient GR algorithms for 2-D ad-hoc wireless networks are proposed in this chapter: the Optimal Range Forward (ORF) algorithm and the Optimal Forward with Energy Balance (OFEB) algorithm. In algorithms 6.3 and 6.4 respectively,both of them are compared to the existing GR algorithms, the Most Forward within Radius (MFR) algorithm and the Nearest Forward Progress (NFP). For each current source node, the distance to the destination node (d_{CD}) is compared to the threshold distance which is determined by equation 6.9, in order to determine whether a relay node is required or if the data packet can be transmitted to the destination node directly. MFR selects as the next hop node the node nearest to the maximum range allowed in the system. NFP selects the node nearest to the sender. Therefore both algorithms do not make use of the optimal range that minimises the energy consumption as derived in this chapter. The new ORF algorithm selects as the next hop the node nearest to the optimal transmission range (best location

as shown in Fig. 6.5, determined by the optimal transmission range) within the maximum allowed range and therefore minimises the energy consumption. In Fig. 6.5, the red dots represents nodes, the blue dot is the source node. the yellow dot is the destination node, the square is the best location of next hop node. Δd is the distance to the best location, R_{max} is the maximum transmission range. and R_{opt} is the optimal transmission range. The new OFEB algorithm selects the next hop node as the node (within the maximum transmission range) that minimises equation 6.14.

$$ f(E_{res}, \Delta d) = \alpha \frac{\Delta d}{R_{opt}} - (1 - \alpha) \frac{E_{res}}{E_{cap}}. \tag{6.14} $$

This is a node that uses the best combination of energy reserves and needs the minimum energy to be reached. The weight factor α determines the relative significance placed on these two requirements. Therefore. OFEB is superior in concept and performance as will be seen. In equation 6.14. Δd is the distance between the neighbour nodes and the best location and E_{res} is the residual energy of the neighbours. Intuitively, without considering the energy balance. some nodes may be frequently selected as the relay nodes. and their energy may be drained out very soon compared to other nodes. Since E_{res} and Δd use different units. they are normalised as shown in equation 6.14. E_{res} is normalised with respect to the default energy capacity of each node (E_{cap}) to define $E_{res_{normalised}}$; Δd is normalised with respect to the optimal transmission range to define $\Delta d_{normalised}$.

6.4 Simulation results

The simulation is carried out in a 2-D ad-hoc network model, as shown in Fig. 6.5. where N_n nodes are randomly distributed in the area. R_{max} is the maximum transmission range of each node. R_{opt}. which determines the best location of the next hop node. is the optimal transmission range computed based on equation 6.13 ($R_{opt} = 90.1 \, m$ for $n = 2$). Δd is the distance between the best location and the neighbour node. In the simulation. the location information (coordinates) of each node is obtained by using GPS and is shared with its neighbours through

Propagation factor (n)	2	Node energy capacity (E_{cap})	0.001 J
Number of nodes (N)	50-500	Normalised simulation time (t)	10^6 sec
Network length	500 m	Optimal transmission range (R_{opt})	90.1 m
		Maximum transmission range (R_{max})	250 m

Table 6.1: Parameters of simulation

periodic broadcasting. The location information of the source and the destination nodes is included in the transmitted packet. Therefore, in the forwarding scheme of each relay node, the next hop node can be selected according to the local geographic information and the location of the destination node. Using geographic routing, the simulation of a 2-D ad-hoc wireless network (Fig. 6.5) is carried out, and the parameters used in the simulation are listed in Table 6.1. Furthermore, to facilitate the comparison between the different GR algorithms, the source and destination nodes in each algorithm are fixed to (0,0) and (L.L) respectively, and the other nodes are randomly deployed. By running the simulation 1000 times, the average network lifetime and number of successfully received packets are determined.

6.4.1 Comparison of network lifetime and received packets in different GR algorithms

To compare the performance of the proposed GR algorithms to the existing algorithms, Fig. 6.6 shows both network lifetime and number of successfully received packets when the number of nodes deployed in the network is 500. In this chapter the author defines the network lifetime as the time duration until no source to destination connection can be made. In Fig. 6.6. the network lifetime is the time duration before the point at which the fraction of surviving nodes does not change any more (which represents the point at which no more nodes become drained). In order to compare different GR algorithms. the proportion ratio of the network
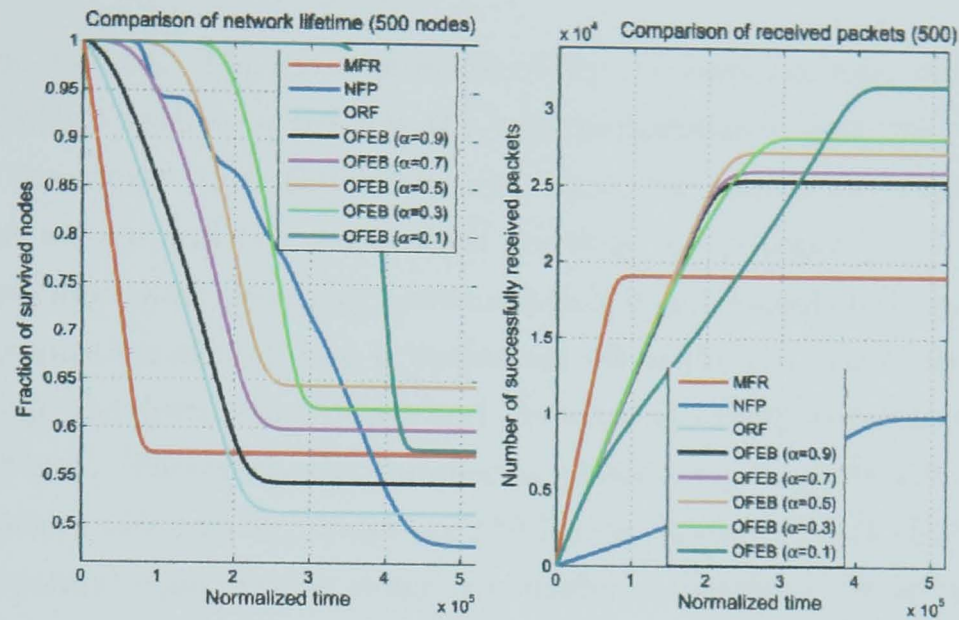
Figure 6.6: Comparison of the network lifetime and the packets received: 500 nodes

lifetime and received packets are compared in Table 6.2, and the results show that the network lifetime of the NFP algorithm is the longest among all algorithms and the performance of MFR is the worst. Since the neighbour node which is closest to the final destination will be selected as the next hop node in MFR, the energy consumed for each hop in MFR is more than the other algorithms, therefore the network lifetime performance of MFR is the worst. Note that, even thouth the network lifetime of NFP is the longest, the number of packets successfully received by the destination is much smaller than the other algorithms. As has been explained the neighbour nodes which is closest to the current source node will be selected as the next hop node in NFP, and this requires more hops and more energy consumption. In the simulation, the average number of hops used by the transmission between the source and the destination nodes is 5.7 in MFR and 51.4 in NFP (for the others see Table 6.2). This shows that the NFP algorithm uses too many hops for one successful transmission and the performance of NFP is limited even though its network lifetime is better than the others. Therefore, the network lifetime should not be the only parameter used to evaluate the performance of the algorithms. The author evaluated the number of packets successfully received by the destination to compare the network

performance as well. The ratio of successfully received packets, show that the OFEB algorithm with $\alpha = 0.1$ has the best performance. and the performance of NFP is the worst. For the MFR algorithm, the minimum number of hops between the source and the destination nodes is the criterion used in selecting the next hop node and the energy consumption is not considered. For NFP, the energy consumption of each hop is optimised while the number of hops between the source and the destination nodes and the network energy consumption are not been considered. Therefore, the number of packets received by the destination and the fraction of surviving nodes are the lowest among all GR algorithms. For ORF, the optimal transmission range is considered to reduce the network energy consumption. Therefore, the number of packets received by the destination and the fraction of surviving nodes are between those of MFR and NFP algorithms. For OFEB, not only the optimal transmission range but also the balance of node residual energy are considered to reduce the network energy consumption and prolong the network lifetime, and different weights (α and $1 - \alpha$) are considered. The results show that, compared to the ORF algorithm, the network lifetime has been significantly prolonged by considering the node residual energy balance in the OFEB algorithm, and the number of received packets increases. Note that, the ORF algorithm can be considered as a special case of OFEB, when the weight factor is $\alpha = 1$. Note that, with increasing weight factor. the time duration before the first node dies is significantly extended. The reason is that nodes with higher remaining energy will be selected as the next hop node. and therefore the loss of the first node is delayed.

6.4.2 Impacts of node density to different GR algorithms

In Fig. 6.7, the impact of node density (number of nodes) on both network lifetime and number of received packets is evaluated. The results show that both performances improve when the number of nodes increases. and the fraction of surviving nodes approaches 58% when the number of nodes is more than 100. Fig. 6.8 shows similar trends to Fig. 6.7. but the improvement in received packets is much less than that of MFR with increasing number of nodes. Furthermore. the fraction of surviving nodes in NFP decreases when the number of nodes increases.

No. of nodes	NFP	MFR	ORF	OFEB($\alpha = 0.9$)	0.7	0.5	0.3	0.1
Network lifetime								
500	1	0.21	0.53	0.53	0.55	0.56	0.64	0.89
No. of received packets								
500	0.31	0.60	0.80	0.80	0.82	0.86	0.89	1
Average of No. of hops								
500	51.4	5.7	10.6	10.7	10.8	10.3	11.5	14.2

Table 6.2: Comparison of network performance in different GR algorithms
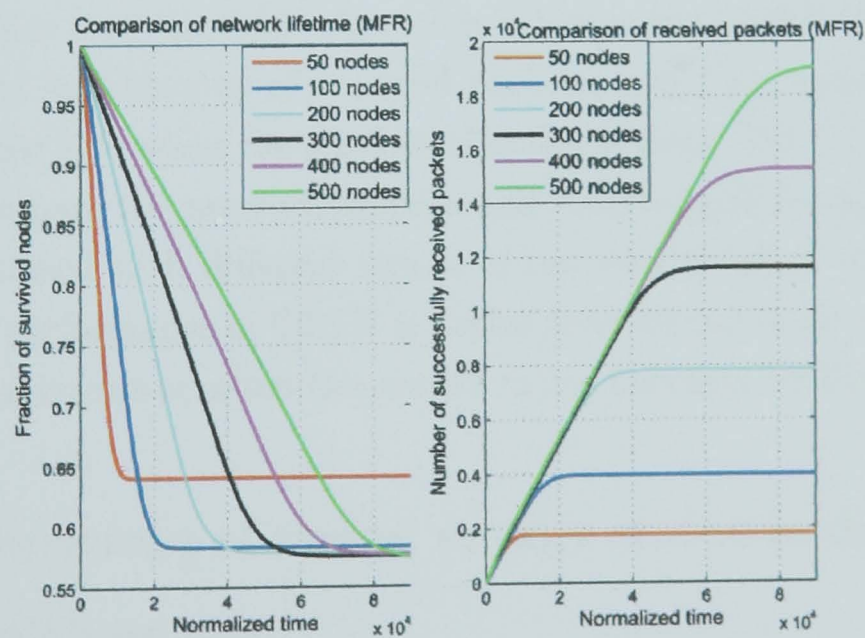
Figure 6.7: Impact on the network lifetime and the packets received: MFR
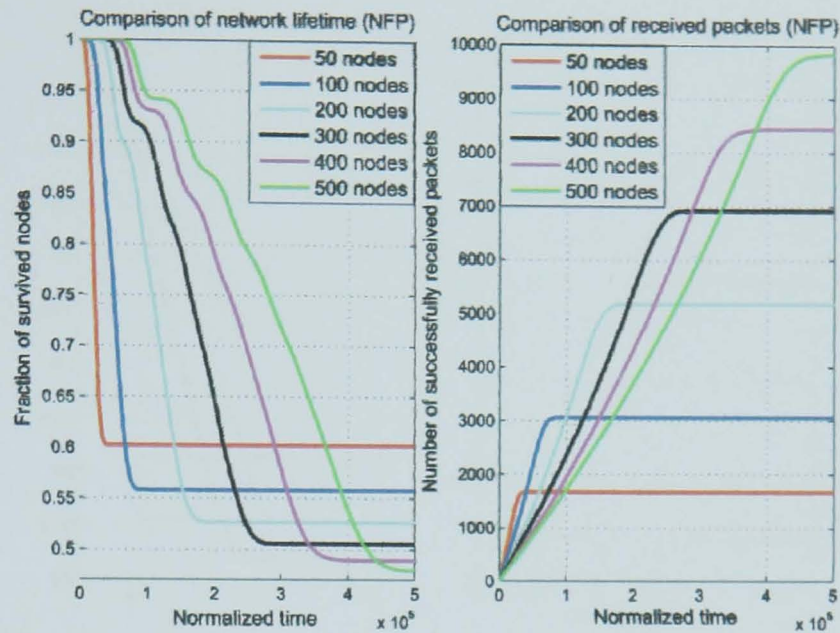
Figure 6.8: Impact on the network lifetime and the packets received: NFP

which means more nodes are drained out. The reason is that the forwarding algorithm in NFP only considers the distance between the neighbour nodes to the current source node if the neighbour nodes are closer to the final destination, and this involves more nodes in the transmission. By comparing Fig. 6.9 and Fig. 6.8, it is clear that the ORF algorithm is better than MFR in terms of both network lifetime and number of received packets, and the fraction of surviving nodes approaches 52% when the number of nodes is large. Fig. 6.10 and Fig. 6.11 respectively compare the network lifetime and received packets when the OFEB algorithm is utilised with different values of the weight factor (α). The results show that, the performance of OFEB is better than all the other algorithms, and the performance improves when the weight factor becomes smaller.

6.4.3 Comparison of nodes' energy status in different GR algorithms

The author noted that the fractions of surviving nodes are different when there are no connections in different GR algorithms. Fig. 6.12 and Fig. 6.13 show the 500-node energy status based on different GR algorithms when the network dies
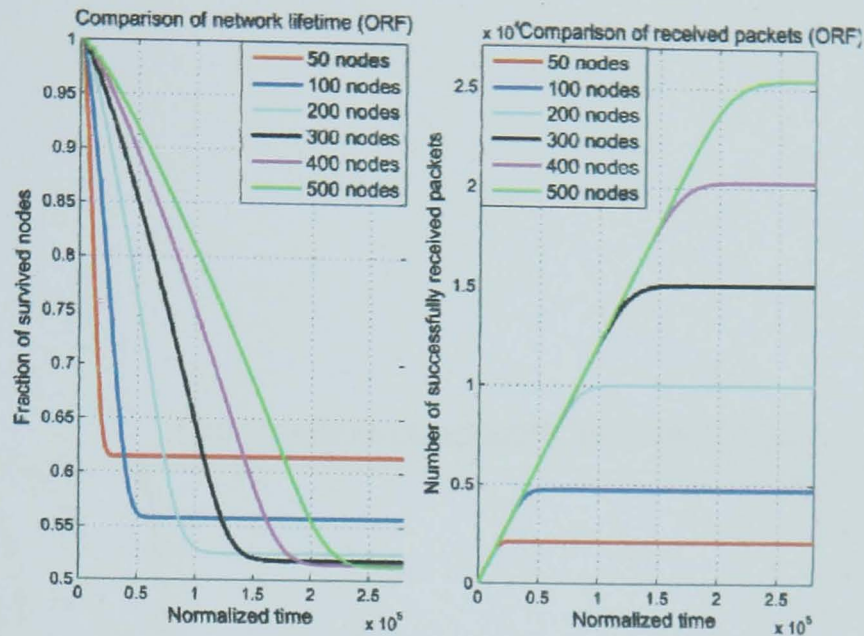
Figure 6.9: Impact on the network lifetime and the packets received: ORF

(no connection between the source and the destination nodes). In all figures, the source node is located at (0,0), the destination node is located at (500,500), and the locations of all the other nodes are fixed in different algorithms, and they have been classified into three types: un-used nodes (represented by star, ∗), used nodes (represented by triangle △) and dead nodes (represented by circle, o). In MFR, the proportion of un-used nodes is very high compared to the other algorithms, which means that the number of nodes involved in the transmission is much lower than the others. Also, the proportion of used nodes is very low in MFR. In ORF, the proportion of un-used nodes is lower than that of MFR and the proportion of used nodes is comparable to that of MFR. In NFP, the proportion of un-used nodes is quite low and the proportion of used nodes is much higher than that of MFR and NFP. By comparison, more nodes have been involved in the transmission between the source and the destination nodes in NFP. However, NFP uses too many hops in each transmission and the performance of NFP is not good even though a large proportion of nodes have been involved in the transmission. In OFEB, the proportion of un-used nodes increases when the weight factor decreases, and all nodes have been involved in the transmission when the weight factor is 0.1. The results show that, by considering the balance of node residual energy, more nodes will be involved in the transmission and the
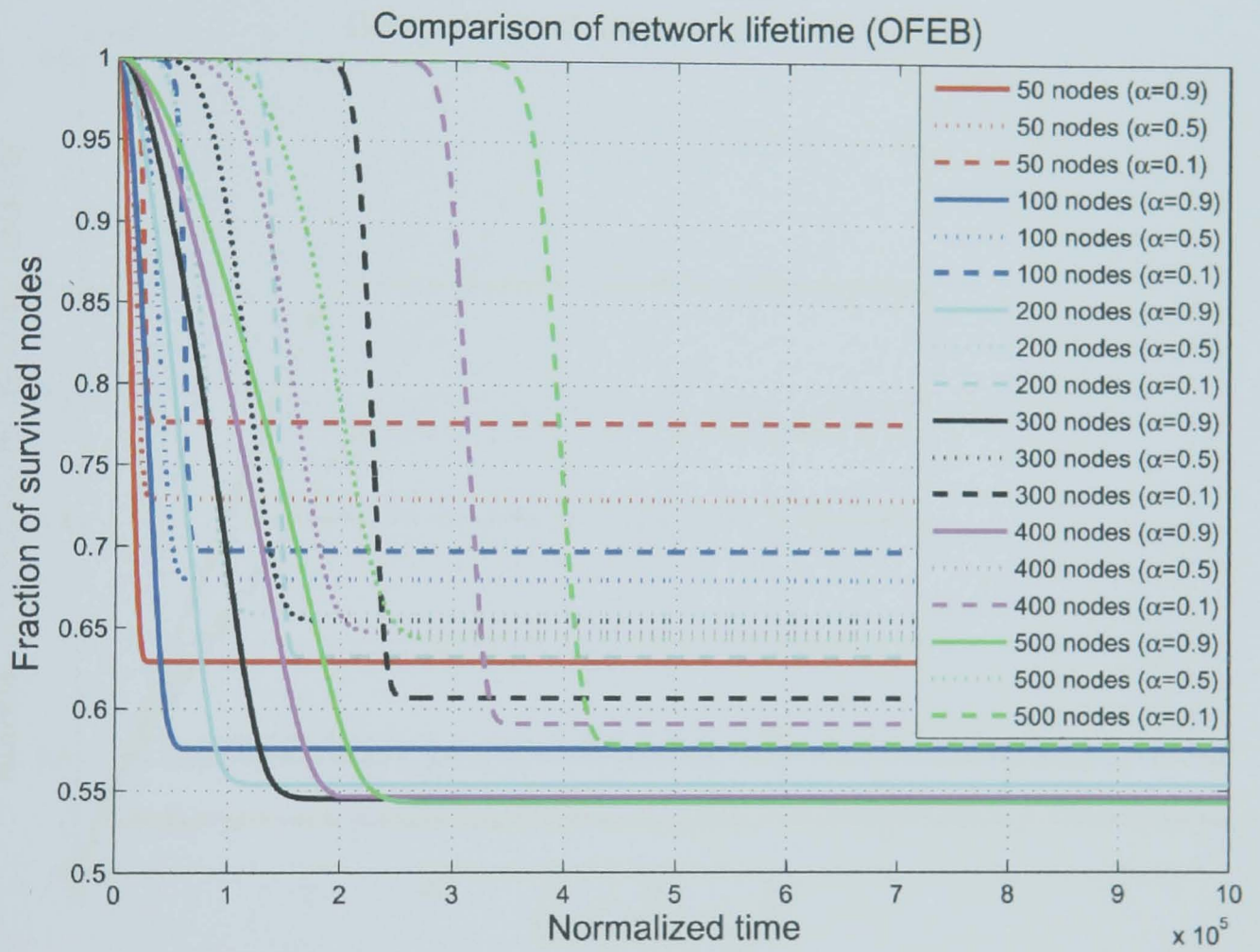
Figure 6.10: Impact on the network lifetime: OFEB
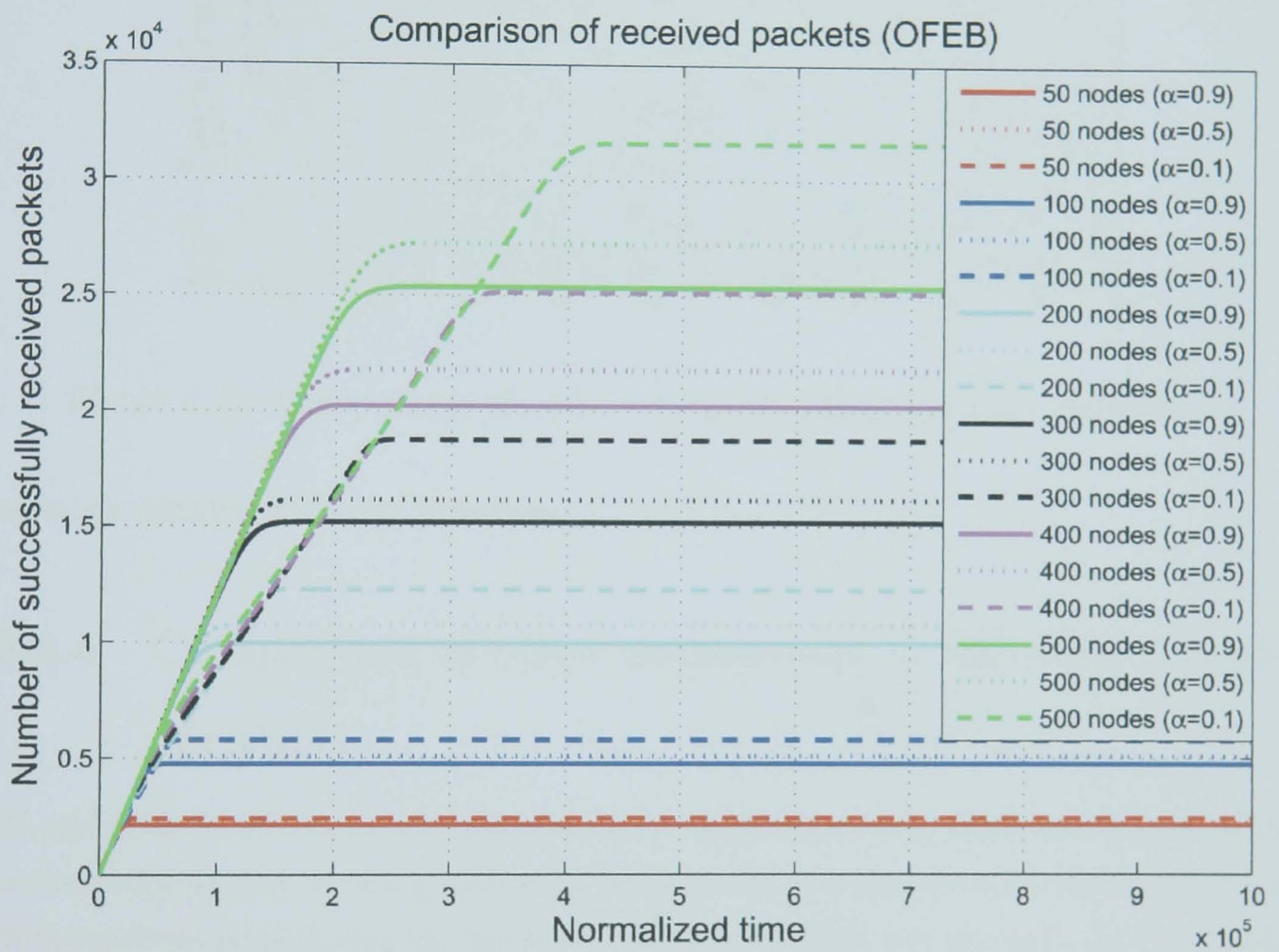
Figure 6.11: Impact on the packets received: OFEB
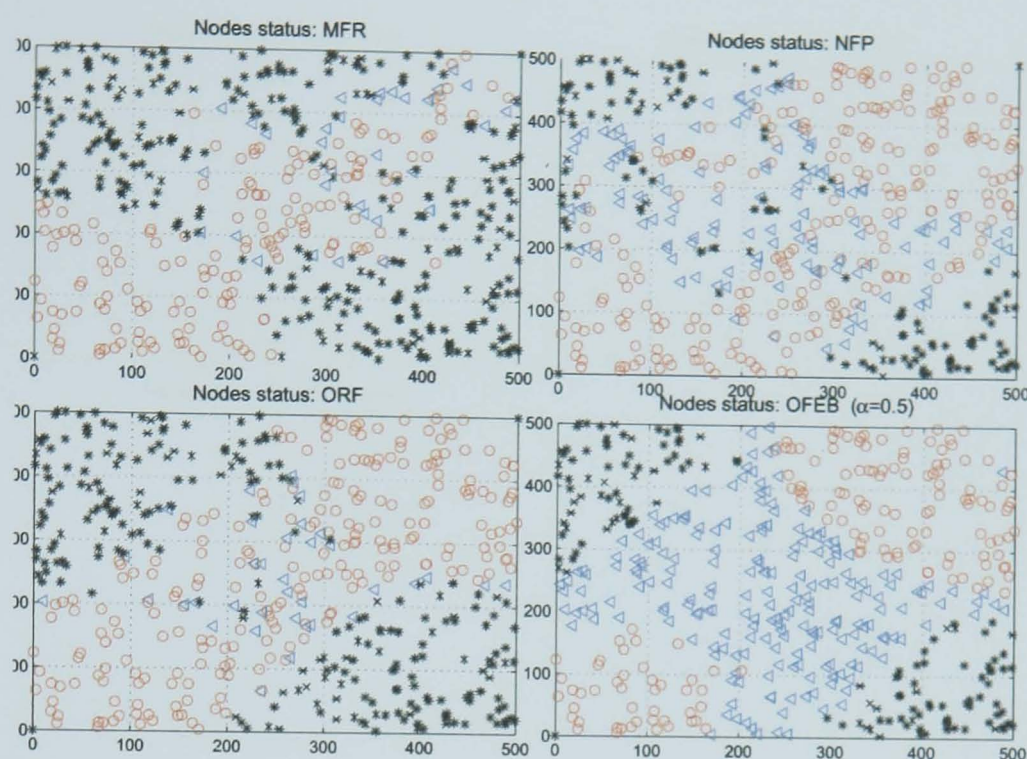
Figure 6.12: Comparison of nodes' energy status in different algorithms

network performance can improve.

6.4.4 Comparison of other parameters in different GR algorithms

In addition to the network lifetime and received packets, there are some other parameters worthy of being analysed, such as the average energy consumption for each received packet and the network throughput (bits per second). In Fig. 6.14, the network lifetime, the number of received packets, the average energy consumption for each received packet, and the network throughput are all compared based on different node densities in different GR algorithms. The number of received packets increases when the node density increases in all GR algorithms. The OFEB ($\alpha = 0.1$) algorithm has the best performance and the performance of NFP is the worst. The network lifetime increases when the node density increases in all GR algorithms, and NFP has the best performance and MFR has the worst performance. As we mentioned, the network lifetime should be considered with the number of received packets to evaluate the performance of the algorithms.
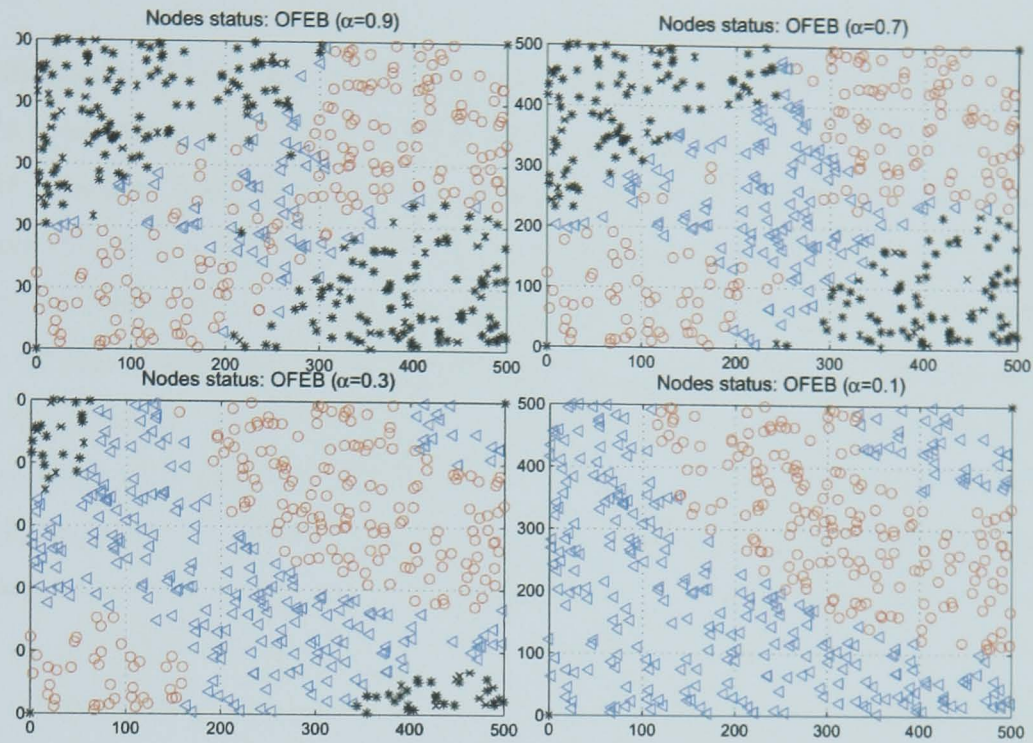
Figure 6.13: Comparison of nodes' energy status in OFEB

The energy consumed for each successfully received packet is lowest in the OFEB algorithm with large weight factor ($\alpha > 0.5$, ORF is a special case of $\alpha = 1$). In NFP, the energy consumed for each successfully received packet increases when the node density increases (whereas it decreases in the other algorithms when the node density increases). The reason is that based on the forwarding scheme used in NFP, when the node density is high, more hops are used for the end-to-end transmission between the source and the destination nodes, therefore the energy consumed for one received packet increases. In MFR, the energy per packet decreases when the node density increases during the period of low node density, and it remains unchange when the node density is high. In ORF, the energy per packet decreases when the node density increases, and the curve of energy per packet in OFEB ($\alpha = 0.5$, $\alpha = 0.7$ and $\alpha = 0.9$) has a similar trend to that of ORF (OFEB $\alpha = 1$). This shows that when the weight factor in OFEB is large, the energy consumed for one received packet decreases when the node density increases. In OFEB ($\alpha = 0.3$), the energy per packet is slightly smaller than that of MFR and larger than that of OFEB ($\alpha > 0.5$). The energy per packet in ORF has a similar trend to that of MFR, and the energy per packet

remains unchange when the node density is high. In OFEB ($\alpha = 0.1$), the energy per packet is smaller than that of NFP but larger than the others, and the energy per packet remains unchange when the node density is high. Note that, when the the number of nodes is 50 in the network (node density is $2 \times 10^{-4}\ m^2$), the energy per packet of FEB ($\alpha = 0.1$) is equivalent to that of the NFP and much larger than that of the other algorithms. As a result, when the node density is low, the optimal transmission range has higher impact on the energy consumption.

For network throughput, MFR and NFP respectively have the best and the worst performances. In MFR, the network throughput is much larger than that of the others and the reason is that the most forward node is selected to be the next hop node in the MFR forwarding scheme. Also, the network throughput increases when the node density increases in MFR. In NFP, the network throughput is much smaller than that of the others. The reason is that the nearest node to the current source node is selected to be the next hop node, therefore it takes much longer time to forward the data packet to the destination node. The higher the node density is, the longer the time taken, thus the network throughput decreases when the node density increases in NFP. In ORF, the optimal transmission range is the metric to select the next hop node, therefore the network throughput is between MFR and NFP, and it increases when the node density increases. In OFEB, the network throughput increases when the node density increases in the low density case. In the high node density case, the network throughput decreases when the weight factor is low ($\alpha = 0.1\ and\ \alpha = 0.3$), and it increases when the weight factor is high ($\alpha = 0.5,\ \alpha = 0.7\ and\ \alpha = 0.9$).

6.5 Summary

In a 2-D ad-hoc wireless network, the author proposed the energy-efficient Geographic Routing algorithms ORF and OFEB to prolong the network lifetime and improve other network performance metrics. The results were compared to the existing GR algorithms including MFR and NFP. The new ORF algorithm selects as the next hop node the node nearest to the optimal transmission range (within the maximum range) and therefore minimises the energy consumption. The new
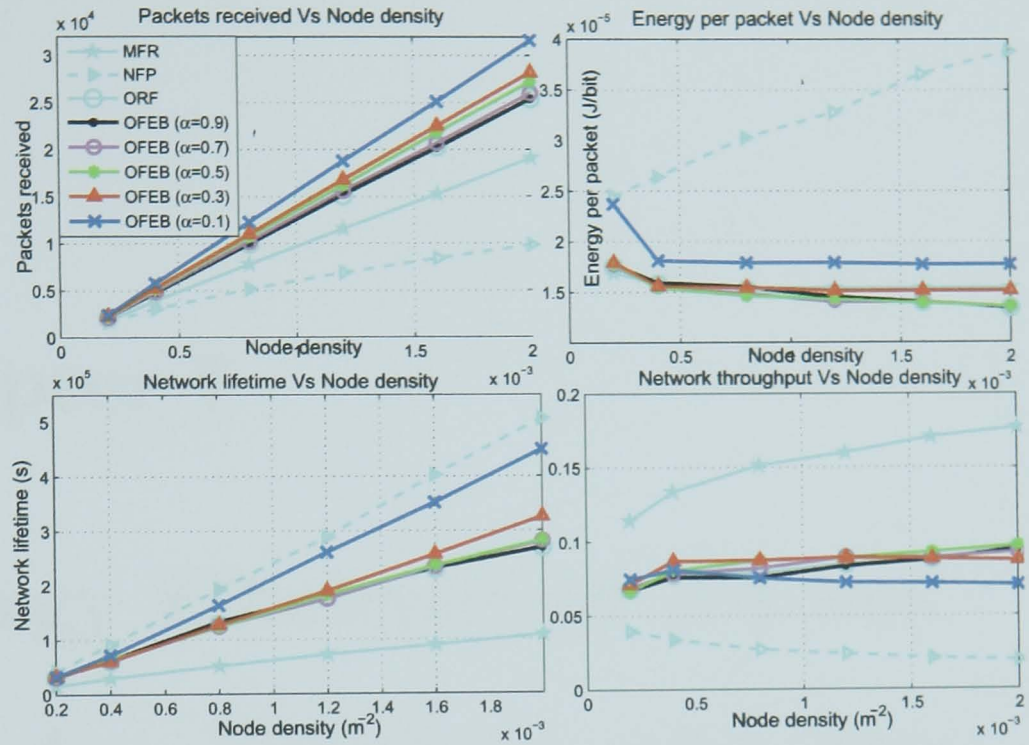
Figure 6.14: Comparison of all simulation results

OFEB algorithm selects the next hop node as the node (within the maximum range) that minimises the value of $[\alpha \frac{\Delta d}{R_{opt}} - (1 - \alpha) \frac{E_{res}}{E_{cap}}]$. This is a node that has the best combination of energy reserves and needs the minimum energy to be reached. The weight factor α determines the relative significance placed on these two requirements. The simulation results show that the OFEB algorithm has the best performance, in which the network lifetime, the network throughput, the number of received packets, and the energy consumed for each received packet have all been compared. Also, in this chapter we introduced a method that can be used to select the optimum location of relay nodes.

Chapter 7

Energy Efficiency in Ad-hoc Wireless Networks with Two Realistic Physical Layer Models

7.1   Introduction

Most transmission and energy consumption models in ad-hoc wireless networks assume an ideal physical layer model, where the probability of the packet being received by the neighbour is 100% once the neighbour node is within the transmission range of the transmitter. In this chapter, we investigate Rayleigh fading and Lognormal fading scenarios to derive the optimal transmission range in ad-hoc wireless networks. In this chapter, based on the hop-by-hop retransmissions (HHRs) model, where a packet is retransmitted between two nodes until it is received and acknowledged correctly, the relationship between expected energy consumption and the distance between two nodes is derived in the two-node model. In an equal-hop end-to-end multihop transmission model, the relationship between the total expected energy consumption, the range of each hop, and the transmission power of each node is derived and analysed. It is shown that min-

imum energy consumption can be achieved by adjusting both the transmission power and the range of each hop. Furthermore. based on a one hop model. an efficiency function is proposed based on the one hop progress and one hop energy consumption. The relationship between expected one hop energy consumption. the range of the hop, and the nodes' transmission power has been derived and the results show that, these two relationships derived through different methods are the same, which validates the relationship.

7.2 Two physical layer models

The received signal power at a receiver, located a distance x from the transmitter. can be expressed as [3]:

$$p_r(x) = \frac{p_t G_t G_r \lambda^2}{(4\pi)^2 x^2 Loss}. \tag{7.1}$$

where G_t and G_r are respectively the gains of the transmitter and receiver. The carrier wavelength is λ and $Loss$ represents any additional losses in the transmission. Thus, with $G_t = G_r = 1$, and $Loss = 1$, the received signal power is

$$p_r(x) = \frac{p_t c^2}{(4\pi)^2 x^2 f^2}, \tag{7.2}$$

where c is the speed of light, f is the carrier frequency and p_t is the signal transmission power at the transmitter.

In the physical layer fading propagation model, $p_r(x)$ represents the average signal power at a distance x from the transmitter. and the probability $(P_b(x))$ of the signal being successfully received at x is derived based on Rayleigh fading and Lognormal fading models. For the Rayleigh fading model:

$$P_b(x) = exp(-\frac{p_{thr}(4\pi)^2 x^2 f^2}{p_t c^2}). \tag{7.3}$$

For the Lognormal fading model:

$$P_b(x) = \frac{1}{2} + \frac{1}{2} erf(\frac{\ln(p_{thr}) - \ln(\frac{p_t c^2}{(4\pi)^2 x^2 f^2})}{\sqrt{2}\sigma}). \tag{7.4}$$
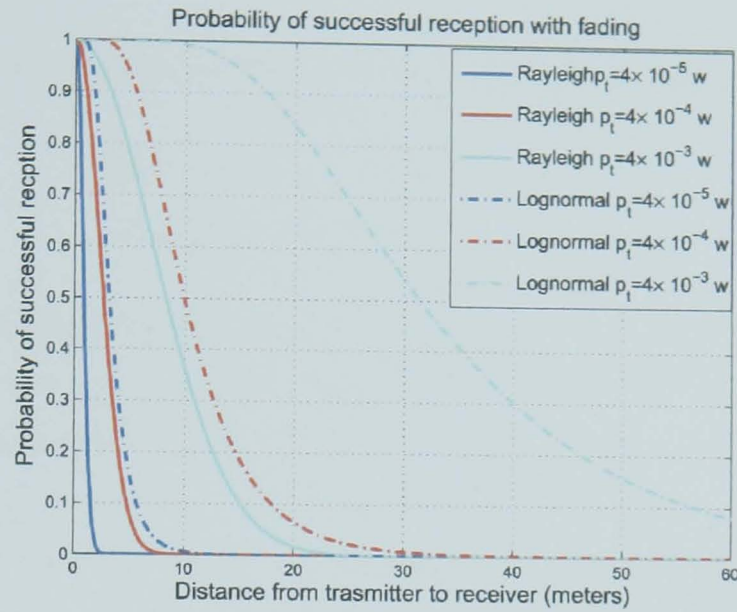
Figure 7.1: Probability of successfully receiving a packet

where σ is the standard deviation ($\sigma = \frac{\sigma_{db}\ln(10)}{10}$, $\sigma_{db} = 4\ db$ in this chapter), c is the speed of light and f is the frequency of the carrier wave, where $f = 2.4 \times 10^9 Hz$, p_{thr} is the signal threshold power needed to maintain performance, where $p_{thr} = 100 \times 10^{-6}$ in this chapter.

In this chapter, the author assume that the transmission range is adjustable. Therefore, each node has different levels of transmission power (p_t), and the transmission power is adjusted to achieve energy efficiency. Based on equations 7.3 and 7.4, the probabilities of the signal being successfully received at a distance x from the transmitter are plotted in Fig. 7.1.

7.3   Energy consumption in a two-node model

Most energy consumption models used in ad-hoc wireless networks assume that the physical layer is ideal, which means the packet will be received if the receiver is within the range of the transmitter. With a real physical layer model, the packet is received by the receiver with a probability ($P_b(x)$), which is a function of the distance to the transmitter. We assume that each signal represents 1 bit data, and the packet length is 1 bit as well. Hence, each signal represents a 1-bit length packet. For a packet transmitted from the transmitter node to the receiver

node. the energy consumed at the transmitter and the receiver is respectively:

$$E_{transmssion} = e_e Packet + E_t$$
$$E_{reception} = e_e Packet. \tag{7.5}$$

where e_e is the energy consumed by the transceivers electronics per bit. Based on [64] and [65], the typical value of e_e is: $e_e = 3.32 \times 10^{-7}$ J/bit. $E_t = p_t \times T$. where T is the bit period, and it is 10^{-6} in this chapter.

Based on the hop-by-hop retransmissions (HHRs) model. where a packet is retransmitted between two nodes until it is received and acknowledged correctly. the author has derived the energy consumption in a two-node model respectively based on the Rayleigh and Lognormal fading scenarios. In a transmission system composed of two nodes (transmitter A and Receiver B). the number of hops is counted as the number of hops needed for the packet and acknowledgment both to be received successfully. With $P_b(x)$ as the probability of the packet being successfully received, the expected number of transmissions from B to A is $\frac{1}{P_b(x)}$ (ie. for Acknowledgment), and therefore the expect number of transmission from A to B is $\frac{1}{P_b^2(x)}$ (Recall that B generates one ACK per successfully received packet and therefore $\frac{1}{P_b(x)}$ ACK transmission from B to A call for $\frac{1}{P_b^2(x)}$ transmissions for A to B). The expected number of receptions at B is $\frac{1}{P_b^2(x)} \times P_b(x) = \frac{1}{P_b(x)}$. and the expected number of receptions at A is 1 (1 represents the fact that the acknowledgment has being received by A. which means that the transmission between the two nodes is successful).

Thus the total numbers of transmissions and receptions are respectively:

$$N_{transmission} = \frac{1}{P_b^2(x)} + \frac{1}{P_b(x)}$$
$$N_{reception} = \frac{1}{P_b(x)} + 1. \tag{7.6}$$

Therefore. based on the energy consumption model (equation 7.5). the energy consumed for transmission and reception of the two-node model is:

$$E_{sum_{transmssion}} = N_{transmission} \times E_{transmssion}$$
$$E_{sum_{reception}} = N_{reception} \times E_{reception}. \tag{7.7}$$

Figure 7.2: Equal-hop end-to-end transmission model

7.4 Energy consumption of an end-to-end multihop transmission model

Based on the end-to-end transmission model shown in Fig. 7.2. one packet (1 bit) is transmitted from the source node to the destination node via equally spaced intermediate nodes. In the equal-hop end-to-end multihop transmission model, shown in Fig. 7.2, the distance between the source and the destination nodes is divided into m equally-spaced hops. where $m = \frac{L}{x}$ (L is the distance between the source and the destination nodes and x is the single hop distance). Thus. based on equation 7.7, the expected energy consumption for one packet being successfully transmitted from the source node to the destination node is:

$$E_{total} = m \times (E_{sum_{transmission}} + E_{sum_{reception}})$$
$$= \frac{L}{x} \times [(\frac{1}{P_b(x)} + \frac{1}{P_b^2(x)})(e_e + E_t) + (1 + \frac{1}{P_b(x)})e_r]. \qquad (7.8)$$

Based on equation 7.8. the total energy consumption (E_{total}) of the end-to-end transmission is a function of the length of each hop (x) and the transmission power of each node (p_t).

7.4.1 Rayleigh fading scenario

Based on equations 7.8 and 7.3. the total energy consumption (E_{total}) of the end-to-end transmission is a function of the length of each hop (x) and the transmission power at each node (p_t), and can be represented by:

$$E_{total} = m \times (E_{sum_{transmission}} + E_{sum_{reception}}) \qquad (7.9)$$
$$= \frac{L}{x} \times [(\frac{(e_e + E_t)}{exp(-\frac{p_{thr}(4\pi)^2 d^2 f^2}{p_t c^2})} + \frac{(e_e + E_t)}{exp^2(-\frac{p_{thr}(4\pi)^2 d^2 f^2}{p_t c^2})}) + (e_r + \frac{e_r}{exp(-\frac{p_{thr}(4\pi)^2 d^2 f^2}{p_t c^2})})].$$

Figure 7.3: Energy consumption of the end-to-end transmission (Rayleigh)

With different static values of p_t, the relationship between E_{total} and x is plotted in Fig. 7.3, where the node transmission power is as shown in the figure. For each different level of p_t, there is a minimum energy consumption (E_{total}), which occurs at the specific transmission range (x). To analyse the relationship between E_{total}, p_t, x and $P_b(x)$ (determined by p_t and x), the corresponding data has been recorded in Table 7.1. Based on Table 7.1, the relationship between E_{total} and x, and the relationship between E_{total} and p_t has been plotted in Fig. 7.4 and Fig.7.5 respectively. In both Fig. 7.3 and Fig. 7.4, E_{total} decreases when x increases before a specific value of x, and it increases when x increases after that point. It is clear in Fig. 7.5 that E_{total} decreases when p_t increases before $p_t = 6.25 \times 10^{-7}w$, and it increases when p_t increases after $p_t = 6.25 \times 10^{-7}w$. Based on Fig. 7.3, Fig. 7.4 and Fig.7.5, it can be seen that there is a minimum E_{total} for specific p_t and x, and this shows that the minimum energy consumption occurs when $p_t = 6.25 \times 10^{-7}$ and $x = 7.1$. Furthermore, note that the minimum energy consumption for different levels of p_t occurs when $P_b(x)$ is between 69% and 71%. Thus, E_{total} can be minimised by a range of $P_b(x)$ values.

x	5.7	6	6.3	6.6
p_t	0.375×10^{-4}	0.417×10^{-4}	0.458×10^{-4}	0.500×10^{-4}
$P_b(x)$	0.694305132	0.695007184	0.694432725	0.692903154
E_{total}	0.011561697	0.011456074	0.011387549	0.011347901
x	6.8	7.1	7.3	7.5
p_t	0.542×10^{-4}	0.583×10^{-4}	0.625×10^{-4}	0.667×10^{-4}
$P_b(x)$	0.698039534	0.694957014	0.698339877	0.700959086
E_{total}	0.01133012	0.011329779	0.011342915	0.011367662
x	7.7	7.9	8.1	8.3
p_t	0.708×10^{-4}	0.750×10^{-4}	0.792×10^{-4}	0.833×10^{-4}
$P_b(x)$	0.702943912	0.704396449	0.705398395	0.706015895
E_{total}	0.011401686	0.011443234	0.011490966	0.011543845

Table 7.1: Results from the end-to-end transmission model (Rayleigh)
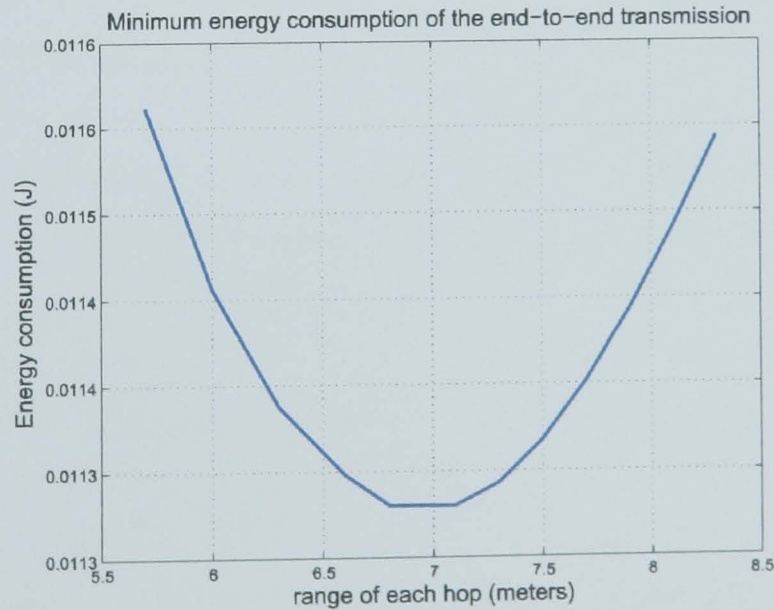
Figure 7.4: Minimum energy consumption for different transmission powers (versus x in Rayleigh model)
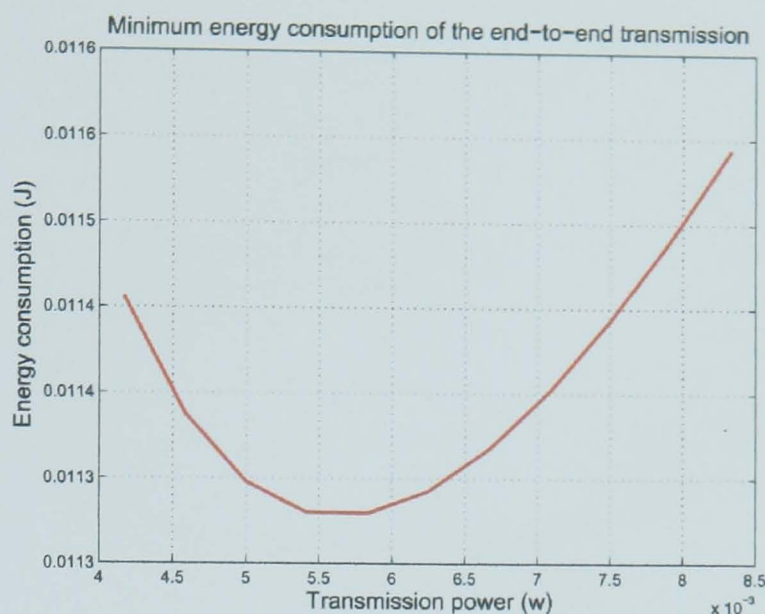
Figure 7.5: Minimum energy consumption for different transmission powers (versus p_t in Rayleigh model)

7.4.2 Lognormal fading scenario

Considering a Lognormal fading scenario, based on equations 7.4 and 7.8, the relationship between E_{total} and x is plotted in Fig. 7.6 (with static value of p_t), where the nodes' transmission power is adjusted as shown in the figure. With different static value of p_t, the relationship between E_{total} and x is plotted in Fig. 7.6, where the nodes' transmission power is adjusted as shown in the figure. For each different level of p_t, there is a minimum energy consumption (E_{total}), which occurs at the specific transmission range (x). To analyse the relationship between E_{total}, p_t, x and $P_b(x)$ (determined by p_t and x), the corresponding data has been recorded in Table 7.2. Based on Table 7.2, the relationship between E_{total} and x, and the relationship between E_{total} and p_t has been plotted in Fig. 7.7 and Fig.7.8 respectively. In both Fig. 7.6 and Fig. 7.7, E_{total} decreases when x increases before a specific value of x, and it increases when x increases after that point. It is shown in Fig. 7.8 that E_{total} decreases when p_t increases before $p_t = 6.25 \times 10^{-7}w$, and it increases when p_t increases after $p_t = 6.25 \times 10^{-7}w$. Based on Fig. 7.6, Fig. 7.7 and Fig.7.8, it can be seen that there is a minimum E_{total} for specific p_t and x. The minimum energy consumption occurs when

Figure 7.6: Energy consumption of the end-to-end transmission (Lognormal)

$p_t = 6.25 \times 10^{-7}$ and $x = 28.3$ for the set of parameters considered. Furthermore, note that the minimum energy consumption for different levels of p_t occurs when $P_b(x)$ is between 79% and 81%. Thus, E_{total} can be minimised by a range of $P_b(x)$ values.

7.5 Energy efficiency with efficiency function

As shown in Fig. 7.9, S is the source node, D is the destination node, and R is the relay node. In order to find the optimal location of the next hop node, which leads to energy efficiency in the entire transmission, an efficiency function (F) is proposed as follows:

$$F = \frac{Progress}{E_{onehop}},\qquad(7.10)$$

where E_{onehop} is the energy consumption for one transmission between S and R, and *Progress* is the progress of the relay node defined as $|SD| - |RD|$. Therefore, to minimise the energy consumption between S and D, the *Progress* of the current hop should be made as large as possible and E_{onehop} should be made as small as possible. Thus, by maximising F, the optimal energy consumption

x	20.4	21.5	22.5	23.4
p_t	0.375×10^{-4}	0.417×10^{-4}	0.458×10^{-4}	0.500×10^{-4}
$P_b(x)$	0.79558552	0.79568542	0.7970329194	0.7996507994
E_{total}	0.00270091	0.00267225	0.0026526634	0.0026399752
x	24.3	25.2	26	26.8
p_t	0.542×10^{-4}	0.583×10^{-4}	0.625×10^{-4}	0.667×10^{-4}
$P_b(x)$	0.80103606	0.80145174	0.8034093139	0.8045887559
E_{total}	0.00263268	0.00262966	0.0026300470	0.0026332205
x	27.6	28.3	29.1	29.8
p_t	0.708×10^{-4}	0.750×10^{-4}	0.792×10^{-4}	0.833×10^{-4}
$P_b(x)$	0.80512687	0.80723434	0.8067329285	0.807848271
E_{total}	0.00263867	0.00264601	0.0026549431	0.0026651742

Table 7.2: Results from the end-to-end transmission model (Lognormal)
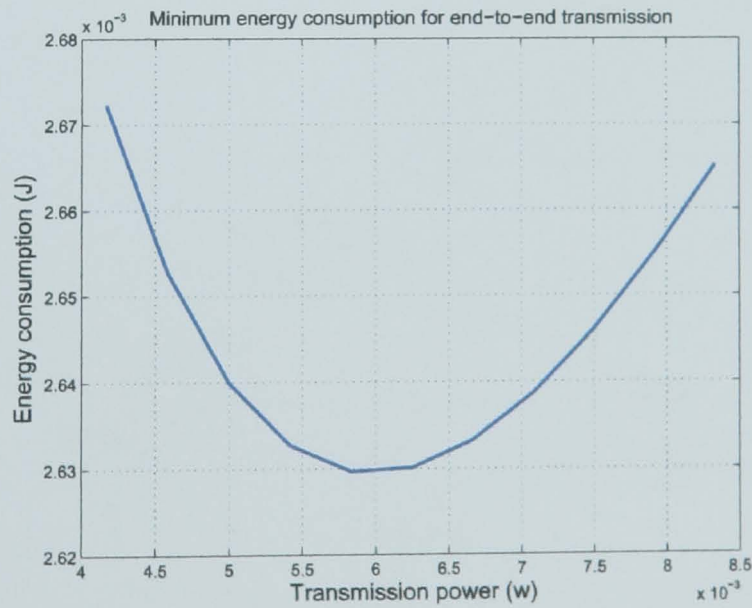
Figure 7.7: Minimum energy consumption for different transmission powers (versus x in Rayleigh model)

Figure 7.8: Minimum energy consumption for different transmission powers (versus p_t in Rayleigh model)
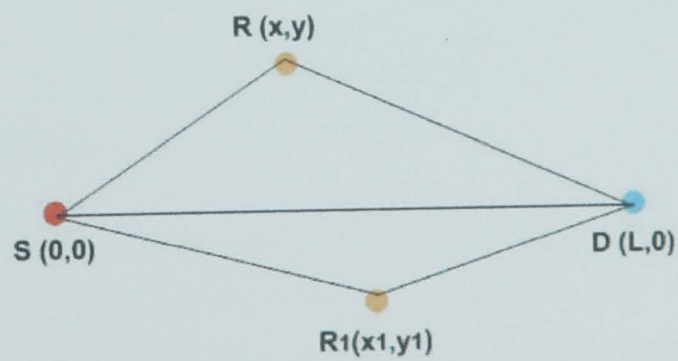
Figure 7.9: Model with the progress metric

between S and D can be achieved. Based on equations 7.5, 7.6 and 7.7, the efficiency Function is:

$$F = \frac{|SD| - |RD|}{(\frac{1}{P_b(x)} + \frac{1}{P_b^2(x)})(e_e + E_t) + (1 + \frac{1}{P_b(x)})e_e}. \tag{7.11}$$

Using the coordinates of each node, it becomes:

$$F = \frac{L - \sqrt{(L - x)^2 + y^2}}{(\frac{1}{P_b(x)} + \frac{1}{P_b^2(x)})(e_e + p_t) + (1 + \frac{1}{P_b(x)})e_e}. \tag{7.12}$$

For a linear network $(y = 0)$, it is:

$$F = \frac{x}{(\frac{1}{P_b(x)} + \frac{1}{P_b^2(x)})(e_e + p_t) + (1 + \frac{1}{P_b(x)})e_e}. \tag{7.13}$$

Since $F > 0$, the maximum of F is equivalent to the minimum of $\frac{1}{F}$, and $\frac{1}{F}$ is expressed as:

$$\frac{1}{F} = \frac{(\frac{1}{P_b(x)} + \frac{1}{P_b^2(x)})(e_e + p_t) + (1 + \frac{1}{P_b(x)})e_e}{x}, \tag{7.14}$$

which is linearly proportional to E_{total}, as shown in equation 7.8. The only difference between equations 7.8 and 7.14 is the length of the network (L). Therefore, the relationship between energy efficiency (E_{total} for the end-to-end model and $\frac{1}{F}$ for the progress model), transmission power (p_t), and the probability of packet being successfully received ($P_b(x)$) are the same based on two different methods.

7.6 Summary

Based on realistic physical layer scenarios, this chapter proposed two methods to achieve energy efficiency in ad-hoc wireless networks. The relationship between the energy cost, the range of each hop, and the nodes' transmission power has been derived based on these two methods. The results show that, these two relationships derived through different methods are equivalent. The results in this chapter can be implemented in an energy efficient geographic routing algorithm, which can form the basis for future work.

Chapter 8

Energy Efficiency in Ad-hoc Vehicular Networks

8.1 Introduction

Green ICT (Information and Communication Technology) is a new focus with the goal of saving energy by optimising mobile network communications and ultimately protecting the natural climate [144]. In terms of the global carbon emissions, some analysts have reported that ICT accounts for $2 - 2.5\%$ of the global harmful emissions, which is equal to the global aviation industry [145]. According to a report by the Ministry of Internal Affairs and Communications of Japan [146], ICT equipment (routers, PC's, and other network systems) consumed about 45,000,000 MWh in 2006 which is 3% of the country total energy consumption and this figure has increased about 20% over the past five years. In this chapter, vehicular ad-hoc networks (VANETs), as shown in Fig. 8.1, are designed to reduce their communication energy consumption.

Based on a realistic transport traffic scenario on a motorway, 'M1' in the UK, this chapter evaluates the energy consumption in a motorway ad-hoc wireless network. This is based on a Geographical Adaptive Fidelity (GAF) topology management protocol [13], where the energy consumption has been analysed for

137
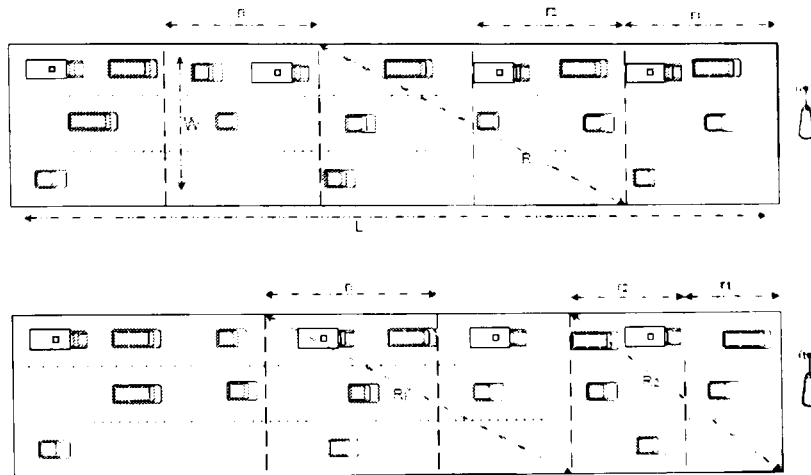
Figure 8.1: Equal-grid and adjustable-grid motorway GAF model.

equal-grid, adjustable-grid and genetic algorithm models. Considering nodes in the VANET network and their transmission ranges, this chapter provides a network model to compute the energy consumption of VANETs and compares their energy efficiency performance. The proposed genetic algorithm model has been found to be more energy efficient than the adjustable-grid model which is better than the equal-grid model.

8.2 Traffic statistics in the M4 motorway in the UK

As a first step, some statistical analysis has been carried out on vehicular traffic profiles observed at inductive loops on the 'M4' motorway in the UK. Fig. 8.2 shows the distribution of vehicles as it is observed at inductive loop (ID) 2244, on the M4, on Tuesday (23/04/2002), Friday (26/04/2002) and on Saturday (27/04/2002). On Tuesday and Friday, there are two peak times (7-8 am and 5-6 pm), which correspond to the morning and evening work rush hours. On Saturday, there are two peak times (11-12 am and 7-8 pm), which correspond to the equivalent leisure rush hours. Fig. 8.3 provides a comparison of vehicle dis-

Figure 8.2: Distribution of vehicles in one day over three inductive loops: 2244, 2246, 6584 in the M4 motorway
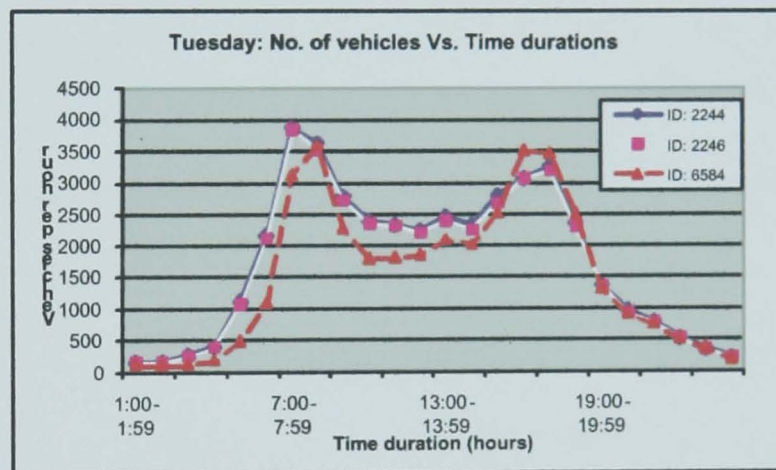
Figure 8.3: Distribution of vehicles over inductive ID 2244 during three days.

tribution around inductive loops (ILs) on Tuesday (23/04/2002). The statistical analysis shows that the distributions of vehicles at the ILs IDs 2244, 2246 and 6584 are very similar. This data clearly show that the transport traffic varies on a specific location on the M4 according to the time of the day as well as varying in different locations on the M4 during a specific time duration. Fig. 8.4 illustrates these trends, where vehicle distributions are shown within different time durations, peak and off peak time, as well as, at different locations between IDs 2244-2256 on Tuesday-02/04/2002.

During a specific time duration, the bit rates and statistical probabilities of different types of data (speech, video, data, RFID) are presented in Table

Figure 8.4: Distribution of vehicles during the offpeak and peak times.

Speech bit rate	64 kb/s	Speech ON/OFF probability	5/35
Video bit rate	320 kb/s	Video ON/OFF probability	5/65
Data bit rate	10 Mb/s	Data ON/OFF probability	15/75
RFID bit rate	10 Mb/s	Data ON/OFF probability	1/12

Table 8.1: Parameters for computing data traffic
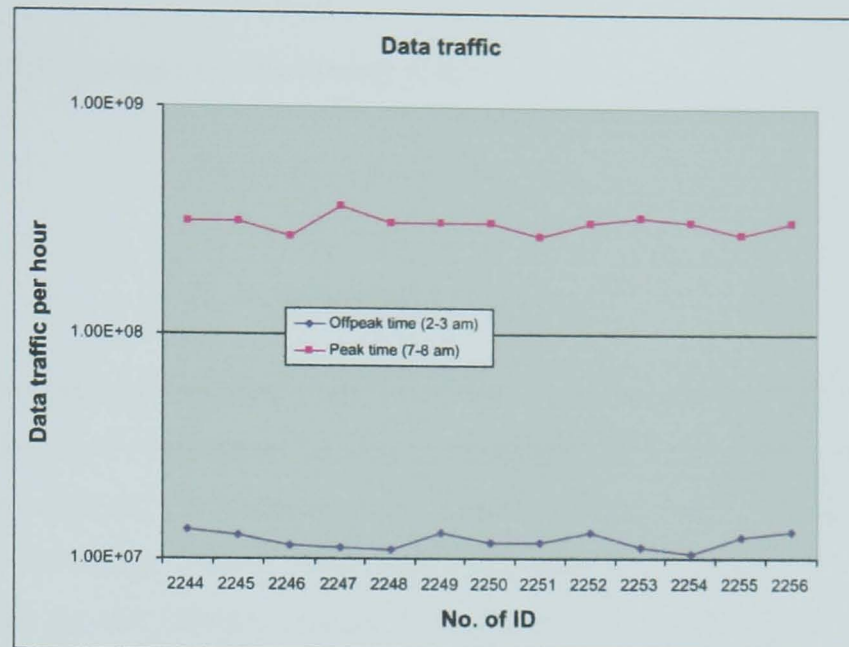
Figure 8.5: Distribution of data traffic during the offpeak and peak times.

8.1 [147]. Therefore, the average traffic transmitted by each vehicle is assumed to be $64 \times 10^3 \times \frac{3}{35} + 320 \times 10^3 \times \frac{5}{65} + 10 \times 10^6 \times \frac{15}{75} + 10 \times 10^6 \times \frac{1}{6} \approx 2.9 Mbits/s$ which is achievable based on current standards and expected near future evolution. Based on vehicle distribution trends within different time durations and at different locations, Fig. 8.5 illustrates the data traffic transmitted by these vehicles.

This result will be taken into consideration in modelling transport traffic on a typical motorway in order to achieve energy efficiency in VANETs. Note that the average speed of vehicles is about 25 m/s (90 km/hour) and the distance between two IDs is 500 metres. Therefore, the average number of nodes distributed between two ILs is about 20, where the author assume that they are uniformly distributed between any two ILs on the M4.

8.3 Preliminaries

The energy consumed by ad-hoc wireless network nodes is the sum of energy consumed for transmitting, receiving and listening. Based on [141] the energy consumed per second by a node in these three states can be respectively calculated

as follows (as mentioned in equations 4.4):

$$E_t = (e_e + e_a R^n)T_t$$
$$E_r = (e_e + e_p)T_r$$
$$E_l = e_l T_l = e_l(1 - T_t - T_r) \qquad (8.1)$$

where e_e is the energy/second consumed by the transceivers electronics, and e_a is the energy/second consumed in the transmitter RF amplifier, and e_p is the energy/second consumed for processing in the receivers and e_l is the energy/second consumed for listening to the radio environment, where $e_l = e_e$, e_e, e_a, and e_p are determined by the design characteristics of the transceivers. Based on [65], the typical values of these parameters are: $e_e = 0.083$ J/S, $e_p = 0.017$ J/S, $e_a = 2 \times 10^{-5}$ $J/S/m^2$; n is the power index of the channel path loss, which is between 2 and 4. R is the node transmission range; T_t and T_r denote respectively the time durations for transmitting and receiving the traffic, which can be expressed as follows (as mentioned in equations 4.5):

$$T_t = D_t/d_R$$
$$T_r = D_r/d_R, \qquad (8.2)$$

where D_t and D_r are the transmitted and received traffic data bits respectively, and d_R is the transmitted or received data rate ($bits/second$) of each network node. Thus, during one second, T_l, which denotes the time for listening to the radio environment, is: $T_l = 1 - T_t - T_r$, where $0 \le T_l \le 1$, thus $0 \le (1 - D_t/d_R - D_r/d_R) \le 1$. For the static traffic data scenario, where $D_t = D_r = D$, the value range of D can be described as follows (as mentioned in equations 4.6):

$$0 \le D \le \frac{1}{2}d_R \times second. \qquad (8.3)$$

In this chapter, the author focus on uplink communication from vehicles to a Base Station (BS). Based on GAF mechanism, our motorway model is divided into virtual grids, and the data traffic is ultimately forwarded to the BS. Since the distance between two BSs is about 4 km, in the model the author consider a 2 km (L=2 km) motorway network section with a BS located at the right end of the network. As the author mentioned before, about 20 vehicles are uniformly

distributed in 500 metres (distance between two IDs), the average number of nodes in the 2 km is 80 which corresponds to a similar trend to that shown in Fig. 8.5 (observe the variation with time of day/rush hour). Vehicles are classified as normal nodes (only transmit data) and head nodes (relay traffic to next grid).

Assume that a constant traffic (D) flows along the motorway network (from the left end to the BS) and the nodes in the network do not transmit data, the relationship between the optimal transmission range and network traffic can be derived as follows. In the equal-grid motorway GAF model, where all the virtual grids are the same size, L and W represent the length and width of the network, respectively, while r and R represent the grid length and the transmission range of nodes in each grid, respectively. Therefore, the number of grids, m, is (as mentioned in equations 4.7):

$$m = \frac{L}{r} \qquad (8.1)$$

and the transmission range (R_i) of nodes in the ith grid is derived based on GAF mechanism as follows:

$$R_i = \sqrt{(2r)^2 + W^2}. \qquad (8.5)$$

The total energy consumed in the ith grid, E_i, is the sum of the energy consumed in the listening, transmitting and receiving states of the nodes in the grid (equation 8.1), thus (as mentioned in equations 4.10):

$$E_i = E_t + E_r + E_l$$
$$= e_p T_r + e_l + e_a R_i^n T_t. \qquad (8.6)$$

Therefore, based on equations 8.2, 8.4 and 8.5, the energy consumed in the entire network can be expressed as follows (as mentioned in equations 4.11):

$$E_{total} = m E_i$$
$$= \frac{L}{r}[e_p D_r + e_l/d_R + e_a(\sqrt{(2r)^2 + W^2})^n D_t]. \qquad (8.7)$$

As mentioned, data traffic is constant through the network, thus $D_t = D_r = D$. To compute the minimum energy consumption of nodes, $\partial E_{total}/\partial r = 0$. For

$n = 2$ (as mentioned in equations 4.14):

$$r^2 = \frac{e_p D + e_l/d_R + W^2 e_a D}{4 e_a D}$$

$$r^* = \sqrt{\frac{e_p D + e_l/d_R + W^2 e_a D}{4 e_a D}}. \qquad (8.8)$$

where r^* is the optimal grid length. Based on equation 8.5, the optimal transmission range, R^*, can be described as follows (as mentioned in equations 4.15):

$$R^* = \sqrt{\frac{e_p D + e_l/d_R + 2W^2 e_a D}{e_a D}}. \qquad (8.9)$$

Equation 8.9 shows that the optimal radio transmission range, R^*, relates to the static network traffic data, D, and width W, where $W = 10m$ in the motorway model.

8.4 Energy consumption in peak time traffic model

In what follows we discuss energy-efficient communication models where the analysis and simulations are based on a 100-second duration.

8.4.1 Equal-grid motorway GAF model

In the equal-grid model, as shown in Fig. 8.1, the entire network is divided into equal grids and the traffic is forwarded grid by grid to the BS. To calculate the energy consumption of the motorway network, the vehicular nodes are classified as normal nodes (N_n) and head nodes (N_h).

The energy consumed by the normal nodes is only for transmitting, which can be derived based on equations 8.1 and 8.2:

$$E_{N_n} = (e_c + e_a R_i^n) D_t / d_R. \qquad (8.10)$$

where $R_i = \sqrt{r_i^2 + W^2}$ (normal nodes are able to transmit data to the head node, no matter where their location is), r_i is the grid length of the ith grid. In the equal-grid model, $r_i = r$.

The energy consumed by the head nodes of the i_{th} grid can be derived using equation 8.7:

$$E_{N_h i} = e_p D_{ri} + e_l/d_R + e_a(\sqrt{(2r)^2 + W^2})^n D_{ti}. \qquad (8.11)$$

where

$$D_{ti} = (L - (i-1)r)W\lambda$$
$$D_{ri} = (L - ir)W\lambda. \qquad (8.12)$$

λ denotes the traffic data (bits) intensity per metres^2 (m^2), which can be calculated from the the data traffic model ($\lambda = 1.16 \times 10^4 bits/m^2/s$).

By using equations 8.10, 8.11 and 8.12, the energy consumption of the entire network is:

$$E_{total} = \sum_{i=1}^{m} E_{N_h i} + (N - m) \times E_{N_n}, \qquad (8.13)$$

where N is the number in vehicular nodes in the motorway network ($N = 80$).

8.4.2 Analysis of network connectivity

Based on [148], the probability of network connectivity (P_b) can be calculated by

$$P_b = (1 - e^{-d2R})^N. \qquad (8.14)$$

where d is the node density, R is the transmission range of nodes, and N is the total number of nodes in the network. To meet $P_b > 99\%$, and using the parameters stated earlier in this section, R is solved to be $R > 113m$. Using the mechanism of equal-grid GAF model, the number of grids is about 36 ($m = 36$), where the energy consumption of the network is 3841 J, which is larger than the minimum energy consumption of the equal-grid model ($E_{min} = 3567$ J).

8.4.3 Adjustable-grid motorway GAF model

Obviously, nodes near the sink will relay more traffic than nodes at the other end of the network. Therefore, to optimise their energy consumption according to

the relationship between optimal radio range (optimal grid length) and network traffic from equation 8.9 (8.8). the nodes near a sink should have a smaller radio range. An adjustable-grid motorway GAF model can lead to lower energy consumption compared to equal-grid GAF model, if properly designed. As illustrated in Fig. 8.1, the adjustable-grid motorway GAF model divides the network into m variable-length grids, where the length of each grid is determined according to equation 8.9.

The energy consumed by the normal nodes is only for transmitting. which can be derived based on equations 8.1 and 8.2:

$$E_{N_n} = (c_e + c_a R_i'')D_t/d_R. \tag{8.15}$$

where $R_i = \sqrt{r_i^2 + W^2}$ (normal nodes are able to transmit data to the head node. no matter where their location is), r_i is the grid length of the ith grid.

The energy consumed by the head nodes of the ith grid can be derived using equation 8.7:

$$E_{N_h i} = c_p D_{ri} + c_l/d_R + c_a(\sqrt{(2r)^2 + W^2})'' D_{ti}. \tag{8.16}$$

where

$$D_{ti} = (L - r_1 - r_2... - r_{i-1})W\lambda$$
$$D_{ri} = (L - r_1 - r_2... - r_i)W\lambda. \tag{8.17}$$

λ denotes the traffic data (bits) intensity per metres^2 (m^2). which is the same as the equal-grid model ($\lambda = 1.16 \times 10^4 bits/m^2/s$).

By using equations 8.15, 8.16 and 8.17. the energy consumption of the entire network is:

$$E_{total} = \sum_{i=1}^{m} E_{N_h i} + (N - m) \times E_{N_n}. \tag{8.18}$$

where N is the number of vehicular nodes in the motorway network ($N = 80$). The energy consumption of the adjustable-grid motorway GAF model is 3012 J. when the number of grids $m = 21$.
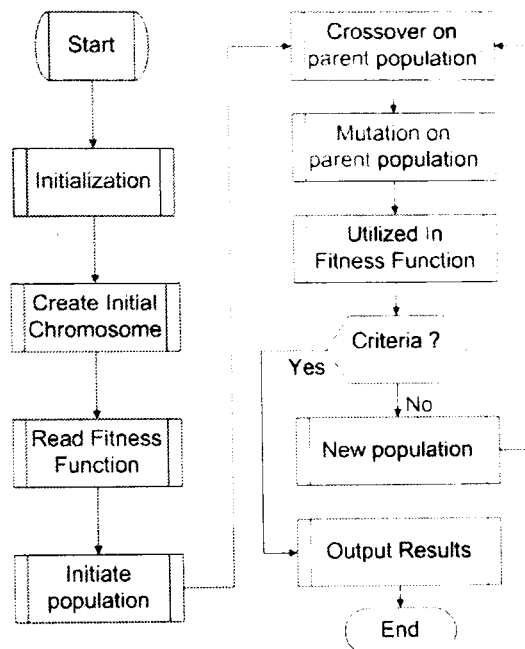
Figure 8.6: Genetic algorithm flow chart

8.4.4 Genetic Algorithm motorway GAF model

Genetic Algorithms (GA) [90][91] are optimisation and search techniques based on the principles of genetics and natural selections. The GA operations are explained in the flow chart shown in Fig. 8.6.

In the GA model, the fitness function is:

$$E_t = \sum_{i=1}^{m} E_i.$$ (8.19)

where

$$E_i = e_p D_{ri} + \frac{e_l}{d_R} + e_a(\sqrt{(r_i + r_{i-1})^2 + W^2})^n D_{ti}.$$ (8.20)

which is constraint by the set:

$$\bigvee = \{(r_1, r_2, \dots r_m) : 0 < r_i < L. \sum_{i=1}^{m} r_i = L\},$$ (8.21)

where r_i is represented by a chromosome in the GA algorithm, based on which new chromosomes are produced in each generation by crossover and mutation operations on parent population, as shown in Fig. 8.6. Given enough generations

147

(about 20000 generations), the minimum of the fitness function (minimum energy consumption) is computed: $E_t = 2946J$, where $m = 20$. This result will be analysed in Section 8.6.

8.5 Energy consumption in off peak time traffic

In the off peak data traffic scenario, the average number of vehicles in the motorway section GAF model is only about 4. Since the maximum number of grids is 4, with the same mechanism of the peak time traffic model, the minimum energy consumption of the equal-grid model is achieved at this number of grids, where $m = 4$. Since the data traffic density is too low and the number of vehicles is very small, the energy consumption results of the adjustable-grid, equal-grid and genetic algorithm models show comparable results in terms of energy consumption.

Fig. 8.5 shows that the average data traffic transmitted by vehicles during the peak time is much larger than that during off peak time and varies at different locations during specific time durations. The huge difference in data traffic calls for enabling vehicles to transmit at different transmission ranges according to time duration and location on a motorway in order to save more energy. Therefore, vehicles adjust their transmission range based on transport traffic density in order to maintain vehicular network connectivity as well as to save more energy. When the number of vehicles in a specific time duration or over a specific location is small, each vehicle adjusts its transmission range to a large value in order to maintain network connectivity. Whereas, when the number of vehicles increases then each vehicle should adjust its transmission range based on the optimal transmission range and total energy relationship functions derived in this chapter so that the total energy consumption can be minimised. As a result, vehicles will be able to automatically tune their wireless communication cards to a transmission range, which corresponds to a specific driving time or a specific location on a motorway in order to save more energy.
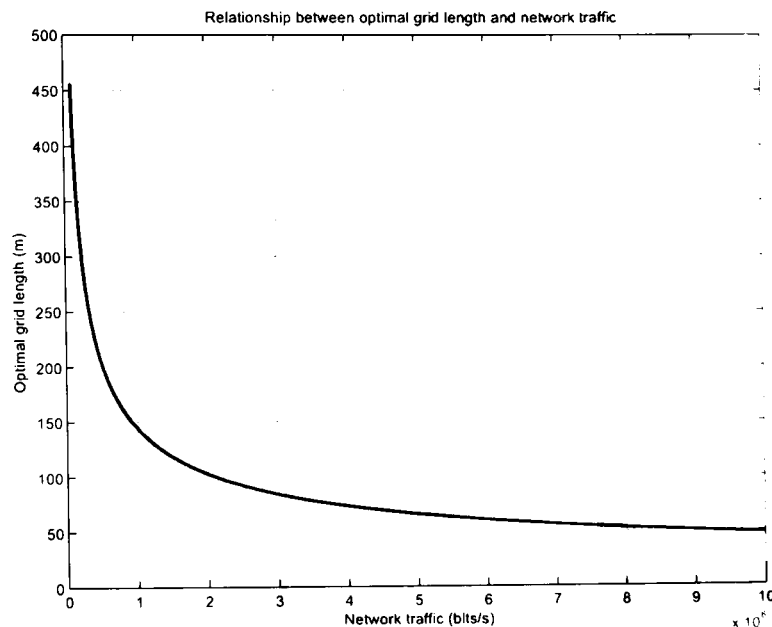
Figure 8.7: Relationship between the optimal grid length and network traffic (n=2)

8.6 Numerical results

The author has conducted simulations to evaluate the energy efficiency of the equal-grid, adjustable-grid and GA models. Eighty vehicular nodes (determined by the M4 motorway traffic model) were randomly distributed in the motorway network which is divided into virtual grids following the GAF models introduced. In each grid, the head node to which all the other nodes transmit was randomly selected. The data is relayed by the head node of each grid until it reaches the sink node. Each simulation was repeated 1000 times, and the total average energy consumption was computed. In what follows the we discuss the results based on the relationships derived and the energy-efficiency GAF models considered.

Based on the relationship between the optimal transmission range and data traffic transmitted by vehicular nodes in Section 8.4. Fig. 8.7 depicts the relationship between optimal grid length and network traffic. Three important points can be observed in the results shown in Fig. 8.7: First, the optimal grid length (or optimal radio transmission range) increases sharply when the network traffic is low, where the number of transmissions is small and therefore the global network energy can be minimised by minimising the number of nodes involved in

the transmission, which corresponds to a large node transmission range. The majority of the network is in the sleeping state when the network traffic is less than 2×10^6 $bits/s$. Second, when the network traffic is large, the optimal transmission range, R^*, takes smaller values and therefore the optimal grid length becomes smaller, and hence, there will be more relaying nodes (more grids).

8.6.1 Comparison of GAF models for energy efficiency

To evaluate the total network energy consumption with dynamic traffic in the equal-grid motorway GAF model, the author evaluated the total energy consumption in terms of the number of network grids, m, based on equation 8.13. The relationship between E_{total} and m is shown in Fig. 8.8. The minimum energy consumption of the equal-grid model is achieved when $m = 27$. Fig. 8.8 shows the optimal transmission range in terms of the number of grids covering a network in the equal-grid model. When the number of grids is small, the length of the grid is large. Therefore, the d^n $(n = 2)$ propagation loss component dominates the energy consumption, thus the energy consumption decreases sharply for $m < 27$ with increase in the number of grids. However, when the number of grids is large, the length of each grid is small. Therefore, the d^n propagation loss component becomes smaller, where the transmitter and receiver electronics energy consumption per bit become large. This linearly increases in turn the energy consumption with the number of grids, as shown in Fig. 8.8, for $m > 27$.

As presented in 8.4, the energy consumption of the adjustable-grid and GA models have been computed. Accordingly, the network energy consumption of the equal-grid, adjustable-grid and GA models are compared in Fig. 8.8. This shows that the network energy consumption of the equal-grid model reaches the minimum energy consumption (3567 J) at $m = 27$, and the network energy consumption of GA model reaches the minimum energy consumption (2946 J) at $m = 20$. Compared to the minimum network energy consumption of the equal-grid model, the adjustable-grid model saves 19.3% energy and the GA model saves 21.1% energy (by comparing the minimum energy consumption of both models). Note that, there is only one single value for the network energy consumption in the adjustable-grid model because in the adjustable-grid model, the length of
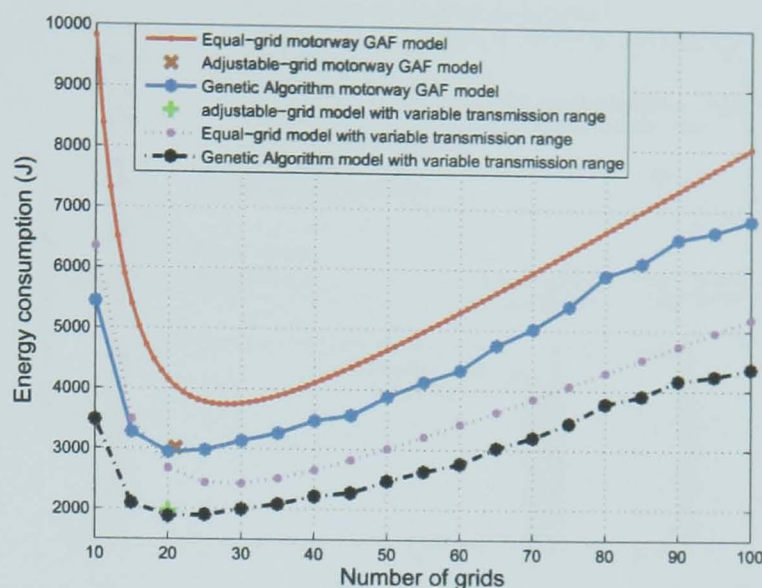
Figure 8.8: Energy consumption comparison

each grid is computed according to the network traffic, and the number (m) of grids is determined once the sum of the length of these grids exceeds the length of the network $(2km)$.

8.6.2 GAF models with variable transmission ranges

In the numerical results obtained so far, the transmission range in each grid is considered to be static based on GAF models. In these any node in one grid is able to communicate with any node of its neighbouring grid, which means that the transmission range in one grid is determined by the size of its neighbour and itself. Here, however, the author assumes that the transmission range, R_i, from one head node to its neighbour head node is only determined by their positions on the motorway: $R_i = \sqrt{(x_i - x_{i-1})^2 + (y_i - y_{i-1})^2}$, where x_i and y_i are the coordinates of the active node in the ith grid.

As a result, Fig. 8.8 also shows the energy consumption of the GAF models which considers variable transmission ranges, and this shows that the models based on the variable transmission range can save more energy than those which are based on a static transmission range. Based on the computation, it has been found that the GAF models based on variable transmission ranges can save energy
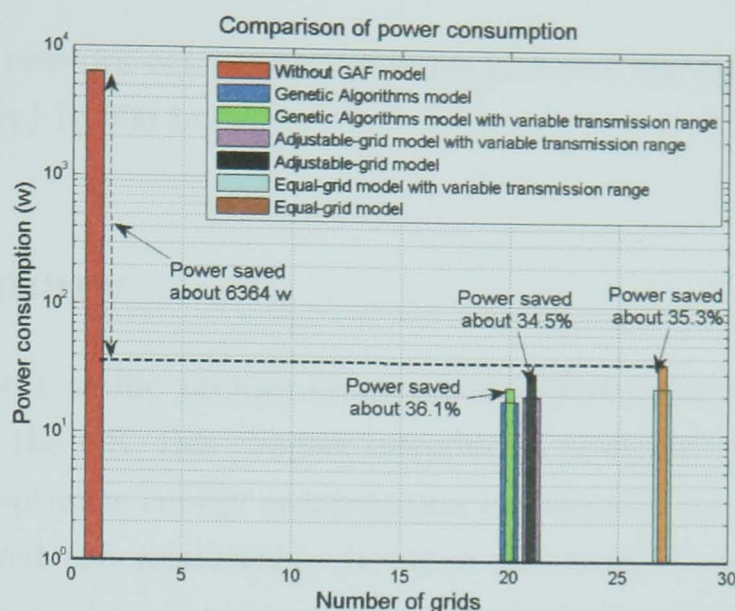
Figure 8.9: Power consumption in three models

by 35.3% in (equal-grid model), 34.5% in (adjustable-grid model), and 36.1% in (GA model), compared to the GAF models which are based on static transmission ranges. Furthermore, the comparison is more clearly shown in Fig. 8.9.

8.6.3 Comparison of power consumption

The results above are all based on 100-second simulations, in which the power consumptions (J/s) of these models are calculated and shown in Fig. 8.9. Without the GAF mechanisms, it is assumed that every vehicle can transmit data directly to the BS. Thus the transmission range of each vehicle is considered to be fixed, and is set to be the network length ($L = 2km$). Based on equation 8.6, the energy consumed by the entire network is computed to be about $6.4 \times 10^5 J$, thus the power consumption is $6.4 \times 10^3 W$, which is shown in Fig. 8.9. Compared to the power consumption without using GAF mechanism, the GAF models proposed in this chapter can reduce the power consumption by 99.4% − 99.7% (about 6364-6381W), and the comparison is given in Fig. 8.9. Note that, in Fig. 8.9, the author only considers the minimum energy consumption of both equal-grid and Genetic Algorithms models, which occur respectively at $m = 21$ and $m = 27$. As an example, if we consider a 60W-bulb, then, the power saved in the 2 km section

of the motorway network can power 100 bulbs and over the entire motorway (300 km approximately) 16,000 bulbs.

8.7 Summary

Based on transport traffic profiles observed at different inductive loops on the M4 motorway in the UK, this chapter introduced, analysed and evaluated three GAF models to optimise energy consumption in vehicular ad-hoc networks. The author has derived the relationship between the number of grids and energy consumption. where the minimum number of network grids can be determined in the equal-grid GAF model, determining the minimum energy consumption in this model. The relationship between the network energy consumption and nodes transmission range has been derived in the adjustable-grid GAF model. This enabled us to find the optimal transmission range, which corresponds to minimum energy consumption in the adjustable-grid model. The performance of these two GAF models is compared to the performance of a genetic algorithm introduced to optimise energy consumption in VANETs. The comparison results show that the GA model is the most energy efficient one and saves 21.1% compared to the equal-grid model, whereas the adjustable-grid model saves 19.3% compared to the equal-grid model. It was determined that a GAF model with variable transmission ranges can save about 35% energy compared to the GAF models based on a static transmission range. This chapter draws the first step towards building a software utility to control the energy consumed in vehicular communication. Consequently, vehicles will be able to tune their communication transmission range based on the driving time or specific locations along their trajectory. Furthermore, the proposed transmission range adjustment mechanism can be deployed in other ad-hoc network scenarios where dynamically varying node densities are expected. for example in social networking.

Chapter 9

Conclusions and Future work

9.1   Conclusions of research work

Energy efficiency is one of the most important issues in ad-hoc wireless networks and forms one of the important constraints in the development of wireless ad-hoc networks. The work in this thesis focused on how to achieve energy efficiency in ad-hoc wireless networks. The energy saving approaches are classified into three main approaches: node states control, optimal transmission range, and topology management or routing algorithms. In this thesis, these three approaches are utilised together in different ad-hoc wireless networks.

In Chapter 1, the author introduced a classification for communication networks and then introduced node characteristics in ad-hoc wireless networks. In relation to energy efficiency, the energy constraints and the definitions of network lifetime in ad-hoc wireless networks have been introduced. To achieve energy efficiency in ad-hoc wireless networks, knowledge of energy consumption states, multihop transmission techniques, topology management and routing algorithms are needed. These were introduced and discussed. Furthermore, this chapter outlined the objectives of this research work and the original contributions, which were supported by a list of publications.

In Chapter 2, the energy efficiency approaches used in ad-hoc wireless networks have been surveyed, and most of these approaches have been classified into

three main categories: multiple power consumption states, transmission range adjustment, and topology management and routing algorithms. As the main user of the multiple power consumption states approach, the IEEE 802.11 PSM has been introduced and discussed, and work related to it has been evaluated. The concept of transmission range adjustment approach has been introduced, and the work based on this concept has been assessed and summarised. The main routing and topology management algorithms have been introduced, and several specific routing and topology management algorithms used in ad-hoc wireless networks have been introduced and evaluated. Furthermore, other energy saving methods, such as hybrid ad-hoc wireless network have been discussed.

In Chapter 3, an energy efficient GAF protocol has been proposed in a linear ad-hoc wireless network. In terms of the network traffic, the attenuation loss factor, the data bit rate, and the optimal transmission range have been derived. The network energy consumption of the equal-grid GAF model has been derived and the optimal grid length has been determined. Furthermore, based on the optimal transmission range and Genetic Algorithms respectively, adjustable-grid models have been proposed, and the related energy consumptions has been evaluated. The results show that, compared to the minimum energy consumption of the equal-grid model, GA and OTR adjustable-grid models respectively save energy by 12.0% and 10.9% under the set of network and transceiver parameters assumed. Note that, the energy consumption model considers the energy consumed in the listening states, which has been neglected in previous work in the literature.

In Chapter 4, an energy efficient GAF protocol has been proposed in a rectangular ad-hoc wireless network. Compared to the linear GAF model proposed in Chapter 3, the rectangular model is closer to real networks, such as VANET on motorways, or rectangular (or square) WASNETs. In a fashion similar to the methods in Chapter 3, the author has derived the relationship between the optimal transmission radio range and network traffic. The analysis of network energy consumption has been carried on in both equal-grid model and adjustable-grid model. The results show that about 78.1% energy is saved by using the adjustable-grid model compared to the minimum energy consumption in the equal-grid model. Furthermore, the network lifetime has been evaluated based on

a new grid-lifetime concept in both an equal-grid and an adjustable-grid models, and the results show that the adjustable-grid model can prolong the network lifetime by 420% compared to the equal-grid model. With the node density control approach, the network lifetime can be prolonged. In this chapter, the energy consumption model has been improved by adding transmission impairments, including the propagation attenuation function, loss factor ($n = 2, n = 4$) and Rayleigh fading.

In Chapter 5, energy-efficient geographic routing algorithms, ORF and OFEB, have been proposed to prolong the network lifetime in a linear ad-hoc wireless network. The ORF algorithm selects as the next hop node the node nearest to the optimal transmission range (within the maximum range) and therefore minimises the energy consumption. The OFEB algorithm selects the next hop node as the node (within the maximum range) that minimises the value of $[\alpha \frac{\Delta d}{r_{opt}} - (1-\alpha)\frac{E_{res}}{E_{cap}}]$. This node has the best combination of energy reserves and needs the minimum energy to be reached. Compared to the existing geographic routing algorithms MFR and NFP, the simulation results show that the OFEB algorithm has the best performance in terms of network lifetime and amount of data received by the destination node. Furthermore, the author has introduced a method to select the optimum locations of relay nodes, and has derived the range of relay node location that result in energy saving.

In Chapter 6, energy-efficient geographic routing algorithms, ORF and OFEB, have been proposed to prolong the network lifetime in a 2-D ad-hoc wireless network. The network lifetime and other network performance metrics have been considered , analysed and improved. Similar to the ORF and OFEB algorithms proposed in a linear ad-hoc wireless network in Chapter 5, the 2-D ORF algorithm selects as the next hop node the node nearest to the optimal transmission range (within the maximum range) and therefore minimises the energy consumption, and the 2-D OFEB algorithm selects the next hop node as the node (within the maximum range) that minimises the value of $[\alpha \frac{\Delta d}{R_{opt}} - (1-\alpha)\frac{E_{res}}{E_{cap}}]$. This node has the best combination of energy reserves and needs the minimum energy to be reached. The weight factor α determines the relative significance placed on these two requirements. The simulation results show that the OFEB algorithm has the best performance. The network lifetime, the network throughput, the number of

received packets, and the energy consumed for each received packet have all been considered. Also, in this chapter we introduced a method that can be used to select the optimum location of relay nodes.

In Chapter 7, two methods have been proposed to achieve energy efficiency in ad-hoc wireless networks in realistic physical layer scenarios. Most transmission and energy consumption models in ad-hoc wireless networks assume an ideal physical layer model, where the packet will be 100% received by the neighbour once the neighbour node is within the transmission range of the transmitter. In this chapter, Rayleigh fading and Lognormal fading scenarios have been investigated to derive the optimal transmission range in ad-hoc wireless networks. Furthermore, the relationship between the total expected energy consumption, the range of each hop, and the transmission power of each node has been derived and analysed based on different approaches in an equal-hop end-to-end multihop transmission model. The results show that, two relationships derived through different approaches are equivalent, which validates the models. The results in this chapter can be used to evaluated the realistic scenarios, and can form the basis for further work.

In Chapter 8, the energy efficiency GAF models were applied in a realistic vehicular ad-hoc wireless network. The associated vehicular traffic is observed at different inductive loops on the M4 motorway in the UK. The equal-grid GAF model and the adjustable-grid GAF models which are based on the optimal transmission range and Genetic Algorithms respectively, have been utilised to achieve energy efficiency in the motorway network. The comparison results show that the GA adjustable-grid model is the most energy efficient one and saves 21.1% compared to the equal-grid model, whereas the adjustable-grid model based on the optimal transmission range saves 19.3% compared to the equal-grid model. Furthermore, the results show that a GAF model with variable transmission ranges can save about 35% energy compared to GAF models based on a static transmission range. This chapter draws the first step towards building a software utility to control the energy consumed in vehicular communication. Consequently, the communication transmission range can be tuned based on the driving time or specific locations of vehicles along their trajectory to save energy.

9.2   Areas of future work

The following areas can be considered for future research:

1. The physical layer models introduced and routing algorithms discussed can be used in Geographic Routing approach to reduce the energy consumption and to prolong the network lifetime.

2. Nodes mobility can be considered and improved routing protocols can be derived to enhance the current energy saving protocols.

3. The relationship between node density and network lifetime can be evaluated, and node density can be used together with other protocols to reduce energy consumption and to prolong the network lifetime.

4. Current energy saving algorithms can be applied to specific ad-hoc wireless networks, such as sensor networks and vehicular ad-hoc networks, and certain constraints in specific networks can be considered.

5. The current work should be utilised in a test bed, which consists of several computers with wireless transceiver and traffic generators. Indoor and outdoor experiments should be carried out to assess the performance of current energy saving algorithms. Also, nodes' mobility can be considered.

6. Some critical nodes in ad-hoc wireless networks can be replaced by nodes with a permanent energy source to prolong the network lifetime. Hybrid ad-hoc networks are worthy of being studied in this context.

Bibliography

[1] H. N. Koivo and M. Elmusrati, *Systems engineering in wireless communications*. Wiley-Blackwell, 2009.

[2] T. Rappaport, *Wireless Communications: Principles & Practice*. Prentice-Hall, Englewood Cliffs, 1996.

[3] P. M. Shankar, *Introduction to Wireless Systems*. JOHN WILLEY & SONS, INC., 2002.

[4] A. Goldsmith, *Wireless Communications*. Cambridge, 2005.

[5] H. Karl and A. Willig, *Protocols and Architectures for Wireless Sensor Netwoks*. Jone Wiley & Sons, Ltd, 2005.

[6] R. Jurdak, *Wireless Ad hoc and Sensor Networks: A Cross-Layer Design Perspective*. Springer, 2007.

[7] I. Akiyldiz, W. Su, Y. Sankarasubramaniam, and E. Cayirci, "A survey on sensor networks," *IEEE communication magazine*, vol. 40, pp. 102–114, 2002.

[8] C. K. Toh, *Ad Hoc Mobile Wireless Networks: Protocols and Systems*. Prentice Hall, Dec. 2001.

[9] I. (2008), "Autonomic computing: The 8 elements," tech. rep., IBM, February 2008.

[10] S. Misra, I. Woungang, and S. C. Misra, *Guide to wireless ad hoc networks*. Springer, 2009.

[11] O. Younis and S. Fahmy, "Heed: a hybrid, energy-efficient, distributed clustering approach for ad hoc sensor networks," *IEEE Transactions on Mobile Computing*, no. 4, pp. 366–379, 2004.

[12] L. Bao and J. J. Garcia-Luna-Aceves, "Topology management in ad hoc networks," in *4th ACM International Symposium on Mobile Ad Hoc Networking and Computing*, pp. 129–140, June 2003.

[13] Y. Xu, J. heidemann, and D. Estrin, "Geography-informed energy conservation for ad hoc routing," in *Proceedings of ACMMobil'01*, pp. 70–84, July 2001.

[14] B. J. Chen, K. Jamieson, H. Balakrishnan, and R. Morris, "Span: an energy-efficient coordination algorithm for topology maintenance in ad hoc wireless networks," *Wireless Networks*, vol. 8, pp. 85–96, September 2002.

[15] M. Stemm and R. H. Katz, "Measuring and reducing energy consumption of network interfaces in hand-held devices," *IEICE Transactions on Communications*, vol. E80-B(8), no. 8, pp. 1125–1131, 1997.

[16] P. Agrawal, "Energy efficient protocols for wireless systems," *Personal, Indoor and Mobile Radio Communications, 1998. The Ninth IEEE International Symposium on*, vol. 2, pp. 564–569, Sept 1998.

[17] D. Estrin, R. Govindan, J. Heidemann, and S. Kumar, "Next century challenges: Scalable coordination in sensor networks," in *Proceedings of the ACM/IEEE International Conference on Mobile Computing and Networking*, (Seattle, Washington, USA), pp. 263–270, ACM, August 1999.

[18] W. R. Heinzelman, A. Ch. and H. Balakrishnan, "Energy-efficient communication protocol for wireless microsensor networks," in *International conference System Sciences*, pp. 3005–3014, 2000.

[19] W. R. Heinzelman, J. Kulik, and H. Balakrishnan, "Adaptive protocols for information dissemination in wireless sensor networks," in *MOBICOM*, pp. 174–185, 1999.

[20] J. M. Kahn, R. H. Katz, R. H. K. (acm Fellow. and K. S. J. Pister. "Next century challenges: Mobile networking for "smart dust"." in *MOBICOM*. pp. 271–278, 1999.

[21] K. Sohrabi, J. Gao, V. Ailawadhi. and G. Pottie. "Protocols for self-organization of a wireless sensor network." *IEEE Personal Communications Magazine*, vol. 7, pp. 16–27. Oct. 2000.

[22] M. Mauve, J. Widmer, and H. Hartenstein, "A survey on position-based routing in mobile ad hoc networks," *IEEE Network*. vol. 15. pp. 30–39. 2001.

[23] I. Stojmenovic, "Position-based routing in ad hoc networks." *IEEE Communications Magazine*, vol. 40, pp. 2–8, July 2002.

[24] W. Feng, H. Alshaer, and J. M. H. Elmirghani, "Green ict: Energy efficiency in a motorway model," *IET special issue on Vehicular Ad-hoc networks*. April 2010.

[25] W. Feng and J. M. H. Elmirghani, "Lifetime evaluation in energy-efficient rectangular ad-hoc wireless networks." *International journal of communication systems*, March 2010.

[26] W. Feng, H. Alshaer, and J. M. H. Elmirghani, "Evaluation of energy consumption and network lifetime in rectangular ad-hoc wireless networks." in *Proceedings of 6th International Conference on Information Technology : New Generations (ITNG)*, pp. 546–551, April 2009.

[27] W. Feng, H. Alshaer. and J. M. H. Elmirghani, "Energy efficiency: Optimal transmission range with topology management in rectangular ad-hoc wireless networks." in *Proceedings of the IEEE 23rd International Conference on Advanced Information Networking and Applications (AINA-09)*, pp. 301–306, May 2009.

[28] W. Feng, H. Alshaer, and J. M. H. Elmirghani, "Energy efficiency for rectangular ad-hoc wireless networks," in *the IEEE 5th International Wireless Communications and Mobile Computing Conference (IWCMC 2009)*, pp. 258–262, June 2009.

[29] W. Feng and J. M. H. Elmirghani, "Optimization of energy consumption in linear ad-hoc wireless networks," in *10th IEEE International Symposium on Communication Theory and Application*, July 2009.

[30] W. Feng, H.Alshaer, and J. M. H. Elmirghani, "Optimization of energy consumption in rectangular ad-hoc wireless networks," in *ChinaCom'09*, August 2009.

[31] W. Feng and J. M. H. Elmirghani, "Green ict: Energy efficiency in a motorway model," in *IEEE Next Generation Mobile Applications, Services and Technologies, September*, September 2009.

[32] W. Feng and J. M. H. Elmirghani, "Energy-efficient geographic routing in 2-d ad-hoc wireless networks," in *IEEE Next Generation Mobile Applications, Services and Technologies, September*, September 2009.

[33] W. Feng and J. M. H. Elmirghani, "Energy efficiency in ad-hoc wireless networks with two realistic physical layer models," in *IEEE Next Generation Mobile Applications, Services and Technologies, September*, September 2009.

[34] W. Feng and J. M. H. Elmirghani, "Energy efficiency in the cluster-based linear ad-hoc wireless networks," in *IEEE Next Generation Mobile Applications, Services and Technologies, September*, September 2009.

[35] W. Feng, A. S. K. Mammu, and J. M. H. Elmirghani, "Energy-efficient geographic routing in ad-hoc wireless networks," in *London Communications Symposium09*, September 2009.

[36] R. Bruno, M. Conti, and E. Gregori, "Mesh networks: Commodity multihop ad hoc networks," *IEEE Personal Communications Magazine*, vol. 43, pp. 122–131, Mar. 2005.

[37] C. Jones. K. Sivalingam, P. Agrawal. and J. Chen. "A survey of energy efficient network protocols for wireless networks," *Wireless Networks*, vol. 7, pp. 343–358. 2001.

[38] I. 802.11, "Wireless lan medium access control(mac) and physical layer(phy) specifications," *IEEE standard organisation*. June 1999.

[39] Y. Zhou, Y. E. Tan, D. I. Laurenson, and S. McLaughlin. "Impact of power saving mac scheme on ad hoc network routing protocol," in *Vehicular Technology Conference. 2005. VTC 2005-Spring. 2005 IEEE 61st*. vol. 4, pp. 2463– 2467, May 2005.

[40] N. Li, H. Wang, and S. Zheng. "An energy-saving scheme for wireless lans," in *International Conference on Communication technology*. pp. 1242– 1245. April 2003.

[41] N. Li, Y. Xu, and S. Xie, "A power-saving protocol for ad hoc networks," in *IEEE International Conference on Wireless communications,Network and mobile computing*, pp. 808– 811. Sept 2005.

[42] M. J. Miller and N. H. Vaidya. "Ad hoc routing for multilevel power save protocols," *Ad Hoc networks*, vol. 6. pp. 210–225. April 2008.

[43] A. V. S. Chandra. "Application-specific network management for energy-aware streaming of popular multimedia formats," in *Usenix Annual Technical Conference*, pp. 329–342. 2002.

[44] L. Huang and T. H. Lai. "On the scalability of ieee 802.11 ad hoc networks," in *MOBIHOC02*. pp. 173– 182. June 2002.

[45] T. H. Lai and D. Zhou, "Efficient and scalable ieee 802.11 ad-hoc-mode timing synchronization function," in *Advanced Information Networking and Applications 2003*. pp. 318– 323. Mar. 2003.

[46] J. R. Jiang, Y. C. Tseng, C. S. Hsu. and T. H. Lai. "Quorum-based asynchronous power-saving protocols for ieee 802.11 ad hoc networks," in *Parallel Processing. 2003 International Conference*. pp. 257– 264. Oct. 2003.

[47] Y. C. Tseng, C. S. Hsu, and T. Y. Hsieh, "Power-saving protocols for ieee 802.11-based multi-hop ad hoc networks," in *INFOCOM 2002*, pp. 317–337, June 2002.

[48] Y. Zhou, D. I. Laurenson, and S. McLaughlin, "An effective power-saving scheme for ieee 802.11-based multi-hop ad hoc network," in *VTC Fall 2004*, Sept. 2004.

[49] B. Chen, K. Jamieson, H. Balakrishman, and R. Morris, "Span: An energy-efficient coordination algorithm for topology maintenance in ad hoc wireless networks," in *MOBICOM 2001*, pp. 85–96, July 2001.

[50] E. Jung and N. Vaidya, "An energy efficient mac protocol for wireless lans," in *INFOCOM 2002*, June 2002.

[51] T. Simunic and S. Boyd, "Managing power consumption in networks on ships," in *ACM DATE2002*, 2002.

[52] H. Zhu and G. Cao, "A power-aware and QoS-aware service model on wireless networks," in *IEEE INFOCOM04*, pp. 1393–1403, Mar. 2004.

[53] M. Anand, E. Nightingale, and J. Flinn, "Self tuning wireless network power management," in *9th ACM Annual International Conference on Mobile Computing and Networking (MobiCom 2003)*, pp. 176 – 189, Sept. 2003.

[54] B. Awerbuch, D. Holmer, and H. Rubens, "The pulse protocol: energy efficient infrastructure access," in *IEEE INFOCOM04*, pp. 1467–1478, Mar. 2004.

[55] H. Idoudi, M. Molnar, and A. Belghith, "Power aware alternation : a novel power saving mechanism for ad hoc networks," in *International Conference on Performance Modeling and Evaluation of Heterogeneous Networks*, July 2005.

[56] J. Zhu, C. Qiao, and X. Wang, "A comprehensive minimum energy routing scheme for wireless ad hoc networks," in *IEEE INFOCOM04*, Mar. 2004.

[57] D. Kim and C. Choi, "Adaptive power management for ieee 802.11 based ad hoc networks," in *World Wireless Congress*, May 2004.

[58] C. Suh, Y.-B. Ko, and J.-H. Kim, "Enhanced power saving for ieee 802.11 wlan with dynamic slot allocation," in *LNCS*, pp. 498–507, 2005.

[59] T. Zhang, P. Gurung, E. V. D. Berg, S. Madhani, and A. Muttreja, "Silent networking for energy constrained nodes," *Press in Computer Communications, Elsevier*, vol. 29, no. 17, pp. 3445–3454, 2006.

[60] S. Thakur, S. Nandi, R. Bhattacharjee, and D. Goswami, "An asynchronous wakeup power saving protocol for multi-hop ad hoc networks," *International Journal of High Performance Computing Applications*, vol. 21, pp. 429–442, 2007.

[61] E. Jung and N. Vaidya, "Improving ieee 802.11 power saving mechanism," *Springer Science+Business Media*, pp. 375–391, June 2008.

[62] F. Ingelrest, D. Simplot-Ryl, and I. Stojmenovic, "Optimal transmission radius for energy efficient broadcasting protocols in ad hoc and sensor networks," *IEEE Transactions on parallel and distributed systems*, vol. 17, pp. 536–547, June 2006.

[63] Q. Gao, K. J. Blow, D. J. Holding, I. W. Marshall, and X. H. peng, "Radio range adjustment for energy efficient wireless sensor network," *Ad hoc Networks*, vol. 4, pp. 75–82, January 2006.

[64] W. R. Heinzelman and A. C. H. Balakrishnan, "Energy-efficient communication protocol for wireless microsensor networks," in *Proceedings of HICSS'00*, vol. 2, pp. 4–7, January 2000.

[65] B. Yin, S. Hongchi, and Y. Shang, "Analysis of energy consumption in clustered wireless sensor networks," in *Wireless Pervasive Computing, 2nd International Symposium on*, pp. 102–114, Feb 2007.

[66] A. Cerpa and D. Estrin, "Ascent: adaptive self-configuring sensor networks topologies," in *Proceedings of INFOCOM'02*, vol. 3, pp. 1278–1287, June 2002.

[67] A. Qayyum, L. Viennot, and A. Laouiti. "Multipoint relaying for flooding broadcast messages in mobile wireless networks," in *HICSS 02*, pp. 3866 3875, Jan. 2002.

[68] P. Jacquet, P. M. hlethaler. T. Clausen. A. Laouiti. A. Qayyum, and L. Viennot, "Optimized link state routing protocol for ad hoc networks." in *INMIC 01*, pp. 62–68, Dec. 2001.

[69] I. Stojmenovi.c and M. Seddigh, "Broadcasting algorithms in wireless networks," in *Intl Conf. Advances in Infrastructure for Electronic Business. Science, and Education on the Internet SSGRR*. July 2000.

[70] W. Peng and X. Lu, "On the reduction of broadcast redundancy in mobile ad hoc networks," in *ACM MobiHoc 2000*. pp. 129 133. Aug. 2000.

[71] V. Rodoplu and T. H. Meng. "Minimum energy mobile wireless networks." *IEEE Journal on Selective Areas Communications*, vol. 17. pp. 1333 1344. Aug 1999.

[72] N. Li, J. C. Hou, and L. Sha, "Design and analysis of an mst-based topology control algorithm," in *IEEE INFOCOM 2003*. pp. 1702 1712. Mar 2003.

[73] J. H. Chang and L. Tassiulas, "Energy conserving routing in wireless ad-hoc networks," in *IEEE INFOCOM 2000*, pp. 22–31. 2000.

[74] S. Banerjee and A. Misra, "Minimum energy paths for reliable communication in multi-hop wireless networks," in *MobiHoc*, pp. 146 156. 2002.

[75] S. J. Park and R. Sivakumar, "Quantitative analysis of transmission power control in wireless ad-hoc networks." in *International Workshop on Ad Hoc Networking (IWAHN)*, pp. 56 61. Aug 2002.

[76] H. Takagi and L. Kleinrock. "Optimal transmission ranges for randomly distributed packet radio terminals." *IEEE Trans. Communications*, vol. COM-32. pp. 246–257. Mar 1984.

[77] Y. Chen, E. G. Sirer. and S. B. Wicker, "On selection of optimal transmission power for ad hoc networks." in *36th Hawaii Int. Conf. Syst. Sci.*, pp. 300–309, 2003.

[78] M. Zuniga and B. Krishnamachari, "Optimal transmission radius for flooding in large scale sensor networks," in *23rd Int. Conf. Distrib. Comput. Syst. Workshops*, pp. 697–702, 2003.

[79] J. L. Gao, "Analysis of energy consumption for ad hoc wireless sensor networks using a bit-meter-per-joule metric." tech. rep., IPN Progress Report, Aug 2002.

[80] F. Ingelrest, D. Simplot-Ryl, and I. Stojmenovic, "Optimal transmission radius for energy efficient broadcasting protocols in ad hoc and sensor networks," *Parallel and Distributed Systems. IEEE Transactions on.* vol. 17, pp. 536 – 547, June 2006.

[81] M. S. . Gokturk, O. Ercetin. and O. Gurbuz, "Energy distribution control in wireless sensor networks through range optimization," in *IEEE International Symposium on Personal, Indoor and Mobile Radio Communications (PIMRC)*, 2008.

[82] O. Ercetin, "Distance-based routing for balanced energy consumption in sensor networks," in *Globecom 2008*, 2008.

[83] T. C. Hou and V. O. K. Li, "Transmission range control in multihop packet radio networks," *IEEE Trans. Communications*, vol. COM-34, pp. 38 44. Jan 1986.

[84] M. Zorzi and S. Pupolin, "Optimum transmission ranges in multihop packet radio networks in the presence of fading." *IEEE Trans. Communications.* vol. 43, pp. 2201–2205, July 1995.

[85] H. Gomez and A. T. Campbell. "Variable-range transmission power control in wireless ad hoc networks." *IEEE Transactions on Mobile Computing.* vol. 6, pp. 87-99, January 2007.

[86] J. Broch, D. A. Maltz, D. B. Johnson, Y. Hu, and J. Jetcheva, "A performance comparison of multi-hop wireless ad hoc network routing protocols," in *MobiCom '98: Proceedings of the 4th annual ACM/IEEE international conference on Mobile computing and networking*, pp. 85-97, 1998.

[87] M. Tarique, K. E. Tepe, and M. Naserian, "Energy saving dynamic source routing for ad hoc wireless networks," in *Modeling and Optimization in Mobile, Ad Hoc, and Wireless Networks, 2005. WIOPT 2005. Third International Symposium on*, pp. 305- 310, April 2005.

[88] J. Kanjanarot, K. Sitthi, and C. Saivichit, "Energy-based route discovery mechanism in mobile ad hoc networks," in *Advanced Communication Technology, ICACT*, pp. 1972–1978, February 2006.

[89] R. Chang and C. Kuo, "An energy efficient routing mechanism for wireless sensor networks," in *Advanced Information Networking and Applications, 2006. AINA 2006. 20th International Conference on*, pp. 1-5, 2006.

[90] R. L. Haupt and S. E. Haupt, *Practical Genetic Algorithms*. A John Wiley & Sons, Inc., 2004.

[91] M. Melanie, *An Introduction to Genetic Algorithms*. A Bradford Book The MIT Press, 1999.

[92] M. Khare and S. S. Nagendra, *Artificial Neutral Networks*. Springer Berlin / Heidelberg, 2007.

[93] A. Ciccazzo, P. Conca, G. Nicosia, and G. Stracquadanio, *An Advanced Clonal Selection Algorithm with Ad-Hoc Network-Based Hypermutation Operators for Synthesis of Topology and Sizing of Analog Electrical Circuits*. Springer Berlin / Heidelberg, 2008.

[94] L. Sun and X. Zhang, "A power-saving routing algorithm based on ant algorithm in mobile ad hoc networks," in *Wireless Communications, Networking and Mobile Computing, 2005. Proceedings. 2005 International Conference on*, vol. 2, pp. 799-802, Sept. 2005.

[95] C. E. Perkins and P. Bhagwat, "Highly dynamic destinationsequenced distance-vector routing (dsdv) for mobile computers." in *ACM SIGCOMM '94*, pp. 234 – 244, 1994.

[96] S. Murthy and J. J. Garcia-Luna-Aceves, "An efficient routing protocol for wireless networks," *ACM Mobile Networks and Applications Journal. Special Issue on Routing in Mobile Communication Networks*, pp. 183–197, 1996.

[97] T.-W. Chen and M. Gerla. "Global state routing: A new routing scheme for ad-hoc wireless networks," in *ICC'98*, pp. 171–175, 1998.

[98] G. Chen, M. Gerla, and T. W. Chen, "Fisheye state routing: A routing scheme for ad hoc wireless networks," in *ICC'2000*, pp. 70–74, 2000.

[99] M. S. Corson and A. Ephremides, "A distributed routing algorithm for mobile wireless networks," *ACM/Balzer Wireless Networks*, vol. 1, pp. 61–81, 1995.

[100] D. B. Johnson and D. A. Maltz. "Dynamic source routing in ad-hoc wireless networks," in *Mobile Computing*, pp. 153–181, 1996.

[101] C.-K. Toh, "A novel distributed routing protocol to support ad-hoc mobile computing," in *International Phoenix Conference on Computers and Communications*, pp. 183–197, Mar. 1996.

[102] R. Dube, C. D. Rais, K.-Y. Wang, and S. K. Tripathi, "Signal stability based adaptive routing (ssa) for ad-hoc mobile networks." *IEEE Personal Communications*, pp. 36–45, Jan. 1997.

[103] V. D. Park and M. S. Corson, "A highly adaptive distributed routing algorithm for mobile wireless networks," in *IEEE INFOCOM '97*, pp. 1405–1413, 1997.

[104] C. E. Perkins and E. M. Royer, "Ad-hoc on-demand distance vector routing," in *IEEE Workshop on Mobile computing Systems and Applications*, pp. 90–100, 1999.

[105] C.-C. Chiang, H. K. Wu, W. Liu, and M. Gerla. "Routing in clustered multihop, mobile wireless networks with fading channel," in *IEEE SICON'97*, pp. 197–211, 1997.

[106] R. Sivakumar, P. Sinha, and V. Bharghavan. "Cedar: A coreextraction distributed ad hoc routing algorithm," *IEEE Journal on Selected Areas in Communications*, pp. 1454–1465. Aug. 1999.

[107] Z. J. Hass, "A new routing protocol for reconfigurable wireless networks," in *International Conference on Universal Personal Communications*, pp. 562–566, 1997.

[108] G. Pei, M. Gerla, X. Hong, and C.-C. Chiang, "A wireless hierarchical routing protocol with group mobility," in *ACM/IEEE MSWiM'99*, pp. 1538–1542, 1999.

[109] J. C. Navas and T. Imielinski, "Geocast–geographic addressing and routing," in *MobiCom '97*, pp. 66–76, 1997.

[110] R. Nelson and L. Kleinrock, "The spatial capacity of a slotted oloha multihop packet radio network with capture," *IEEE Transactions on Communications*, pp. 684–694, June 1984.

[111] G. Finn, "Routing and addressing problems in large metropolitanscale internetworks," tech. rep., USC/ISI, March 1987.

[112] T. C. Hou and V. O. K. Li, "Transmission range control in multihop packet radio networks," *IEEE Transactions on Communications*, vol. 34, pp. 38–44, Aug. 1986.

[113] E. Kranakis, H. Singh, and J. Urrutia, "Compass routing on geometric networks," in *in the 11th Canadian Conference on Computational Geometry*, pp. 51–54, 1999.

[114] M. Grossglauser and M. Vetterli, "Locating nodes with ease: Mobility diffusion of last encounters in ad hoc networks," in *IEEE Infocom '02*, vol. 3, pp. 1954–1964, 2002.

[115] I. Stojmenovic, M. Russell. and B. Vukojevic. "Depth first search and location based localized routing and QoS routing in wireless networks." in *IEEE International Conference on Parallel Processing*. pp. 173–181, 2000.

[116] H. Takagi and L. Kleinrock. "Optimal transmission range for randomly distributed packet radio terminals," *IEEE Transactions on Communications*. vol. 32, pp. 246–257, 1984.

[117] S. Basagni, I. Chlamtac. V. R. Syrotiuk. and B. A. Woodward. "A distance routing effect algorithm for mobility (dream)." in *ACM/IEEE International Conference on Mobile Computing and Networking (MOBICOM)*. pp. 76–84, 1998.

[118] S. Wu and K. S. Candan, "Gper: Geographic power efficient routing in sensor networks," in *IEEE international conference on network protocols*. pp. 161–172, 2004.

[119] H. Zhang and H. Shen, "Eegr: Energy-efficient geographic routing in wireless sensor networks," in *Parallel Processing, 2007. ICPP 2007. International Conference on*, pp. 67–72, Sept. 2007.

[120] C. L. Chen and K. R. Lee, "An energy-proportional routing algorithm for lifetime extension of clustering-based wireless sensor networks." *Journal of pervasive computing*, vol. 3, pp. 304–321, 2006.

[121] C. L. Chen and K. R. Lee, "An energy-proportional routing algorithm for lifetime extension of clustering-based wireless sensor networks." in *The 2nd Workshop on Wireless. Ad Hoc. and Sensor Networks*. 2006.

[122] Y. Xu, J. Heidemann. and D. Estrin. "Geography-informed energy conservation for ad hoc routing," in *ACM MobiCom 2001*. pp. 70–84, July 2001.

[123] Y. Xu, S. Bien. Y. Mori. J. Heidemann. and D. Estrin. "Topology control protocols to conserve energy in wireless ad hoc networks." *IEEE Transactions on Mobile Computing*. pp. 319–332, January 2003.

[124] Y. Xu, J. heidemann, and D. Estrin. "Energy conservation by adaptive clustering for ad-hoc networks," in *Poster Session of MobiHoc'02*. pp. 255 263, June 2002.

[125] Y. Xu, J. Heidemann, and D. Estrin, "Adaptive energy-conserving routing for multihop ad hoc networks," tech. rep.. USC Information Sciences Institute, 2000.

[126] C. Schurgers, V. Tsiatsis, S. Ganeriwal. and M. Srivastava. "Optimizing sensor networks in the energy-latency-density design space." *IEEE Transactions on Mobile Computing*, vol. 1. pp. 70 80. 2002.

[127] C. Sengul and R. Kravets. "Titan: On-demand topology management in ad hoc networks," *ACM Mobile Computing and Communications Review (MC2R)*, vol. 9. no. 1, pp. 77–82. 2005.

[128] P. Bose, L. Devroye, W. Evans, and D. Kirkpatrick, "On the spanning ratio of gabriel graphs and beta-skeletons." *SIAM Journal of Discrete Math.* pp. 412 – 427, 2006.

[129] X. Li, P. Wan, and Y. Wang, "Power efficient and sparse spanner for wireless ad hoc networks," in *IEEE International Conference on Computer Communicationsand Networks*, pp. 564–567. 2001.

[130] R. Rajaraman, "Topology control and routing in ad hoc network: a survey." in *ACM SIGACT*, vol. 33. pp. 60–73, 2002.

[131] M. Cheng, M. Cardei. S. Jinhua, C. Xiaochun, W. Lusheng. X. Yingfeng. and D. Ding-Zhu. "Topology control of ad hoc wireless networks for energy efficiency." *IEEE Transactions on Computers*, pp. 1629 1635. 2004.

[132] S. Naghian and J. Tervonen, "semi-infrastructured mobile ad-hoc mesh networking," in *Proceedings of IEEE Personal. Indoor and Mobile Radio Communications*, vol. 2. pp. 1069–1073. 2003.

[133] R.-S. Chang. W.-Y. Chen, and Y.-F. Wen. "Hybrid wireless network protocols," *IEEE Transactions on Vehicular Technology*. vol. 52. pp. 1099 1109. July 2003.

[134] O. Dousse, P. Thiran, and M. Hasler. "Connectivity in ad-hoc and hybrid networks," in *Proceedings of IEEE INFOCOMM computer Communication Review*, vol. 34, pp. 1079–1088, 2002.

[135] D. Wei and H. A. Chan, "Mesh networking backbone with equalized power consumption cells to prolong the lifetime of large sensor networks," in *ICCT'06 International Conference on Communication Technology*, pp. 1–4, 2006.

[136] M. Moh, R. Kukanur, X. Lin, and S. Dhar. "On energy-efficient self-organizing routing for wireless mobile networks," in *Globecom IEEE*, pp. 1–6, November 2007.

[137] M. Saleemand and M. Sheikh. "An empirical analysis of ad hoc routing protocols for hybrid wireless sensor networks," in *ICEE '07*, pp. 1–6, 2007.

[138] F. Ingelrest, D. Simplot-Ryl. and I. Stojmenovic. "Broadcasting in hybrid ad hoc networks," in *Wireless On-demand Network Systems and Services. 2005*, pp. 131 – 138, 2005.

[139] O. Younis and S. Fahmy, "Heed: a hybrid, energy-efficient, distributed clustering approach for ad hoc sensor networks," *IEEE Transactions on Mobile Computers*, pp. 366–379, 2004.

[140] A. Bedir and A. Alouani, "A simple power based control strategy for hybrid electric vehicles," in *Vehicle Power and Propulsion Conference. 2009*, pp. 803 – 807, 2009.

[141] M. Bhardwaj, T. Garnett, and A. P. Chandrakasan. "Upper bounds on the lifetime of sensor networks," in *Proceedings of ICC'01*, pp. 785–790, June 2001.

[142] M. Karkooti and J. R. Cavallaro. "Cooperative communications using scalable, medium block-length ldpc codes," in *Wireless Communications and Networking Conference. 2008. WCNC 2008. IEEE*, vol. 3, pp. 88–93, March 2008.

[143] G. V. Merrett, A. S. Weddell, A. P. Lewis, N. R. Harris, B. M. Al-Hashimi, and N. M. White, "An empirical energy model for supercapacitor powered wireless sensor nodes," in *17th International IEEE Conference on Computer Communications and Networks*, pp. 81–86, August 2008.

[144] R. Bundgen, "White paper green ict," tech. rep., T-Systems Enterprise Service GmbH, 2008.

[145] R. Hodges and W. White, "Go green in ict," tech. rep., GreenTech News, 2008.

[146] S. group, "Ict system and network for reducing environmental impacts," tech. rep., inistry of Internal Affairs and Communications of Japan, Mar. 2007.

[147] B. R. Qazi, . A. de Grado Vivero, O. Y. K. Alani, and J. M. H. Elmirghani, "Pico cellular mac protocol for multimedia communication," in *AINA 2009*, 2009.

[148] C. Bettstetter, "On the minimum node degree and connectivity of a wireless multihop network," in *International Symposium on Mobile Ad Hoc Networking & Computing archive Proceedings of the 3rd ACM international symposium on Mobile ad hoc networking & computing*, pp. 80–91, 2002.